Membrane Transport Activity of Isophthalate Amphiphiles

by

Ryan Knoy
B.S. in Chemistry, Northern Arizona University, 1998

A Thesis Submitted in Partial Fulfillment of the
Requirements for the Degree of
M.Sc. in Chemistry
in the Department of Chemistry

We accept this thesis as conforming
to the required standard

[redacted]

Dr. T.M. Fyles, Supervisor (Department of Chemistry)

[redacted]

Dr. D. A. Harrington, Departmental Member (Department of Chemistry)

[redacted]

Dr. P. Wan, Departmental Member (Department of Chemistry)

[redacted]

Dr. R. W. Olafson, Outside Member (Department of Biochemistry and Microbiology)

[redacted]

Dr. D. H. Paul, External Examiner (Department of Biology)

Supervisor: Dr. Thomas M. Fyles

Abstract

This research addresses the issue of the minimum structural requirements to form cation conducting channels in lipid bilayers. A suite of fifteen alkoxy substituted isophthalates has been assessed. Two surveys were conducted to demonstrate cation channel formation: one in planar bilayers using the voltage-clamp technique and the second conducted in vesicle bilayers using a pH stat technique. In both techniques, membranes were formed from a mixture of 8:1:1 phosphatidylcholine, phosphatidic acid, and cholesterol. In the bilayer clamp experiment, membranes were formed between two aqueous compartments of 1M alkali chloride salts (NaCl, KCl, CsCl). A transmembrane potential was applied and the transmembrane current was measured. Compounds were introduced as solutions in methanol or dimethyl sulphoxide and experiments were controlled to provide equivalent conditions for channel formation to all compounds. Only one active compound was uncovered from planar bilayer clamp experiments under the conditions of the survey. 5-(12-Tricosanoxy-)-isophthalic acid consistently induced step changes in conductance in the three alkali chlorides. The step-changes in conductance were characterized as behaving according to Ohm's law, with cation selectivity manifest as $Cs^+ > K^+ > Na^+$. A range of conductance values (15.4 pS to 16 pS for K^+) was observed in some experiments, indicating flexibility in the active structure.

This active isophthalate was used as a model for two new homologs, in order to probe the dependence of alkoxy length on cation channel formation. These two homologs and the original suite of fifteen were examined in vesicles through the pH stat technique. The homologs synthesized were inactive in vesicles; however, two of the others were found to

be active in vesicles. Using a modified voltage-clamp procedure, one of the isophthalates gave irregular current-time records and the other gave consistent, well-defined activity of typically short duration. For the isophthalate producing irregular current-time traces, the magnitude of the current observed is consistent with the vesicle results. Under the modified conditions, one of the synthesized homologs (5-(-13-pentacosanoxy-) -isophthalic acid), also gave infrequent single channel openings. From the seventeen compounds examined, channel forming activity was observed for four compounds. The research provides reasonable evidence that defined cation-channel forming structures can be formed from relatively small amphiphiles.

Examiners:

[redacted]

Dr. T. M. Fyles, Supervisor (Department of Chemistry)

[redacted]

Dr. D. A. Harrington, Departmental Member (Department of Chemistry)

[redacted]

Dr. P. Wan, Departmental Member (Department of Chemistry)

[redacted]

Dr. R. W. Olafson, Outside Member (Department of Biochemistry and Microbiology)

[redacted]

Dr. D. H. Paul, External Examiner (Department of Biology)

Table of Contents

List of Tables

List of Schemes

List of Figures

Acknowledgements

First and foremost, I would like to express my gratitude to my advisor, Dr. Thomas M. Fyles, for his infinite patience and advice throughout all of the various stages of this research. Tom was always readily available, and I can not thank him enough for his support. I would also like to express my gratefulness to Mr. Todd Sutherland for sharing his extensive computer knowledge. I want to convey my appreciation to Mr. Chi Wei Hu for his help in mastering the pH stat technique and Ms. Keetah Eggers for the helpful discussions I had with her.

I want to thank Dr. David Harrington for what I learned in his instrumentation course and for being on my committee. Thanks also to Dr. Peter Wan, Dr. Robert Olafson and Dr. Dorothy Paul for agreeing to be committee members. This research would not have been possible without Mr. Bob Dean and Mr. Terry Wiley of the Electronics Shop. Thanks also to Mr. Roy Bennett and Mr. Richard Robinson of the Machine Shop, who did a fine job fabricating equipment which was used in this work. Mr. Paul Eggers deserves a round of applause for his help and advice with computers. I can not thank Sr. Miguel Labayen enough for letting me use his computer at a critical stage in this research, and for his support, friendship and interesting conversations. Michel Sieffert introduced me to the Max Plank Institut für Polymerforschung, and the conversations I had with him were an important contribution to this research. I am ever grateful to Dr. Klaus Müllen at MPIP for contributing the compounds that are the focus of this work. Finally, I would like to convey my gratitude to Ms. Susanne Reiser, who was instrumental in the application process.

For Melanie and Buck

Chapter 1: Overview of cation channels

The transport of sodium, potassium and calcium across membranes in biological systems is achieved almost exclusively through multiple transmembrane spans of proteins.[1] The importance of transmembrane cation-conducting channels in biological systems can not be overstated. Potassium, sodium, and calcium transmembrane channels have an immense role in biological processes such as the regulation of nerve impulses,[2] the frequency and duration of the heartbeat,[3] and the passage of water and salts in mammalian kidneys[4] and intestines.[3]

In the past two decades, chemists and biologists have collaborated in designing small, synthetic ionophores in an attempt to mimic the cation-transport efficacy of naturally occurring transmembrane proteins. Synthetic ionophores which are cation channels are analogous to naturally occurring channels by definition: the channel must insert into and span the membrane[5] and provide a hydrated, ionophilic pathway for cation-conduction. This is usually achieved with amphiphilic structures that are lipid-soluble (lipophilic) which are able to "bind" cations through electophilic donor moieties.[5] For both naturally occurring proteins and synthetic ionophores, the functioning of cation channels involves complex interactions with phospholipid bilayers which constitute the structural core of biological membranes. Indeed, the enormous work performed by protein cation channels can hardly be addressed without mentioning the membranes in which channels function to form conducting pathways. The interplay of protein and lipid essentially directs the function and regulation of cellular membranes.[5] Membranes are the structural barriers which must be spanned for cations to flow from one aqueous compartment to another. They not only isolate the cell from pathogens, but are essential for establishing and

regulating electrochemical gradients which are vital for driving basic biological processes.

If the membrane could be alluded to as a wall, the amphiphilic character of phospholipids is responsible for the spontaneous formation of this wall, whereas the proteins imbedded within are directly involved in the coordination of the construction of this wall and regulation of what passes through it. The phospholipid bilayer can be defined as a reconstituted version of a biological membrane. The greatest distinction between a bilayer and a natural membrane is that the former is void of proteins. Phospholipids and sterols are in a predominantly lamellar phase, separating aqueous phases as in a natural membrane. The majority of membrane lipids exist in the lamellar phase or bilayer phase under physiologically pertinent conditions.[5]

1.2 Phospholipids

In the last few years, research has been conducted to probe the role of phospholipids in regulating the interactions of imbedded proteins. Recent research suggests that lipids are not merely the building blocks of membranes, but play a key role in modulating the conformational equilibrium of membrane proteins and in determining when a structure is "active" or "inactive." Lipid packing energetics have been demonstrated to have a significant influence on single-channel conductance activity of a natural ionophore, Alamethicin.[6] The regulation of many biological processes relies on a complex interdependence of proteins, phospholipids, and cholesterol.

The high electrical capacitance of natural membranes and phospholipid bilayers is directly attributed to the amphiphilic character of polar lipids and a molecular

geometry which permits neat lateral stacking into monolayers, and opposition of monolayers to form sheets, or bilayers (a lyotropic lamellar phase).[7]

Phosphatidylcholine (PC) **1**, is a naturally derived mixture of lipids, having molecules substituted with a variety of acyl chains and typically one degree of unsaturation.

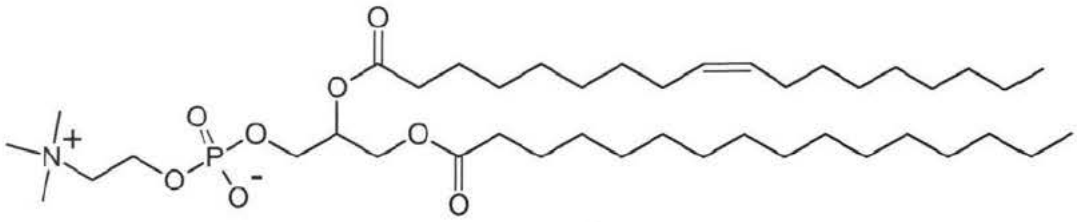

1

Phosphatidylcholines from natural sources have mixed, acyl chains of an even number of carbons, predominantly 16 or 18 carbons in length. Egg PC has mostly saturated fatty acids in the *sn*-1- position and unsaturated acids in the *sn*-2- position,[8] as depicted for compound **1**. *Cis* double bonds effectively kink the acyl chain and lower the phase transition temperature (T_m) for the transition from liquid crystalline to gel phase. They have the most pronounced lowering effect on phase transition temperature when placed in the middle of the acyl chain.[5] The mixed acyl chains of egg PC have a prominent effect on the thermotropic behavior and the conformation of the acyl chains in lamellar phase. Spectroscopic, X-ray and neutron diffraction studies have indicated that the saturated chain substituted at the *sn*-1- position is perpendicular to the plane of the bilayer throughout its length, whereas the typically monounsaturated acyl chain in position *sn*-2- starts out nearly parallel to the plane of the bilayer before bending at C2 to position the rest of the chain perpendicular to the plane of the bilayer.[5] Most natural lipids have either a negatively charged headgroup (phosphatidic acid, phosphatidylserine) or a zwitterionic head group (phosphatidylcholine, phosphatidylethanolamine).[7] The

zwitterionic head group of PC provides sufficient electrostatic repulsion to give an overall columnar geometry which promotes adaptation of the lamellar phase, whereas other lipids with smaller headgroups (and less electrostatic charge) are effectively pinched down around the headgroup to take on a conical shape and overall spherical packing morphology.

1.3 Membranes as capacitors

In mammalian cells, energy is continually spent on pumping sodium cations outside the cell and potassium cations inside the cell. Ionic gradients give rise to electrical transmembrane potentials when a conducting pathway is opened. These electrical potentials drive key biological processes such as the phosphorylation of ADP to ATP.

Table 1: Ionic Concentrations and Equilibrium Potentials for Mammalian Skeletal Muscle

Ion	Extracellular (mM)	Intracellular (mM)	$[Ion]_o/[Ion]_i$	Equil. Potential (mV) *
Na^+	145	12	12	+67
K^+	4	155	0.026	-98

* calculated[2] using Nernst equation at 37°C: $E_K = ((RT)/F) \ln([K]_o/[K]_i)$

Membranes can be regarded as capacitors because in living systems they are continually storing charge. The cell membrane is an effective capacitor not only because of these gradients, but because membranes are thin (40 Å), which leaves a narrow gap between two pools of electrolyte, and have high electrical resistance (10^8 Ω for a Paramecium membrane and as high as 10^{15} Ω•cm for a pure phospholipid bilayer).[2] Capacitance can be modeled using the simple equation for two conducting parallel plates,

$$C = (\varepsilon \varepsilon_0 A)/d \qquad \text{Equation 1}$$

where A is the area of the plates, d is the thickness of the insulator, ε is the dielectric constant of the insulator in between, and ε_0 is the polarizability of free space (8.85×10^{-12} $CV^{-1}m^{-1}$).[2] Membrane capacitance is crucial since the charge that is held gives rise to transmembrane potentials (Table 1) when conducting pathways are present.

1.4 Protein transmembrane cation channels

Potassium channels formed by transmembrane domains of proteins are remarkable in that they have high selectivity over other physiological cations, as much as 10000: 1 for K^+ over Na^+.[3] The voltage-gated potassium channel from the bacterium *Streptomyces lividians*, now called KcsA, is one of the most studied natural potassium channels. A crystal structure of 3.2 Å resolution for this potassium channel has been obtained by MacKinnon and co-workers.[9] Figure 1 represents the orientation of the two transmembrane domains of alpha helices forming the potassium channel in a bilayer, with the narrowest part of the channel positioned toward the extracellular face.[3] Four helices form an aqueous "bowl" in the midplane of the bilayer, the most hydrophobic region. As with other membrane proteins, aromatic residues are found near the membrane-water interface.

Cation selectivity is thought to be attributed to a highly conserved, "signature" pore sequence: Thr-Xxx-Thr-Thr-Xxx-Gly-Tyr-Gly.[10] This sequence is found in the pore helix, before a turn to a Gly-Tyr-Gly sequence.[3] Generally, cation channels in nature were previously considered to stabilize cations in transit by cation-π interactions[11] and/or interactions with carbonyl oxygens.[10]

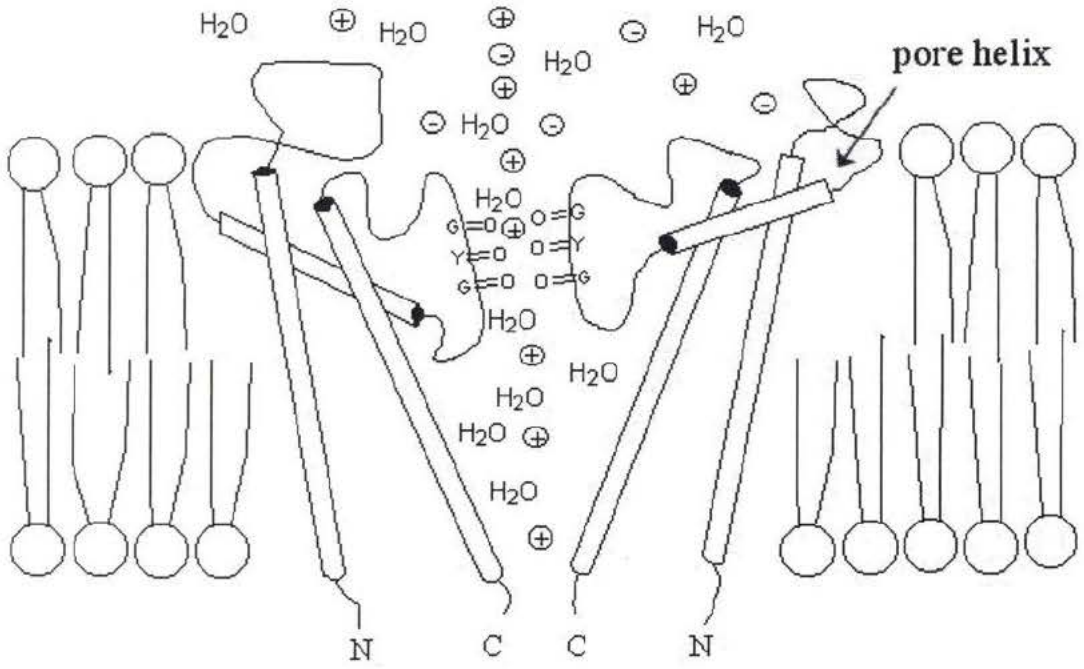

Figure 1: Cross section representing two of the four transmembrane-domains of alpha-helices (depicted as cylinders) which form the *S. lividians* potassium channel[13]

Interestingly, from crystallographic data, the tyrosine residue from the Gly-Tyr-Gly sequence was found to be directed away from the interior of the channel, and the aromatic rings of this particular residue were surmised to be "unable to contribute any cation-π interactions"[3] towards cation stabilization. Although the peptide backbone was not resolved on the atomic scale by X-ray crystallography, the inward positioning of the amide carbonyl oxygens, especially of the Gly-Tyr-Gly sequence, is undoubtedly a critical factor in cation translocation.[3] Below this ionophilic throat region, which has been posed as a "cation selectivity filter," an aqueous compartment opens into the bowl. The aqueous bowl is thought to be critical in stabilizing cations in transit: cations must be hydrated, especially in a hydrophobic environment (amongst acyl chains). In Figure 1, negatively-charged C termini were found to be positioned about the intracellular opening and could provide a stabilizing presence.[3] Only a very few protein structures are

currently available. In the future, data from crystallographic studies such as these will revolutionize what can be known in terms of the chemical structure of a cation channel. However, most of our present knowledge on how cation channels function comes from studies with vastly smaller molecules. Until proteins in their natural state can be readily characterized and are a common occurrence, small molecule studies will continue to provide the most detailed molecular information on cation channels.

1.5 Gramicidin and other naturally occurring ionophilic pore-formers

A range of antibiotic substances, such as Gramicidin A, Amphotericin B, and Alamethicin, have all been demonstrated to form cation-conducting pores or channels.[2]

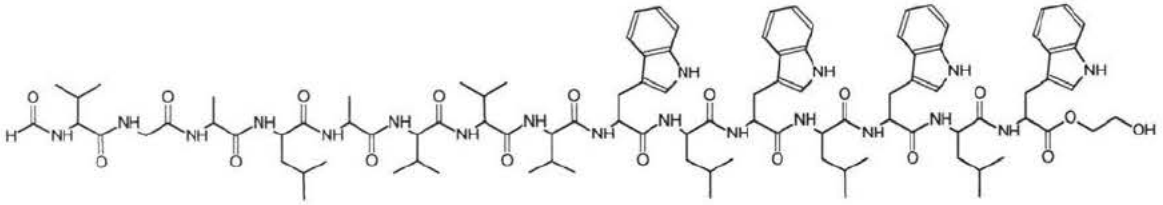

2

Gramicidin, **2**, a pentadecapeptide from the bacterium *Bacillus brevis*, [4] is an example of a cation channel which spans the bilayer by dimerizing through hydrogen bonds in an end to end fashion. Each oligopeptide, composed of alternating D- and L- amino acids, is wound in a β helix, the center of which forms an aqueous pore 4 Å in diameter.[2] Gramicidin exhibits behavior of a water-filled pore[2] and it has been estimated that a single gramicidin channel passes about 10^8 water molecules per second at low ionic strength,[2] with six to ten water molecules within the pore at any time.[2,4] Thus, where water is stabilized, cations are as well. Between two pools of 100 mM CsCl, Gramicidin induces step-changes in conductance of about 30 pS and demonstrates cation selectivity

$Cs^+ > K^+ > Na^+$ [4] with lifetimes ranging from 30 ms to 60 s depending on the electrolyte.[2] Single-channel conductances for the sodium cation are about 15 pS, corresponding to a cation flux of 10^6 to 10^7 cations per second.[5]

In addition to the active gramicidin dimer, other naturally occurring antibiotics utilize aggregates to form cation conducting structures. Whereas the gramicidin dimer is thought to demonstrate true self-association through hydrogen bonding, other antibiotics are thought to "self-assemble" based on the incomplete miscibility[5] of such compounds in membranes. Aggregates of the eicosapeptide Alamethicin are thought to arise as a result of lateral phase separation,[5] resulting in aggregates of varying size as "staves" are inserted into and withdrawn from "the barrel" which forms the aqueous pore. The polyene antibiotic Amphotericin B has a hydrophobic heptaene unit, or lipophilic side, and a hydrophilic, ester-linked polyol chain, or ionophilic edge.[12] Amphotericin B self-associates in a barrel stave fashion, with the least lipophilic, oxygen-enriched moieties directed inward to stabilize cations, and the most lipophilic hydrocarbon part interacting with the non-polar acyl chains of phospholipids. The stability of this pore is thought to depend on the ability of Amphotericin B to bind cholesterol,[5] a prevalent molecule in mammalian membranes. The naturally-occurring ionophores presented serve as models for how aggregation of smaller subunits yields supramolecular cation-conducting structures.

Of particular interest is whether the conductance exhibited by the cation-conducting molecule is rectified. Conductance can be ohmic in character as for Gramicidin (equal amounts of current at both signs of potential), or rectified (i.e. "voltage-gated") as with Alamethicin[5] (greatly diminished current response at one polarity). Rectification can

also arise in mixed electrolyte systems for channels that display cation selectivity (as with Gramicidin, greater conductance for a particular cation over others). In such cases, a non-zero reversal potential is typically produced, manifest as a current-voltage interdependence that does not cross the origin, that is, zero current flows through the conducting pathway at a transmembrane potential significantly offset from zero voltage. As discussed in 1.6.6, the reversal potential is often used as a measure of cation selectivity for synthetic channels.

1.6 Synthetic Cation Channels

From the examples provided by biological systems, cation transport can be divided into five groups based on how the transporter functions. Bimolecular channels (1), such as Gramicidin dimers, are able to span the bilayer. Aggregates of oligopeptides (2) act as cation channels in biological systems. In vertebrates, invertebrates, plants and bacteria, the functional potassium cation channel is a tetramer.[13] In the *Streptomyces lividians* channel, each of four subunits has two transmembrane α helices connected by a pore region of ca. 30 amino acids.[9] Some additional groups of channels are: carriers (3) which shuttle through the bilayer (Valinomycin), non-peptide aggregates (4) which function by a group of molecules acting in concert to form hydrophilic pores (such as the antibiotics Alamethicin and Amphotericin B), and disrupting agents (5) that create ill-defined conduction pathways (Melittin from Bee venom and other toxins) are also formed. In all these cases, cation channel formation is not typically achieved unimolecularly (with the exception of a very few synthetic molecules). The examples from natural systems suggest that insertion requires that the structure be amphiphilic. One strategy in uncovering new cation channel architectures involves examining

molecules of varying degrees of lipophilicity, to increase the probability of finding the right interplay of hydrophilic and hydrophobic attributes.

The remainder of the introduction will illustrate a trend in achieving cation channel-formation with increasingly smaller molecules, which often times involves aggregation. Aggregation can be achieved either through (1) concerted attractive forces, like hydrogen bonding (self-assembly) or (2) lateral phase separation of the active structure(s) out of the bulk lipophilic phase and into defect phase(s), usually through "incomplete miscibility", as suggested by Yeagle.[5] An increasing number of researchers are designing channel-forming structures using aggregates of small amphiphiles which can work in concert to span the bilayer membrane. Small amphiphiles are of interest because they are typically less intensive to synthesize, and those that actively form channels can elucidate the elementary structural characteristics that are fundamental for channel formation and cation stabilization.

1.6.1 Peptide/crown ether hybrid

Meillon and Voyer[14] designed a cation channel by incorporating a 21 amino acid oligopeptide to serve as a backbone for six 21-crown-7-ether rings (**3**), which could conceptually act as a hydrated pore through the hydrophobic midplane of a bilayer. Since the most stable conformation of **3** is the α helix conformation, this oligopeptide coils to assist in aligning the array of crown ethers.

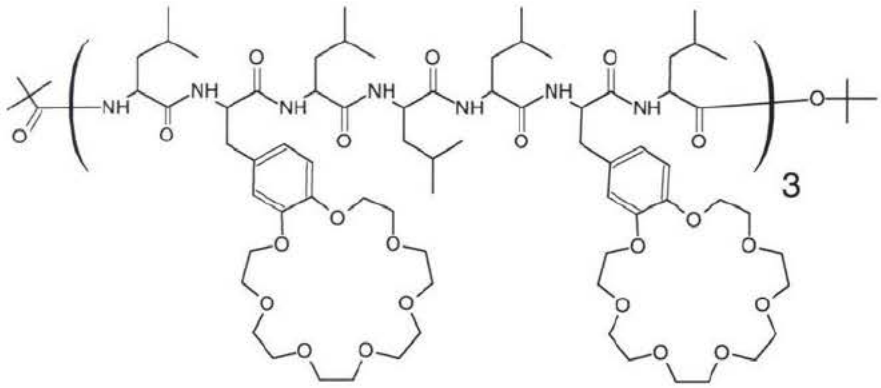

3

In solution with hydrated diphytanoyl phosphatidylcholine (DPPC), this oligopeptide has an IR absorption which correlates with an α helical conformation (1656 cm^{-1} amide I band). Single-channel conductance was examined for **3** using the bilayer voltage clamp technique. In DPPC bilayers using 1M potassium chloride as electrolyte, step changes in conductance of 1 second lifetime for the open state were observed in proportion to a cation flux of 35 pS at + 100 mV.[14] Interestingly, the same experiment conducted using glycerol monooleate (GMO), which has a neutral headgroup, yielded step-changes in conductance of significantly smaller magnitude (10 pS) and lifetime (200 ms). This is indicative of a stabilizing effect from the zwitterionic phosphatidylcholine headgroup. The lower conductivity for the GMO bilayer could imply that cations are not moving as easily into the channels or possibly they are not as well hydrated as in the DPPC bilayer experiments. The shorter lifetime in GMO is evidence that the insertion of **3** is less stable when situated in the bilayer with neutral headgroups, whereas the same molecule in the zwitterionic DPPC bilayer was open five times longer. It is conceivable that lone pairs of electrons on the terminal crown ether oxygens are drawn toward the positive charge on choline, the outermost part of the headgroup presumably exposed to the surface.

However, it is no wonder that insertion of this bulky channel by introduction into the bulk electrolyte was reportedly problematic.

1.6.2 Cyclic peptide tubes: self-assembly of a cation channel

Ghadiri[15] has designed and tested cyclic peptides consisting of an even number of alternating L- and D- amino acids that spontaneously stack in a lipophilic environment.

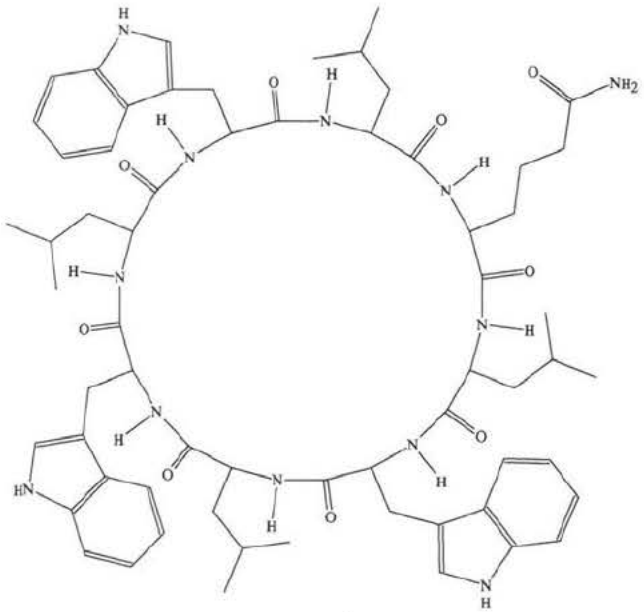

4

The cyclic eight amino acid peptide *cyclo*[-(L-Trp-D-Leu)$_3$ L-Gln-D-Leu] **4** was designed with concentric face-to-face convergence in mind, through hydrogen bonding perpendicular to the concentric rings.[15] The formidable enthalpic contribution of eight hydrogen bonds between each pair of rings holds the tube together, overcoming the entropic cost of aligning the rings linearly. In planar bilayer voltage clamp experiments, this supramolecular cyclic peptide structure yielded step changes in conductance of 55 pS in 500 mM NaCl and 65 pS in 500 mM KCl, but "the single-channel conductance was

shown to be independent of the applied voltage in the range 10-100 mV,"[15] implying that these step changes are not ohmic in character (the term "ohmic" referring to equal current response at both polarities of a given transmembrane potential). In this case, the channel is not acting as a defined resistor at both signs of potential (i.e. not an ohmic conductor).

1.6.3 Diazacrowns as supramolecular structures in cation channels

Gokel and coworkers[16, 17] have investigated diaza-18-crown-6 macrocycles linked by saturated dodecyl chains to form a transmembrane cation-channel. Their approach incorporated diazacrowns to serve as both head groups and as "cation relays" in the hydrophobic interior of phospholipid bilayers. They recognized the potential of the diazacrown architecture as a "flexible framework." The idea was that the structure of these floppy, polar macrocyclic-linked amphiphiles could more readily adapt a membrane-spanning configuration, such as **5**.

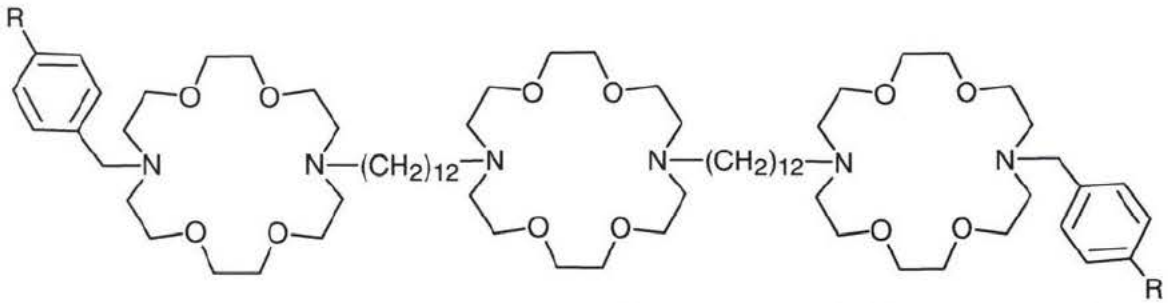

5 R = H, OCH_3, NO_2

The three most active structures in planar lipid bilayer voltage clamp experiments are based on the structure of compound **5**. The single channel conductivity traces from analogs of **5** were reported to be very similar to those observed for peptide channels, with discrete step changes in conductance. Planar lipid bilayers were formed by painting L-α-

lecithin, a soybean lipid mixture with 20% PC.[1] The proton substituted structure exhibits step-changes in conductance with a reported cation flux of 12.8 pS in 500 mM NaCl at a transmembrane potential of ±100 mV,[16] and when the current of single transitions was plotted against the transmembrane potential, a straight line was fitted through them.[1] These step-changes in conductance were ohmic in nature and not rectified.[1] "Very little difference" in cation flux for these three analogs was observed, but open times were reportedly longest of the three for the methoxy substituted structure, and shortest for the nitro substituted. In vesicles, the hydrogen substituted channel was reported to have a relative rate of 38% of the activity observed for gramicidin, whereas the nitro substituted one was 30%, and the methoxy substituted derivative had the highest relative rate of the suite of 10 compounds at 43%.[16]

This supramolecular architecture in **5** was also outfitted with terminal fluorophores to examine how the head groups were positioned in the bilayer. The terminal methoxy(p-phenyl) groups at both ends of the above molecule were replaced with (2(3-N-methylindolyl)ethyl (MeInE) and dansyl (8-(dimethylamino) naphthalenesulfonyl). The dansyl substituted molecule yielded ohmic, non-rectified step-changes in conductance of 9 pS at ± 100 mV in 500 mM NaCl.[17] Fluorescence energy transfer (FET) experiments were performed by employing a doxyl substituted phosphatidylcholine, which bore a nitroxide radical. The energy transfer takes place when the indole and naphthyl moieties fluoresce and this radiation is absorbed or "quenched" by the unpaired electron of the nitroxide radical. This quencher was covalently attached to the middle of one of acyl chains of the phospholipid. It was concluded from these FET experiments that the active structure was monomeric and that the fluorophore was approximately 14 Å from the

middle of the bilayer,[17] which by their calculations puts the headgroup at the surface if the bilayer was 30 Å thick.

The question of whether variations in transport efficiency were based in the solubility differences of the candidate ionophores in bilayers was tested by performing partitioning coefficient experiments between octanol and water. It was observed that these compounds all favoured the hydrophobic solvent by a factor of greater than 10^{10}.[16] Therefore, the hypothesis is not supported by this observation, even though there is quite a leap structurally between octanol and phospholipids. The step-changes in conductance are support for the validity of future analogs to be designed around the diaza-18-crown-6 moiety.

1.6.4 Bola-amphiphiles

Fyles and coworkers[18, 19, 20, 21, 22] have synthesized bola-amphiphiles, which have been demonstrated to induce cation transport in planar lipid bilayers and vesicles. A modular "tinker toy" set of macrocycles, linkers and headgroups was used to synthesize a variety of bola-amphiphiles (Compounds **6a** – **6e**). Ion-selectivity through the aggregation of pore-formers was to be achieved by modifying the central linkage unit of previous bola-amphiphiles designs (not presented here). The linker was shortened and the number of functionalities present was decreased[18] to effect a shorter, more slender molecule more conducive to aggregation (**6a** – **6e**). The suite of compounds was demonstrated to be considerably more active than previous bola-amphiphiles[18]. The dianionic bis macrocyclic pore former **6a** induced ohmic step changes in conductance in planar lipid bilayer voltage-clamp experiments.[19] Compounds **6a** through **6e** were made increasingly hydrophobic by substituting ether oxygens in the macrocycle with

methylenes (M), and ester linkers with thioethers (L). These modifications in compounds **6b** to **6e** decrease the number of direct donor interactions with cations in transit.[20] Additional modifications include overall length of the bola-amphiphile (**6c** is three atoms longer than **6b**, while **6d** is one atom shorter) and conformation (**6a** through **c** prefer an extended conformation while the thioether linked bola-amphiphiles adopt a "U" conformation.[20]

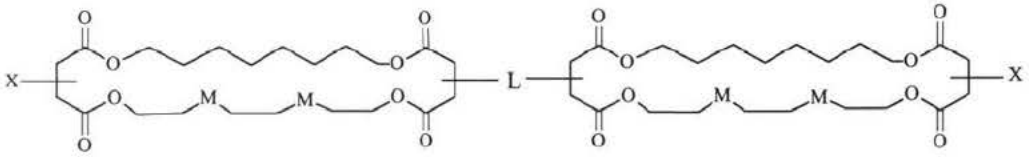

6

	6a	**6b**	**6c**	**6d**	**6e**
L	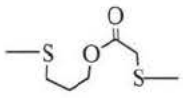	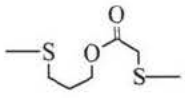	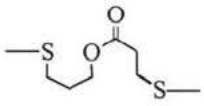	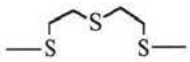	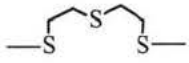
M	O	CH_2	CH_2	CH_2	CH_2
X	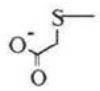		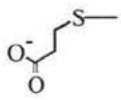		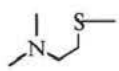

The bola-amphiphile **6a** is cation selective in the order $Cs^+ > K^+ > Na^+$, and yielded specific conductances of 33 pS (Cs^+), 14.3 pS (K^+), 9.9 pS (Na^+).[19] The uniformity of these step-conductance changes from voltage clamp experiments imply an ordered, symmetric (uniform) active structure.[18] The active model for **6a** was surmised to be an aggregate of "a few" molecules.[19] It was concluded that the ion selectivity of **6a** was consistent with the negative head group charge.[19] The cesium cation has the most diffuse surface charge[19] and is the least solvated, hence it is the least restrained passing by the anionic carboxylate headgroup of **6a**.

The greatest difference observed in vesicles between **6a** and analogs **6b** through **6e** is that the former has a kinetic order of nearly two while the later four analogs all have a kinetic order of approximately one (exponential). Analogs **6b** and **6c** yielded the unprecedented "shark fin" type of event in planar bilayer voltage-clamp experiments,[20] which is distinctly different from a normal "square top" step-change in conductance.* Shark fin type events are exemplified by a sudden rise from the baseline to the "active" conductance level, followed by a prolonged deterioration in conductance as the channel gradually closes (over several seconds) to the baseline "zero" conductance level. This type of closing is genuinely different as it is definitely not a discrete transition as typified by previous cation channel behavior. Shark fins were concluded to be an artifact of the opening and closing processes of these bola-amphiphiles.[20]

Compounds **6d** and **6e** were reportedly difficult to examine in planar bilayers as they provoked bilayer breakage. Interestingly, compound **6d** promoted metastable sharkfins, typically 10 seconds in duration or longer. Some of these sharkfins lost their discrete transition appearance in opening, and have the appearance of "humps" of current in the current as a function of time trace. The shark events were shown to be voltage dependent: opening rise time and duration of the events decreased at lower transmembrane potentials, although maximum amplitude varied widely (4 pA to 15 pA at a transmembrane potential of 120 mV). Fyles and coworkers concluded that an aggregate of "U" shaped monomers could provide the active structure.

The headgroups of the bis-macrocyclic structure of **6a** were modified to increase the molecular dipole of a known channel-forming architecture. The asymmetric headgroups of analogs **6f** and **6g** were shown to exhibit voltage gating behavior. Macroscopic

* see Figure 8, page 42 for a typical "square top" step-change in conductance

currents promoted by a large population of channels formed by **6f** in planar bilayer voltage clamp experiments were analyzed to examine the voltage gating behavior of this analog. A voltage ramp-potential was applied (-100mV to +100mV). Significant levels of current were observed only at *cis*-negative potentials over a period of 10 to 15 minutes.[21]

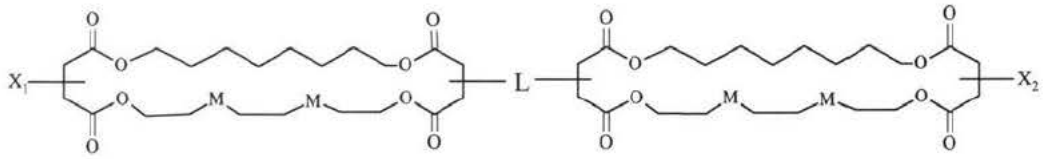

6

	L	M	X_1	X_2
6f	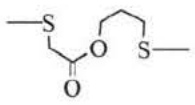	O	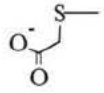	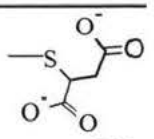
6g	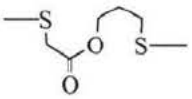	O	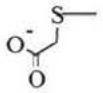	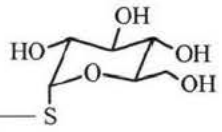

After this period, the rectified behavior of **6f** diminished until current was carried at both negative and positive potentials.[21] The analog **6g**, substituted with thioacetate at one terminus and thioglucose at the other, demonstrated a nearly linear current-voltage response. This ohmic response for **6g** was attributed to random lateral orientation in the bilayer, whereas this random positioning was evident for **6f** only after a period of 10 to 15 minutes. The hypothesis for **6f** was that this compound was positioning itself across the bilayer with the succinate group (X_2) directed towards the side of introduction, which was cis. This is consistent with the succinate group being more polar than the thioacetate terminus (X_1), since this group presents a higher energy barrier in "flip-flopping" to the opposite side as the compound diffuses through the bilayer. Interestingly, in experiments

when **6f** is added to the other side of the bilayer (*trans*), the rectification of the current is reversed, that is, current carried only at *cis*-positive potentials. In either case, bulk current measurements show that channels formed by **6f** initially only permit current to flow in the direction of the molecular dipole, from the single-charged terminus to the more polar succinate terminus of double the negative charge. A linear (ohmic) current-voltage dependence is only observed upon mixing **6f** directly into the phospholipid mixture before bilayer formation, which is consistent with this theory. Although bola-amphiphiles have demonstrated the impressive feat of voltage-gated channel formation, the complexity of the synthesis of such molecules still drastically limits the structural diversity of such bola-amphiphiles, and hence limits the number of possible candidate channels that can be characterized.

Channel forming compounds of lower complexity have been designed and tested. Acyclic bola-amphiphiles, such as the hexaester 7, are directed at finding whether a macrocycle or ionophilic linker is necessary to induce cation transport.

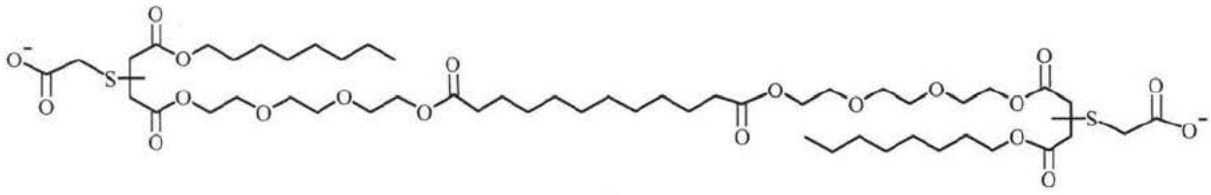

7

The structural fundamentals in forming a cation conducting structure can be elucidated by finding structural elements that still promote cation channel formation. The way to accomplish this most readily is by synthesizing inherently simple molecules. The hexaester bola-amphiphile 7 is essentially **6**, but an ester on each end is lost upon converting the macrocycles to linear chains, and the linker is void of ionophilic moieties. This is an example of the streamlining trend among synthetic ionophore channel

molecules: simplifying structural designs to clarify the fundamentals of channel-forming structural elements. Compound **7** has demonstrated cation transport activity in PC/PA/cholesterol vesicles,[22] but yielded inconsistent activity in planar bilayer experiments. Insertion of this floppy molecule into the lipid bilayer was found to be problematic. Two analogs of this molecule with amides replacing the esters (diamide, hexamide) have been prepared, but to date the hexaester is the most active of these acyclic bola-amphiphiles.

1.6.5 Zwitterionic sterol derivatives

Regen[23, 24, 25] has designed relatively small ionophores around a sterol sulfonic acid derivative with an amide group on the other end linking either a polyamine **8** or oligoether chain **9** terminated with ammonium.

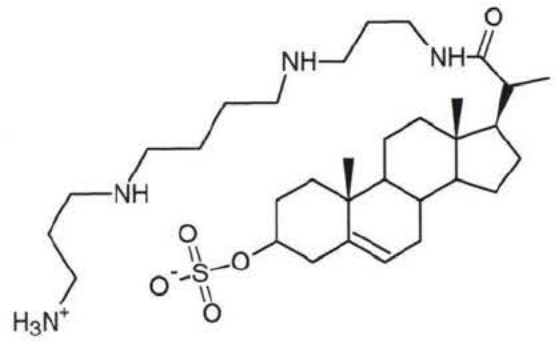

8

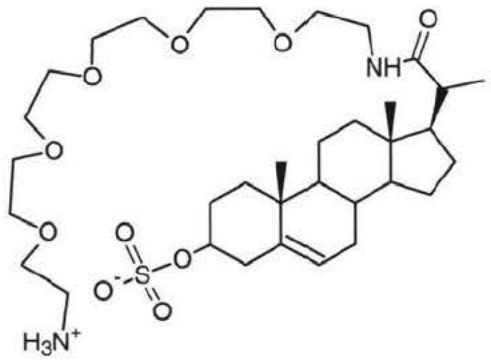

9

This essentially combines a relatively hydrophobic, naturally occurring sterol to anchor the ionophore among the acyl chains of phopholipids with a hydrophilic ion stabilizing moiety rich in electron lone pairs in a molecule of low molecular weight.

These molecules could technically be called zwitterionic due to the ammonium sulfate headgroup, although the ionic charges are literally on opposite covalently bonded ends of the molecules. Regen has been interested in designing mimics of the naturally occurring

heptaene antibiotic Amphotericin B, and the two molecules above indicate a trend to simplify previously active structures that induced cation transport in vesicle experiments. Previous designs were of the same basic structure, with an oligo(ethylene glycol) moiety instead of the sulfonyl moiety of the above compounds.[23]

Ionophore **8** is remarkably similar in structure to squalamine, an antimicrobial sterol found in nature.[24] From ^{23}Na NMR experiments utilizing a membrane-impermeable shift reagent, ionophore **8** was found to be inactive for sodium cation transport in egg phosphatidylcholine (PC) and egg phophatidylglycerol (PG) vesicles. As Regen notes, if the nitrogens of the polyamine moiety were protonated, there would be a net repulsion between incoming sodium cation and the amines.[25] This compound was found to transport cations by dissipating transmembrane pH gradients imposed on vesicles formed from egg PG vesicles (which has a negatively charged headgroup), but was barely active in the same experiment performed with egg PC vesicles (zwitterionic headgroup, positively charged choline facing outward). Intravesicular pH was monitored with pyranine, the deprotonation of which produces a fluorescing phenolate anion. The sterol ionophore **8** dissipated a pH gradient with 1 mol % of compound following pseudo first order kinetics in fluorescence intensity versus time.[25]

The hypothesis that the enhanced activity of **8** in PG relative to PC is attributed to the insertion stabilized by the close proximity of the zwitterionic headgroup of this sterol to the negatively charged phospholipid headgroup (PG). This implies that **8** is stuck in the PG bilayer deeper than in the PC bilayer, facilitated by a net attraction between lipid and ionophore headgroups instead of a neutral balance of charge resulting from the close proximity of two zwitterionic headgroups. If this hypothesis is correct, the gel to liquid-crystalline phase transition should be perturbed as a result of the close packing of

phospholipid acyl chains being disturbed.[5] Regen *et. al.* examined this hypothesis through differential scanning calorimetry experiments and found that the results were consistent with this theory: "10 mol % of 1 in DPPG significantly lowers the gel to liquid-crystalline phase transition temperature of the main transition (40.7°C to 40.4°C) and eliminates the pre-transition peak".[24] As the authors mentioned, this type of sterol derivative **8** might be applicable as a bactericide since the outer monolayer in bacterial plasma membranes tend to be negatively charged.

The oligoether sterol ionophore **9** was demonstrated by Regen *et. al.* to actively transport sodium cations but was inactive with respect to proton transport. After ^{23}Na NMR experiments with 0.4, 0.6, 0.8 and 1.0 mol % of ionophore **9** in PC vesicles in the presence of extravesicular, membrane-impermeable shift reagent, the rate constants for each run were found to have a second order dependency on the amount of ionophore present (mol %). From these kinetic results, Regen proposed a working model for **9** wherein the thermodynamically favoured species is the monomer but dimers are responsible for transport. To test if this ionophore was active as a membrane-spanning structure and not as a carrier, experiments were performed where the acyl chain length of the PC used to make vesicles was varied. Upon plotting the observed rate constant against the mole percent of **9** for three phosphatidylcholines, the slope decreased by a factor of greater than 300 on going through the series: dimyristoleoyl (C14:1), dipalmitoleoyl (C16:1), dioleoyl (C18:1) phosphatidylcholines (PC)[25]. This is compelling evidence of a channel rather than a carrier mechanism because a channel will have problems spanning the bilayer if it is too thick.

1.6.6 Linear oligoether quaternary ammonium ion pairs

Y. Kobuke and coworkers[26] have designed and tested what are the simplest and arguably smallest published cation channel-forming amphiphiles. Their design strategy centers around a supramolecular approach: a trimethylammonium cation with a 5,10,15,20-tetraoxa-tetracosane tail paired with a hydrophobic carboxylate (**10**), phosphatidic acid (**11**), and a saturated dialkyl phosphate (**12**). Most synthetic amphiphiles have a hydrophobic region to stabilize insertion into the bilayer and a hydrophilic area to stabilize water and cations within the hydrophobic interior of the bilayer. Kobuke achieves both of these attributes in linear pairs of molecules **10**, **11**, and **12**.

The ingenuity and simplicity of using the tetraoxa alkyl substituted ammonium cation as the hydrophilic cation-stabilizing half, drawn into the interior of the bilayer by a saturated, hydrophobic counteranion, has been shown to form a cation channel-forming structure in bilayer voltage clamp experiments. The facile syntheses of these amphiphilic ion-pairs allow a "mix and match" approach of combining several ions and counterions to find the right degree of lipophilicity.

10

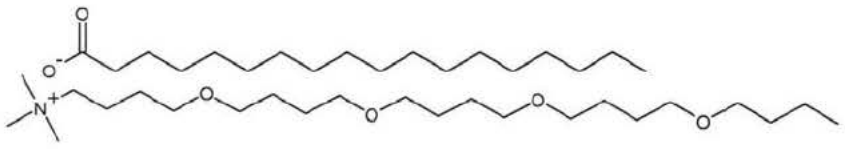

11

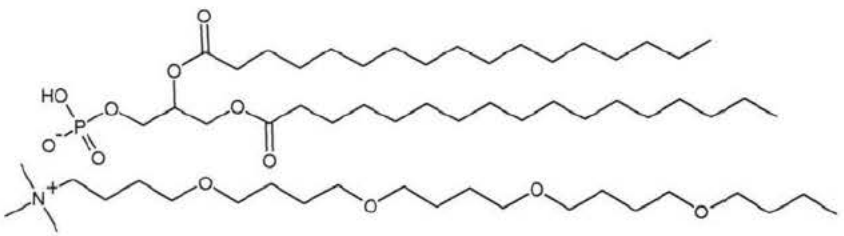

12

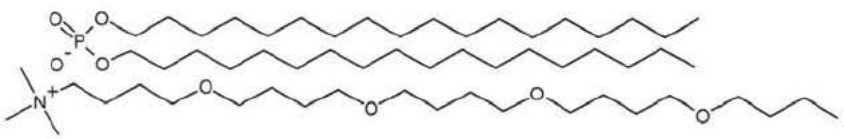

If several quaternary ammonium ions and several phosphate or carboxylate derivatives were available, a mix and match pairing survey could be performed to maximize the diversity of the amphiphiles examined with minimal effort. Planar lipid bilayers were formed from soybean lecithin in n-decane. The amphiphilic ion pair **10** above employs a stearate as the counteranion with a saturated alkyl tail. Although it was reported that "successful observations were limited," this ion pair induced ohmic, non-rectified step-changes in conductance of 7.2 pS in 500 mM KCl [26] with 10 - 30 ms open times (but was reportedly in the "open" state 30% of the time). Pair **11** shows the same quaternary ammonium oligoether paired with naturally occurring phosphatidic acid as the counter anion. This pair yielded less well-defined step changes in conductance with conductivities reportedly varying from 4 to 25 pS. Multiple openings were observed for **11**, not only openings upon openings of the same magnitude but there was also "coexistence of heterogeneous channels".[26] The evidence of varying conductivities under the same experimental conditions suggests that the number of pairs involved in aggregation fluctuates, yielding an ill-defined pore size. The average number of open channels increased with the magnitude of the transmembrane potential. Although the I-V curve was somewhat non-linear, the response was non-rectified, that is not voltage gated.

Ion pair **12** is the same quaternary ammonium cation paired with dioctadecyl phosphate. This ion pair exhibited ohmic, non-rectified step changes in conductance of 10 pS in voltage clamp experiments. A reversal potential was also found for **12**. The reversal potential is the voltage at which zero current flows under a defined transmembrane concentration gradient. A reversal potential of +34.9 mV for ionic pair **12,** showing cation selectivity for the cation over the anion, was obtained by performing an experiment with 100 mM KCl in the *cis* side of the bilayer and 500 mM KCl in the

trans side. A fourth pair employing cardiolipin as the counter anion (not pictured) was found to be completely inactive. The explanation for this inactivity is that the four acyl moieties of cardiolipin effectively "mask" the oligoether tail of the quaternary ammonium.

1.6.7 Simple oligoethers as cation channels

Regen[8] in the early 1990's looked at oligo(ethylene oxide) derivatives for their surfactant properties and use as antimicrobial agents. Only one of the compounds, **13**, examined includes an aromatic moiety. The activity of this surfactant in liposomes of PC and POPC was found to be independent of cholesterol content.[8] This compound was also found to be highly active in lysing human erythrocytes, demonstrating its surfactant property.

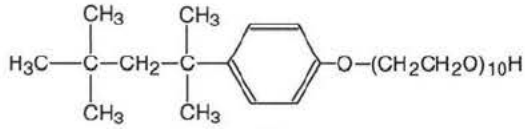

13

Troiano[27] and co-workers have looked at the nonionic surfactant octaethyleneglycol mono *n*-dodecyl ether (so called $C_{12}E_8$) **14** under variable transmembrane potentials in planar lipid bilayers of 1-pamitoyl-2-oleoyl phosphatidylcholine (POPC). They focused on the reduction in transmembrane potential required to cause phospholipid bilayers to either rupture or undergo reversible electrical breakdown.[27]

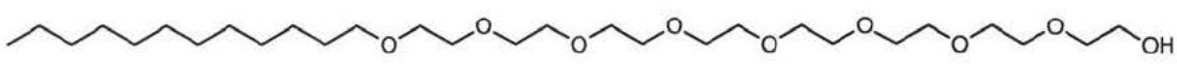

14

For 10 μs pulses, pure POPC ruptured at a mean transmembrane voltage of 450 mV; upon addition of 10 μmol of $C_{12}E_8$ this potential was reduced to 301 mV,[27] one-third less. Although this study is not interested in the rupture of bilayers *per se*, compound **14** is of interest because it is relatively small and has been found to actively insert into phospholipid bilayers.

1.7 Proposed survey of cation-transport capability of ether-isophthalates

The introduction has illustrated a trend in research on synthetic cation channels: increasingly smaller, simpler amphiphiles to the point where the molecules are essentially surfactants. Such small molecules have not previously been considered to be capable of transmembrane channel formation. From the case studies examined in the introduction, cation-channel forming compounds share defining characteristics. All of the compounds discussed thus far have ionophilic moieties which are typically amines, ethers, and carbonyls. Cations need the stabilizing presence of lone pairs of electrons when crossing the hydrophobic interior of the bilayer. Stabilizing cations effectively means stabilizing water, since the cations in transit will never be completely desolvated. Cation channels are always amphiphilic, meaning they have a polar, hydrophilic region and a non-polar lipophilic end, since at least a portion of the molecule must be soluble in the phospholipid bilayer. Lastly, channel-forming compounds are typically conical to columnar in shape. The channel must structurally span the bilayer to some degree and shield cations in transit from the sea of hydrophobic acyl chains which compose the core of the bilayer.

What is to be gained from smaller structures? Regen states that they were seeking the simplest molecules that could form cation channels and thereby avoid "unnecessary multiplicities in structure."[28] Repetitive structural elements, such as macrocycles, cloud

the issue as to what are absolutely necessary components in the structure of a cation channel. A direct correlation can be derived between structure and function for smaller amphiphiles, whereas this correlation becomes less well-defined for more elaborate molecules. Furthermore, more complicated structures (such as macrocycles) are typically synthetically more intensive. Most chemists will agree that the more involved the synthesis is for a class of candidate channels, the fewer the number of compounds that can be produced in the same time. Therefore, the synthesis of more elaborate structures inherently limits the diversity of the analogs to be examined. Self-assembly of a number of smaller molecules to achieve a cation conducting structure could very well be more efficient than producing the equivalent channel with a synthetically intensive, unimolecular transmembrane structure. Kobuke has already demonstrated the advantages of self-assembling simple ionic pairs of amphiphiles to achieve cation-conducting structures.[26,29,30] Insertion of smaller amphiphiles should be easier from the standpoint that there should inherently be less phospholipid packing disruption upon insertion of a scaled-down structure. If a supramolecular structure can be promoted in the bilayer through non-covalent interactions, this may be easier than the insertion of a unimolecular structure, and therefore smaller amphiphiles should have some advantage in being readily incorporated into phospholipid. Even though there is an entropic cost in the organization of a supramolecular structure, there can be an overall energetic savings in a spontaneously forming superstructure.

The overall objective of this project was to survey ether derivatives of isophthalic acid (abbreviated as ISA) by both planar bilayer voltage-clamp experiments and pH stat vesicle experiments. "ISA" will refer to the diacid and "isophthalate" will be used to refer to the predominantly dicarboxylate (deprotonated) form. These are suitable

compounds for examination as cation channels. The reasoning that these compounds are worthwhile for such a survey is fivefold. In general, isophthalates: (1) have amphiphilic character and therefore are complementary to the phospholipid environment, (2) are conical to columnar in shape, (3) have an ionophilic ether moiety and an aromatic ring, which could stabilize cations in the hydrophobic interior of the bilayer, (4) are easily synthesized and (5) have previously been demonstrated to hydrogen bond in the solid state[31-33], in 2D crystals [34,35], in toluene [36,37] and in basic aqueous phase[38]. Two key intramolecular interactions, strong hydrogen-bonding and weak van der Waals interactions (alkyl chain crystallization), were manipulated to investigate the self-assembly process.[36]

The ether isophthalates examined were originally synthesized by Dr. Müllen's group at the Max Plank Institut für Polymerforschung (MPIP) in Mainz, Germany. These compounds were originally synthesized to study properties such as their ability to self-assemble in the solid state[34,35,37,39,40] and their liquid crystalline behavior.[32,39] The suite of molecules were found to have an "adjustable balance" between polar and apolar interactions as alkyl length was varied.[39] Scanning Tunneling Microscopy (STM) was used in solvent codeposition studies of these compounds.[34] 5-Monoalkoxy isophthalic acid (ISA) derivatives, C_{12}ISA, C_{16}ISA, C_{18} ISA were found to form ordered monolayers upon physisorption from 1-phenyloctane at a liquid/graphite interface.[31,34] In both 2D and 3D structures, the pure acid of the monoalkyl C_{16}ISA derivative was found to form closely packed, interdigitated arrays of hydrogen-bonded ribbons.[31]

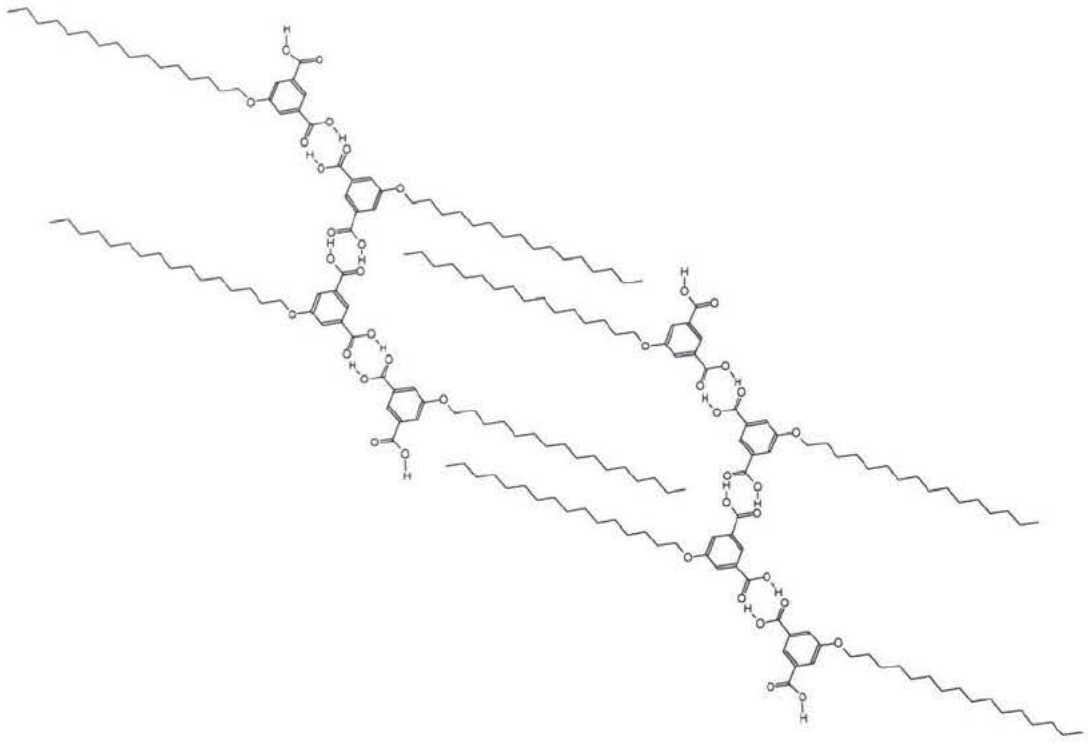

Figure 2: Representation of a two-dimensional slice from a crystal structure of C_{16}ISA

In the 3D structure, two sets of planes were observed: hydrogen bonded strands in one plane and alkoxy chains in the other, meeting at an angle of 51°.[31] Figure 2 represents a two dimensional projection from single-crystal X-ray analysis in which the hydrogen-bonded strands are in the plane of the page.[31] The X-ray crystallography allowed Müllen's coworkers to conclude that hydrogen bonding was present not only between neighboring isophthalic acids on the same monolayer, but also with isophthalic acids on the layers above and below.[34]

Solvent codeposition was observed when an alcohol (ethanol, 1-octanol, 1-undecanol)[34] was used or when a diamine Lewis base (pyrazine, pyrimidine, 4,4'-bipyridine)[35, 32] was introduced. Upon analysis, 5-octadecyloxy isophthalic acid

and 1-octanol were found to be interdigitated,[34] indicating a close, ordered interaction between carboxyls and hydrogen bond formation.

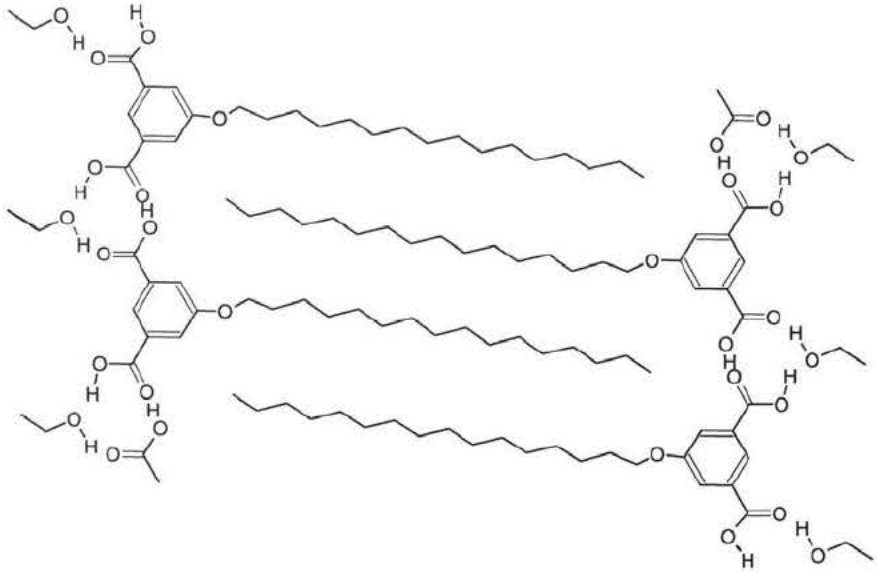

Figure 3: Hydrogen-bonded sheet structure of C_{12}ISA· EtOH solvate[35]

Molecular sheets of C_{12}ISA crystallized from ethanol (Figure 3) were found to form molecular ribbons similar to the sheet motif observed for the C_{16}ISA· pyrimidine solvate.[35] One molecule of ethanol is inserted in between the hydrogen-bonded strands of ISA to yield cross-linked "ribbons" (projection on plane of sheet in Figure 3). The ethanol-solvate ribbons are not flat, but have an angle of ca. 35° [35] between the plane of the hydrogen-bonded chain and the plane of the alkoxy groups.

Interdigitated solvated crystal structures were obtained using Lewis bases, such as pyrazine and pyrimidine, as hydrogen bond acceptors. The crystal structure analysis of the respective ISA solvates has led Müllen's coworkers to conclude that these diamines

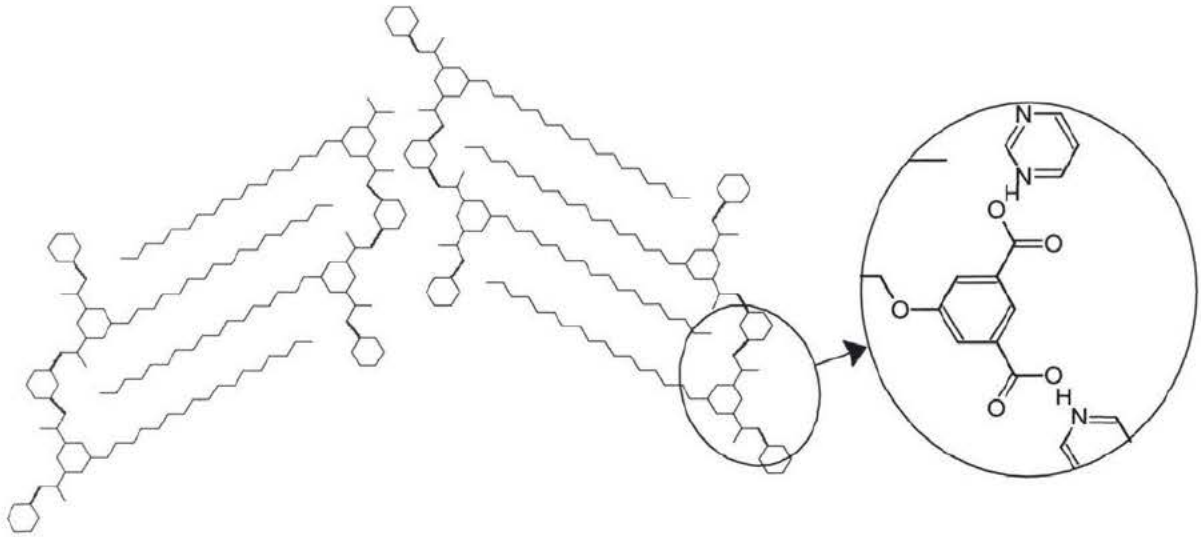

Figure 4: Interdigitated solvated molecular ribbons of C_{16}ISA•½pyrimidine.[35,36]

increase the stability of the monolayer.[31] The interdigitated close-packing of the C_{16}ISA· pyrimidine solvate is pictured in Figure 4. In this case, each carboxyl group forms a hydrogen bond to one nitrogen atom of pyrimidine.[36] This hydrogen-bonding motif in conjunction with the crystallization of the alkoxy moieties give rise to ribbon-type structures,[36] which interdigitate in a head-head-tail-tail arrangement[35] to effect a herringbone configuration.[36]

The pyrazine solvate of a monoalkoxy ISA derivative forms a cross-linked array of ribbons of interdigitated chains as illustrated in Figure 5[35] to form a more rigid, flatter sheet structure where the phenylene rings of ISA in one hydrogen- bonded plane are coplanar, but form an angle with the plane of the pyrazines.[36]

Intermolecular hydrogen bonding occurs between the hydroxy group of the carboxylic acid of one molecule and the carbonyl oxygen of its lateral neighbour.[35]

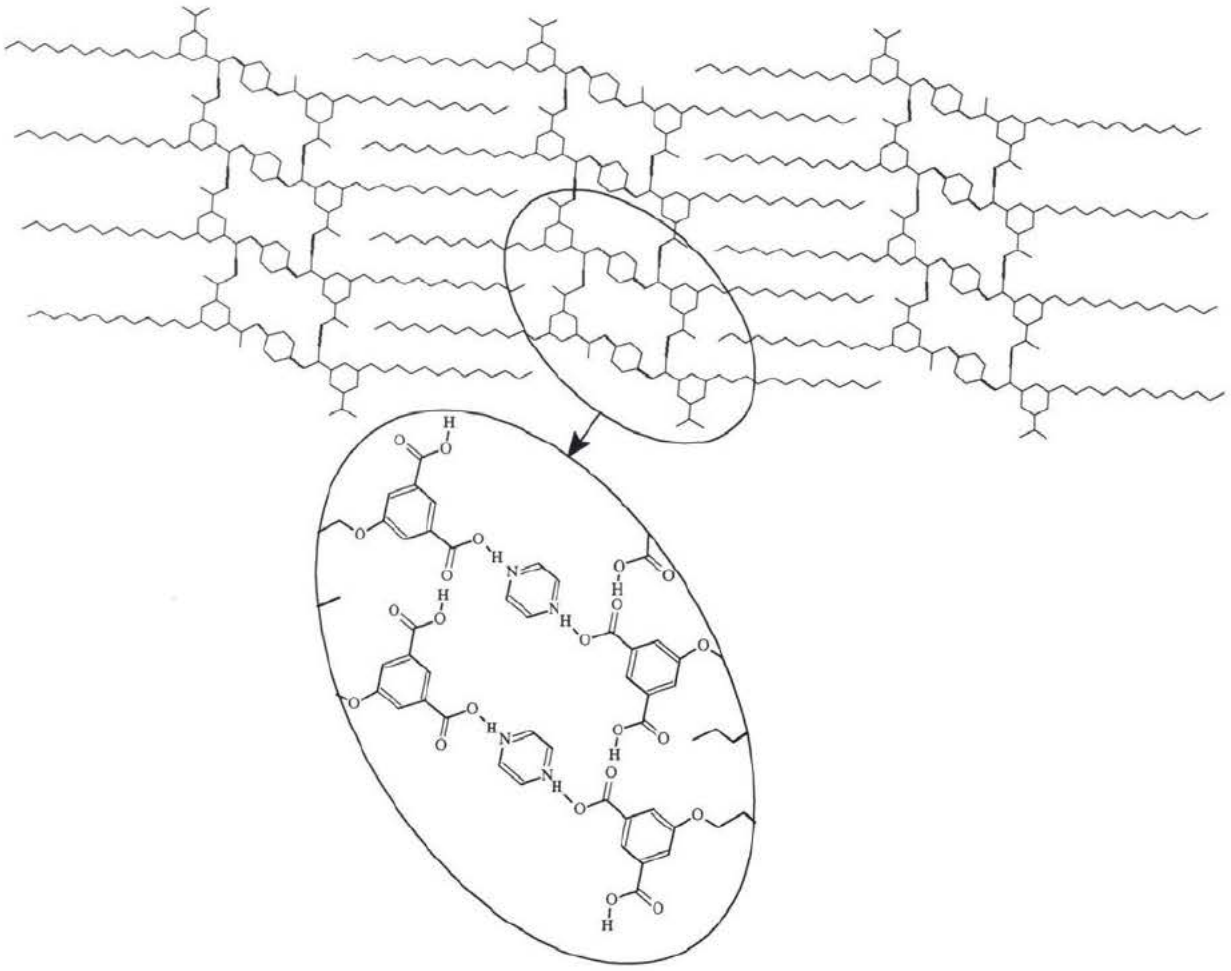

Figure 5: Depiction of cross-linked molecular sheets of 5-dodecyloxy ISA•½pyrazine[35,36]

The remaining carboxylic acids are hydrogen-bonded to the lone pairs of electrons of the aromatic nitrogens of pyrazine.[35] This nearly planar, non-covalent crosslinking yields a supramolecular structure where one of the carboxylic acid groups is slightly rotated out of the plane of the molecule, to effect a staggered layering offset by about half the width of the hydrogen-bonded double strand in the alkoxy direction.[35] Interestingly, the two dimensional structure for pure monoalkoxy ISA on graphite bears only a small resemblance to its crystal structure, whereas the two dimensional structures for the

supramolecular diamine assemblies on graphite are reportedly identical to the projection planes of the corresponding crystal structures.[36]

The stability of the hydrogen bond and its dependence on molecular orientation can be observed in the infrared spectra.[41] In the pure diacids, absorption is observed at 1686 cm^{-1} indicating dimerization by hydrogen bonding of pure ISA.[35] The IR spectra of hydrogen-bonding by carboxylic acids with aromatic diamines show absorption at 1708 cm^{-1} for the carbonyl[35] and an O-H stretch at 2506 cm^{-1}.[35,41] In all examples with aromatic Lewis bases, an absence of a strong absorption around 1720 cm^{-1} was reported,[35] indicating that carbonyls are not free to absorb IR radiation. The carbonyl absorption of monomeric carboxylic acid is known to occur at higher frequency than the absorption that occurs in hydrogen-bonded structures.[41]

ISA derivatives have been shown to aggregate in solution. An ester ISA derivative, 5(3,4,5 tridecyloxy benzoate) isophthalic acid **15**, has been shown to take on the preferential formation of hexameric aggregates in toluene (above 10 mM).[37]

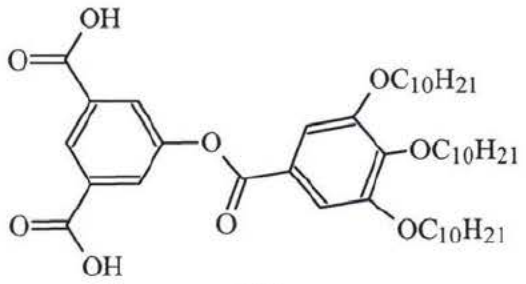

15

VPO measurements carried out in toluene at 40°C with **15** supported the presence of an aggregate of 4600 (benzil standard) to 4900 (polystyrene standard) g/mol.[37] This supports the existence of a hexameric aggregate in toluene. Figure 6 illustrates the

proposed hexamer for 5-decyloxy isophthalic acid as determined from X-ray crystallography.[37] The cavity enclosed by the hexamer is 14Å in diameter,[37] which presents an aperture over three times larger in diameter than the aqueous pore of Gramicidin (which has been estimated to be 4Å in diameter[2]).

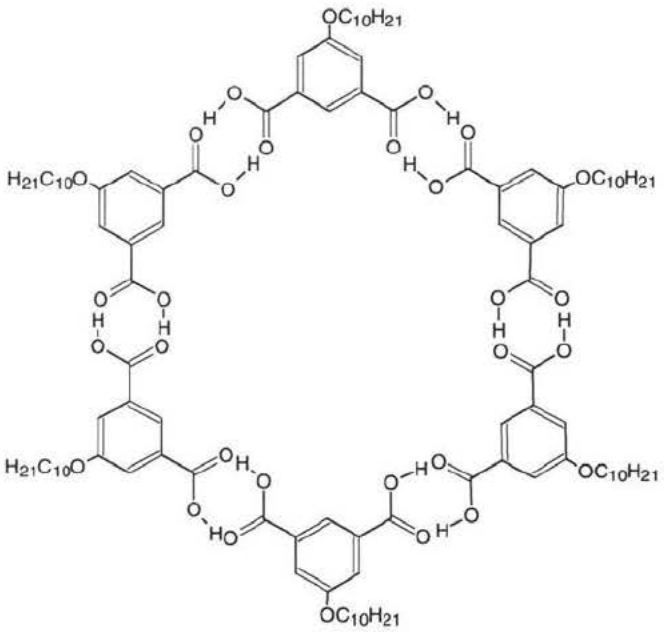

Figure 6: Proposed hexameric aggregate of 5-decyloxy isophthalic acid [37]

Since the isophthalic acids surveyed will be predominantly deprotonated at the pH of the bilayer clamp experiment, evidence of supramolecular assemblies of isophthalates (the predominantly deprotonated species) are of the greatest interest. Fibrous precipitates of partially neutralized ISA's had previously been investigated by SEM,[40] or Scanning Electron Microscopy. "Blob" structures were observed in the aqueous phase from 5-octadecyloxy ISA (150 mM) which had been neutralized with 1.5 equivalents of potassium hydroxide.[38] Formation of supramolecular structures was promoted by repeated heating and cooling cycles of the solutions.[38] Agglomerates of lath-shaped crystals were observed by TEM (Transmission Electron Microscopy). From TEM and electron diffraction studies, the precipitates observed were concluded to be single crystals

where the molecules adopt a layer structure[38] and not "fibers". Wide-angle X-ray diffraction studies indicate one crystalline species and a triclinic alkyl chain packing.[38] The crystal packing motif derived from X-ray and Electron Diffraction Studies is illustrated in Figure 7.[38] This type of interdigitated packing in aqueous phase is the best evidence that this motif may provide a membrane-spanning structure in planar bilayers or vesicles. Alkyl chain packing has been described as lipophilic,[38] and this is suggestive that these aggregates may truly be lipophilic and soluble in a phospholipid mixture. The potential for controlled aggregation exists, so the investigation of cation channels through aggregation is reasonable.

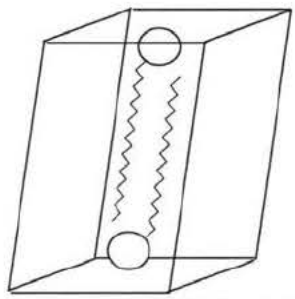

Figure 7: Proposed molecular orientation of C_{18}ISA· 1.5KOH in lath-shaped crystals

1.8 Ether Isophthalates

Fifteen alkoxy derivatives of isophthalic acids were synthesized in Germany under Dr. Klaus Müllen's direction, and were fully characterized in pure and solvated form before sending these compounds (**16** through **30**) to Canada for investigations into the cation-transport activity of these compounds. As far as we know, this is the first research of its kind using isophthalic acids (ISA's) as potential cation channel-forming structures.

There were two goals of this thesis. The principal goal of this research was to assess the cation transport efficacy of alkoxy isophthalic acids in planar lipid bilayers using the

voltage-clamp technique with an emphasis on reliably detecting formation of channels. Due to the number of compounds examined, a survey protocol was implemented (as discussed in 2.2). Once an active compound was uncovered, a secondary goal was to characterize the transport activity. In order to expand the capabilities in this second goal of what can be known about the activity of a channel-forming species from the bilayer voltage clamp technique, homologs were synthesized so that crucial structural elements could be determined (discussed in chapter 3). To clarify what was observed in the first goal, a survey was conducted in liposomes by the pH stat technique (discussed in chapter 4).

Scheme 1 shows the 5-monoalkoxy substituted ISA derivatives available for the project. Compounds **16** through **21** in Scheme 1 and the 4,6 dialkoxy derivatives **22** through **24** in Scheme 2 are arranged by increasing alkyl length. As the alkoxy moiety is lengthened, the balance between polar and non-polar attributes is shifted. In surveying these molecules, the right combination of these attributes will yield a lipophilic structure, the first step in becoming a functioning cation channel. The candidates are divided into 3 groups based on substituents and overall molecular shape: alkoxy (Scheme 1), dialkoxy (Scheme 2), and rigidified naphthyl, fluorinated, and diazacrown substituted (Scheme 3).

16

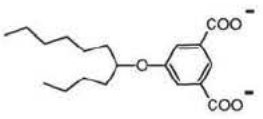

17

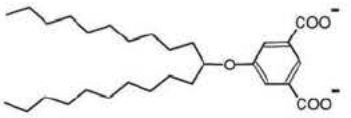

18

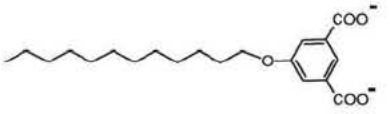

19

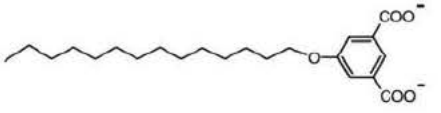

20

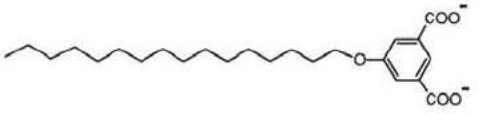

21

Scheme 1: 5-Monoalkoxy isophthalates

Isophthalates are quite amphiphilic at the pH of the bilayer clamp experiment. Compounds **16** and **17** are mono-alkoxy substituted, but the ether linkage is in the middle of the alkyl chain, which could provide the molecule with more nonpolar character than the other *n*-monoalkoxy derivatives and a more columnar morphology than the other mono-alkoxy homologs (**18** through **21**). The isophthalates in Schemes one through three are predominantly deprotonated at the pH of the electrolyte in the voltage clamp

experiment. The pKa values for a typical isophthalate **17** have been estimated to be 4.4 for the first carboxylate (pKa_1) and 3.4 for the second (pKa_2) using the ACD/I-Lab web service.[42] This pKa prediction assumes zero ionic strength. However, the pKa value change will be rather small for a change in ionic strength.

Above pH 5, the isophthalate is present predominantly as the dianion, and in this form will have the greatest charge on the headgroup. This is not only important in maximizing the solubility in phospholipid, but also to ensure that the channel is as water soluble as possible so that it does not precipitate from solution once introduced.

22

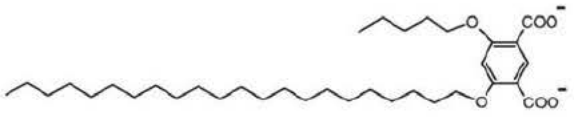

23

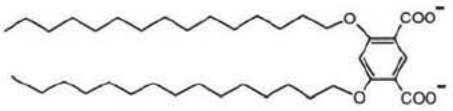

24

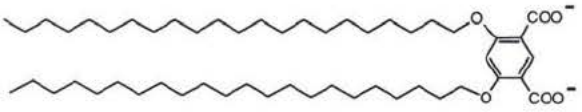

Scheme 2: 4,6-Dialkoxy isophthalates

The dianionic isophthalate can be expected to have a driving attraction to positively charged choline of PC and thereby aid in inserting into the bilayer, especially when the hydrophilic alkyl tail would prefer to be in a hydrophobic environment. The overall conical geometry of the mono-alkoxy derivatives can be alluded to as amphiphilic "nails," and may have an advantage in incorporating into phospholipid bilayers over the

dialkoxy *meta* substituted isophthalates in Scheme 3 which are relatively splayed and more columnar in shape.

The naphthyl and partially fluorinated ether isophthalates in Scheme 3 have an element of rigidity that is not present in the saturated hydrocarbon counterparts in Schemes 1 and 2.

25

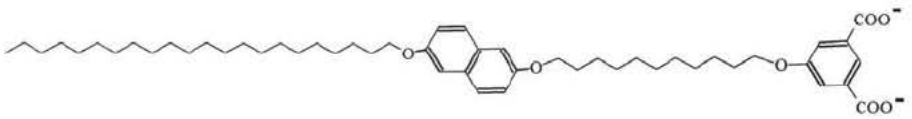

26

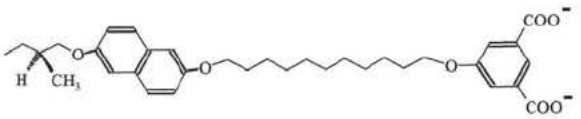

27

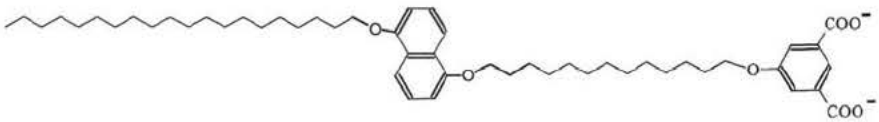

28

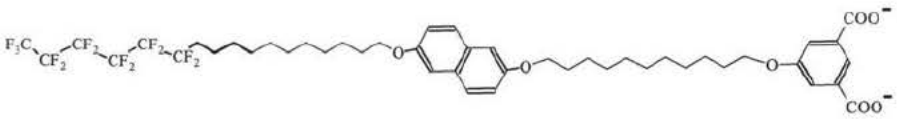

29

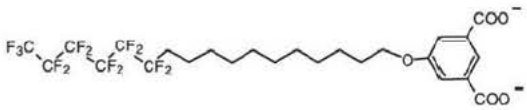

30

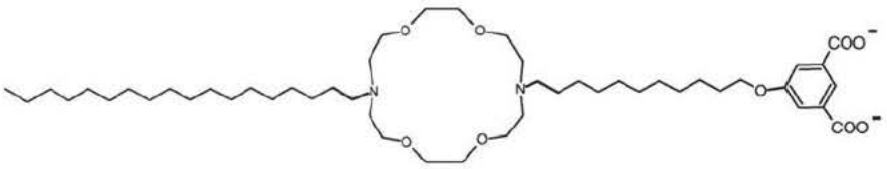

Scheme 3: Naphthyl-, fluoro-, and (diaza-18-crown-6) 5-alkoxy isophthalates

The ether-linked naphthyl substituents of isophthalates **24** to **27** could stabilize cations among the hydrophobic acyl chains through attraction to lone pairs on the ether oxygens and through cation/π interaction. In addition, the conjugated aromatic system of the naphthyl moieties add an element of rigidity to the overall structure, which could aid in aggregation and insertion. If this conjugated aromatic structure were inserted among the acyl chains it could have the potential to disrupt the acyl chain packing of the phospholipid. An isophthalate with an alkoxy-linked diazacrown (**30**) was examined to see if this scaled down derivative of Gokel's tris-diaza architecture could induce cation transport. Isophthalate **30** is more amphiphilic than Gokel's design, having a dianionic headgroup and a completely non-polar alkyl "tail," which would orient the amphiphile with the isophthalate headgroup adjacent to the lipid headgroups. In light of the hydrogen-bonding evidence and ordered-aggregation in the aqueous phase, these ISA derivatives provide a range of hydrophilic and hydrophobic attributes. The right combination of lipophilicity, ionophilic moieties, and supramolecular organization should yield a well-defined cation-transporting structure.

Chapter 2: Survey of cation transport activity of isophthalate derivatives using the bilayer clamp technique

2.1 Bilayer voltage-clamp technique

The bilayer voltage-clamp simulates the transmembrane potentials that occur across biological membranes by applying a transmembrane voltage across a solvated, proteinless membrane, or bilayer. Bilayers were formed in decane across a 0.25 mm aperture, positioned between two pools of alkali salt electrolyte. Since the transmembrane potential is applied through electrodes to the two pools, a cation gradient is not essential to the experiment.

The experimental setup for the voltage clamp experiment is represented as a block diagram in Figure 8. The Delrin™ (polyacetal) cell has two cylinders carved out which are partially overlapping; into one of these cylinders a bilayer cuvette (polystyrene or polyacetal) is inserted. In the side of the cuvette there is a thin region with a 0.25mm diameter hole. This is the hole over which the bilayer is formed. The cuvette (*trans*) and the empty cylinder of the cell (*cis*) are filled with 1M electrolyte to equal levels so as not to create a pressure gradient. As shown in Figure 8, electrical contact to the bilayer clamp is made from each pool of electrolyte by silver/silver chloride electrodes, which meet 3M agar salt bridges in 3M wells of the respective salts. These bridges are employed to minimize liquid-junction potentials.[43]

The amount of current passed from a single-channel conductance is extremely small, on the scale of several picoamperes (pA). For this reason, it is imperative that the bilayer is an effective insulator before introducing an ionophore. Furthermore, the bilayer cell needs to be isolated from the lab environment to inhibit electrical and vibrational noise.

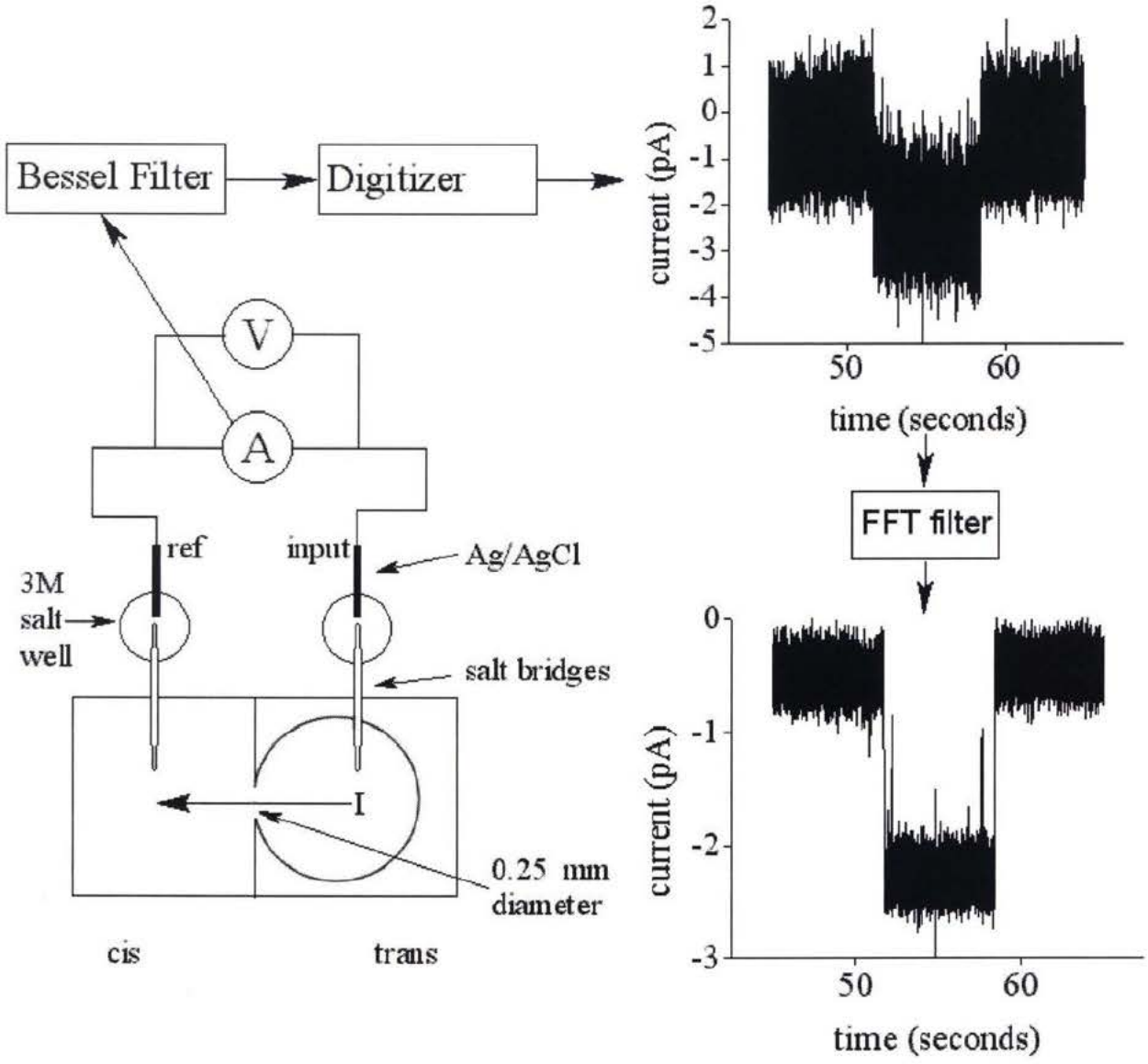

Figure 8: Diagram representation of a bilayer voltage clamp experiment and the flow of data, illustrating the effect of 100 Hz lowpass filtering on a step conductance change.

The cell was placed inside an aluminum Faraday cage to shield the bilayer from external electromagnetic noise. The cage acts as an antennae which grounds externally generated electromagnetic radiation and prevents it from being manifest in the measurement (current). The cage floats atop a pneumatically-stabilized table to minimize the transfer of vibrations from the building to the electrical signal.

The only buffer in the electrolyte used for bilayer clamp studies is bicarbonate due to absorption of atmospheric carbon dioxide, therefore the pH will decrease somewhat over the life of the solution. Freshly made 1M KCl was found to have a pH of 5.4, whereas the same solution sitting for over two months had a pH of 5.1. The potassium chloride solution used in the bilayer clamp experiments was freshly made every ten days to two weeks. One molar cesium chloride and sodium chloride solutions had much longer lifetimes. Both of these solutions were at pH 6.4 after eight months storage. At these electrolyte pH's, isophthalates can be said to be predominantly in dianionic (dicarboxylate) form.

Bilayers were formed across the aperture (0.25 mm dia.) in the cell. Bilayers were formed between the two pools of electrolyte by either painting or dipping. Bilayers were painted with a 10/0 camel hair brush that had been mostly trimmed around the base. PTFE tape was used to wrap the base of the brush so that the remaining bristles were slightly splayed. The aperture in the cuvette was prepared for use by applying coats of the 8:1:1 phosphatidylcholine:phosphatidic acid:cholesterol mixture and gently drying under nitrogen. Minuscule drops of lipid mixture were applied in downward brush strokes underwater, with the cuvette inserted into the cell and filled with electrolyte. A signal was observed on the oscilloscope once the phospholipid mixture was plugging the hole. The bilayers were made to thin through successive downward brush strokes. The membrane thins and eventually a planar bilayer is formed, encircled by a torus of decane.[44]

Measuring the specific electrical capacitance of the bilayer is the best method for assessing the condition of the bilayer.[45] The thickness of the membrane is gauged by measuring the capacitance between the two pools of electrolyte across the bilayer. A

sufficiently thin bilayer membrane is critical to the outcome of the experiment because if the membrane is too thick, a cation channel will not be able to span the bilayer and a transmembrane conductance will not be observed. The capacitance measured is a function of both thinness and area. The bilayers used in the survey were 200 to 220 pF in capacitance. If the solvent annulus is assumed to be small, the capacitance can mostly be attributed to the thickness of the membrane and not the area. In addition to gauging the thickness of the bilayer, the shape of the "square wave" used to measure capacitance is used to assess the stability of the bilayer. The tops of the square waves should appear parallel for a stable bilayer. Sloped square waves indicate a bilayer which is deteriorating and/or not uniform. This type of bilayer was not used for experiments.

After phospholipid had been introduced to the system, solvated phospholipid monolayers formed on the surface of the electrolyte. From this state, bilayers could be formed by opposition of monolayers, or the "dipping" technique. The cuvette was *gradually* lifted, to draw the aperture through the air water interface, and then slid back into place. This was repeated several times until a signal was observed on the oscilloscope. The dipping technique readily produced high capacitance bilayers. The technique was often used in conjunction with brushing: bilayers were formed by dipping, and if the capacitance was inadequate the membrane was thinned by brushing.

Once a bilayer of sufficient transmembrane capacitance was formed, the bilayer was examined for electrical leakiness to assess the uniformity of the membrane and how well it was forming a seal between the two aqueous compartments of electrolyte. To assess leakiness, a continuous transmembrane potential (typically $\pm$ 100 mV) was applied over a period of 40 minutes and polarity was switched every 10 minutes. The bilayer clamp applies a continuous transmembrane potential and measures the resulting current. At *cis*

negative potentials, current travels through the membrane from *trans* to *cis*, as shown in Figure 8. The baseline signal, which is current as a function of time, is examined to make sure that the bilayer has been an effective insulator throughout the 40 minute baseline period. A few (two to five) very small spikes (0.1 to 0.3 pA in magnitude) are typical. Bilayers which exhibited more than one spike greater than 0.4 pA in magnitude over 40 minutes of baseline were not used.

The occurrence of single-channel conductances as a function of time is a stochastic process. The number of channels open at a given time is a completely random affair, since the number of channels actively conducting is varying from moment to moment.[43] Stochastic refers to the probability of a given integral number of occurrences (from the Greek *stochastikos* ("skillful in aiming"): involving chance or probability, probabilistic [46]). Since channels are discrete molecules or discrete aggregates of molecules, the population of channels in the "on" state in an area of the bilayer will continually fluctuate,[2] even at so-called "equilibrium," therefore the occurrence of single-channel conductances is a random phenomenon. At any given time an integral number of channels will be "on." For a given amount of time, all-points histograms can aid in determining what the mean current levels are. The probability of a given level being in the "on" state will be proportional to the relative populations of the respective distributions for the time period. Therefore, all-points histograms are commonly used to find what the predominant levels are, how the populations are distributed about the means, and what the relatively probability is for a given integral number of occurrences.

2.2 Survey Method

The survey was designed to find compounds which induced cation channels. Due to the relatively large number of compounds to be examined by these techniques, it was imperative to adopt a survey protocol to ensure reproducibility. That is, experimental variables, such as lipid preparation, salt type, buffer, cleaning regiment, were held as constant as possible so that results from day to day could be compared reliably. Bilayers used in the survey were formed using a mixture of 8:1:1 PC:PA:cholesterol. Consistency from one bilayer to the next was important to make sure that the 15 candidate channels examined were given an equal chance to exhibit activity in the bilayer voltage-clamp experiment. All compounds were introduced at a stock solution concentration of 1.4 mM. Those that were not soluble in methanol were brought into solution in DMSO. The experimental candidates were each given at least three independent experiments to induce activity. If activity, however irregular, was observed for any one of the three experiments, the candidate was given additional trials. Solutions of the candidate channels were injected on the *cis* side of the bilayer, ten microlitres at a time, as closely as possible to the bilayer without rupture. Consecutive aliquots were injected on the *cis* side every ten to fifteen minutes. Active compounds usually induced activity by the second or third injection. The candidate channel had to demonstrate the same type of well-defined activity over several experiments to be deemed as "active."

Given the challenges of stable bilayer formation, many electrophysiological researchers employing the voltage clamp technique focus on a single compound, adjusting experimental variables (phospholipid mixture, method of compound introduction) until some sort of activity is observed. This activity may not be well-defined and may appear to the outside observer as an irregular signal, but since they are

working with one candidate over a large number of experiments, even an irregular signal is eventually characterizable (as discussed in the next section). This is *not* the case in this survey. Only well-defined step changes in conductance are addressed in this thesis.

With the format of the survey as presented, there is an inherent tradeoff in the bilayer clamp experiment. Not every active compound in the suite will be active with the concentration, experimental time, candidate injection method, and lipid mixture used in the survey. A few channel compounds *may reliably* be discovered under the survey, and these results *will be directly comparable* as the data were collected under the same conditions. The conditions of the survey are not varied for each compound until some sort of activity is observed since this traditional approach is impractical for such a large number of compounds.

2.3 What constitutes an observation?

The activity of interest is a well-behaved single-channel transmembrane conductance. Single-channel conductances, like the one shown in Figure 8, can be identified as discrete step-changes in conductance, from one defined conductance level (the baseline, or zero level in this case) to a level where a conducting pathway is actively facilitating the passing of current. The defining act of a cation channel is to allow an electrical current of cations to flow across a membrane.[43] The primary objective is to interpret the observed conductance in terms of function. The record from the voltage clamp yields only one type of information: current amplitude as a function of time. The unitary current of a single conductance is measured as the difference between the "off" state (baseline) and the "on" state (higher conductance level). Under a transmembrane potential, single-

channel activity can be identified as regular, discrete step changes in conductance from a baseline level ("off" state") to state(s) of higher conductance ("on").

Filtering is a tool which aids in clarifying how well-defined a step-change in conductance is. Step-changes in conductance, like the one in the upper right of Figure 8, have the character of a single-channel conductance, but it is not completely clear that a transition is occurring from one level to a new, distinctly different level. Low-pass filtering allows only the most infrequently occurring data to pass through. The current as a function of time signal is filtered to remove high-frequency background noise that is not due to the activity of the channel.[43] The trace in the upper right of Figure 8 has only passed through the 8-pole Bessel filter (1 kHz lowpass), whereas the trace at lower right is the same data passed through another low-pass filter (100 Hz) which utilizes a Fast Fourier Transform (FFT). The step-change in conductance is better defined after filtering away noise (between 100Hz and 1kHz) to visually clarify that a discrete transition from one level to another is being made. Even with filtering, there can still be some ambiguity whether a discrete transition is manifest in the current as a function of time trace. Figure 9 compares four different traces to exemplify what is mean by ambiguous behavior (B) and what is implied by well-defined behavior (D). Three levels of clear single-channel conductances are apparent in trace D.

All of the traces in Figure 9 have been filtered at 100Hz. In A of Figure 9, a section of typical baseline is shown from a DMSO control experiment. Methanol has previously been established as a suitable solvent for introducing candidate channels in bilayer clamp experiments.[12] Control experiments were conducted to verify that DMSO did not promote deterioration of the membrane.

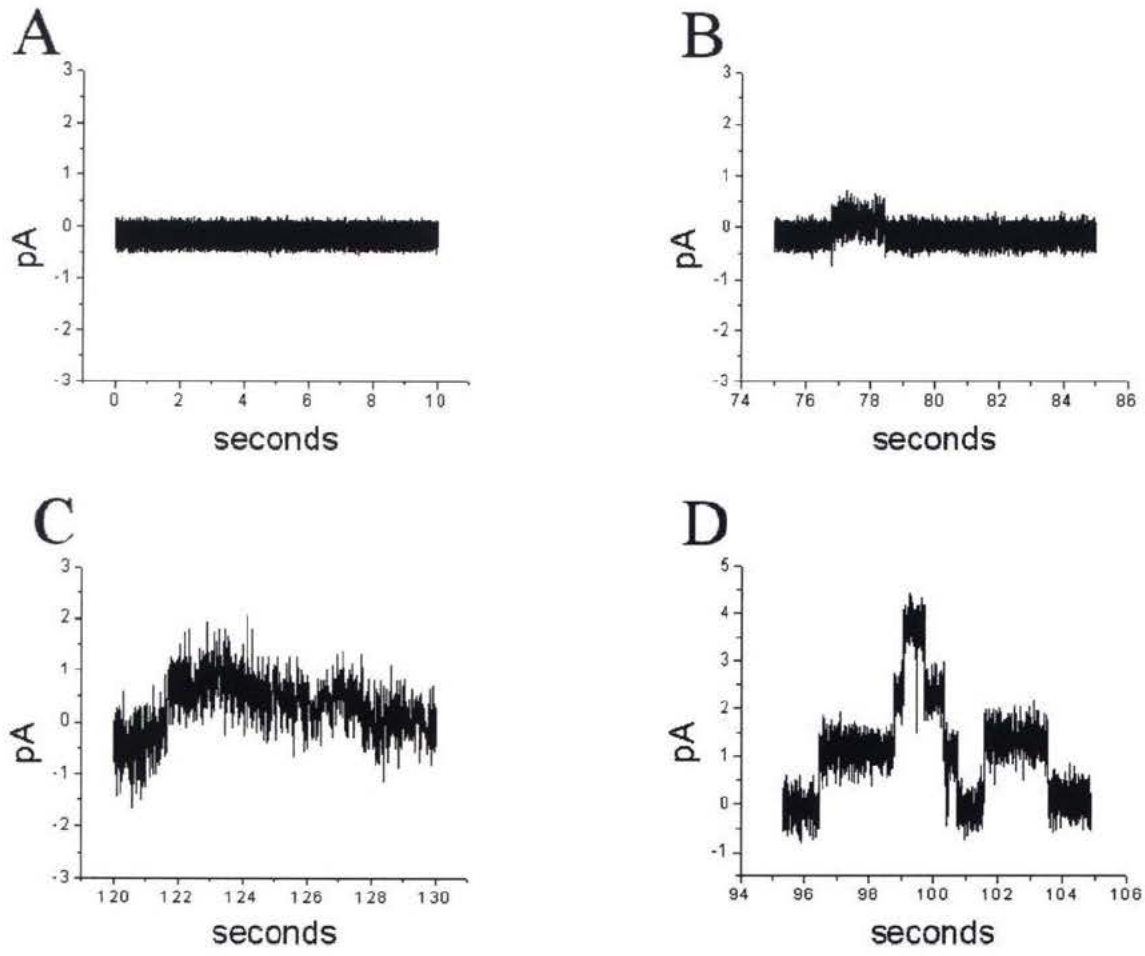

Figure 9: Typical sections of data (100 Hz low-pass filtered) from the survey: (A) Baseline of control experiment after injecting 50 µL DMSO (B) Questionable step-changes in conductance (C) Irregular behavior which is difficult to characterize (D) Three stacked levels of clear step-changes in conductance.

Successive aliquots of dimethyl sulphoxide were injected the same way the candidate channels were introduced. Over a 100 microlitres of DMSO could be injected without detriment to the bilayer. In control experiments, the baseline remained stable and flat throughout without signs of leaking or delayed rupture – bilayers were typically stable for two to four hours throughout a series of control injections.

The trace B can be characterized as ambiguous in character. Even after 100Hz low-pass filtering, it is very difficult to determine whether a discrete transition to a higher conductance level has occurred. In contrast, trace D is a clear example of step-changes in conductance. The transitions are of sufficient magnitude to avoid over-lap of the noise bands of each level, which is what makes the "questionable" example difficult to interpret.

The trace C of Figure 9 illustrates typical irregular "noise-like" behavior, which can result from a variety of situations. The bilayer could be breaking down and leaking current. The phospholipid could be hydrated and/or partially oxidized. Residual chloroform or detergent could be affecting the bilayer, or some other disrupting agent could be causing havoc. This type of irregular looking behavior can also result if a sundry of well-defined conducting pathways are activated at once (i.e. too much of an active compound). This results in a relatively large amount of current (tens of picoamperes). Too many overlapping step-changes in conductance at once end up looking noisy.

As previously mentioned at the end of the section 2.2, some compounds will be inherently hard to characterize. Trace C could be the result of a *single compound* producing "some sort" of ill-defined current fluctuations under voltage clamp conditions. It is not that the compound is in some incomplete state of forming a channel, but rather forming a geometrically irregular pathway for conductance. This survey will ignore this possibility (trace C) in favor of well-behaved channels (trace D).

2.4 Transport action of isophthalate derivatives

2.4.1 Experiments in 1M KCl

The survey of the 15 compounds available uncovered only one reliable channel forming compound, isophthalate **17.** Isophthalate **17** was consistently found to be active in bilayer voltage clamp experiments in 1M potassium chloride. Figure 10 depicts typical channel activity induced by **17** in planar lipid bilayers, and the same type of activity was observed over several experiments. This was the only compound that was active under the bilayer voltage- clamp survey.

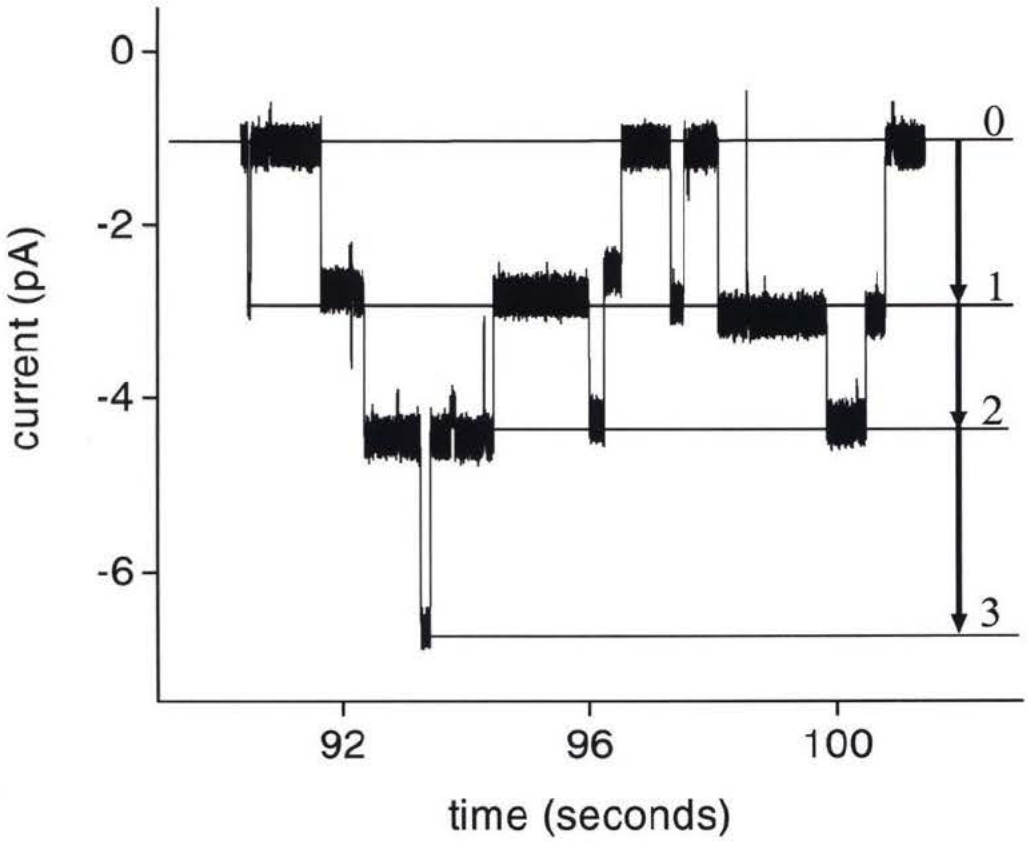

Figure 10: Three levels of step changes in conductance induced by isophthalate **17** at a transmembrane potential of -120 mV (1M KCl).

Figure 10 is from a typical bilayer clamp experiment at negative transmembrane potential showing more than one level of single- channel activity from **17**. Channels that are open induce negative currents at this polarity of applied potential. Three levels of conductances in the "on" state appear in Figure 10 (i.e. actively spanning the bilayer and conducting). The regularity of these step-changes in conductance, meaning that the levels are flat and equally spaced, implies that the conductance pathways are well-defined over the duration of the openings. As illustrated, most single-channel potassium cation conductances were of one to three seconds duration, although longer events have been observed. Some events of shorter duration (less than a second) are clear. These short-lived openings (such as the very first event at the beginning of the trace) have previously been described as "flickering" events and seem to indicate faster "open-close" transitions.[12]

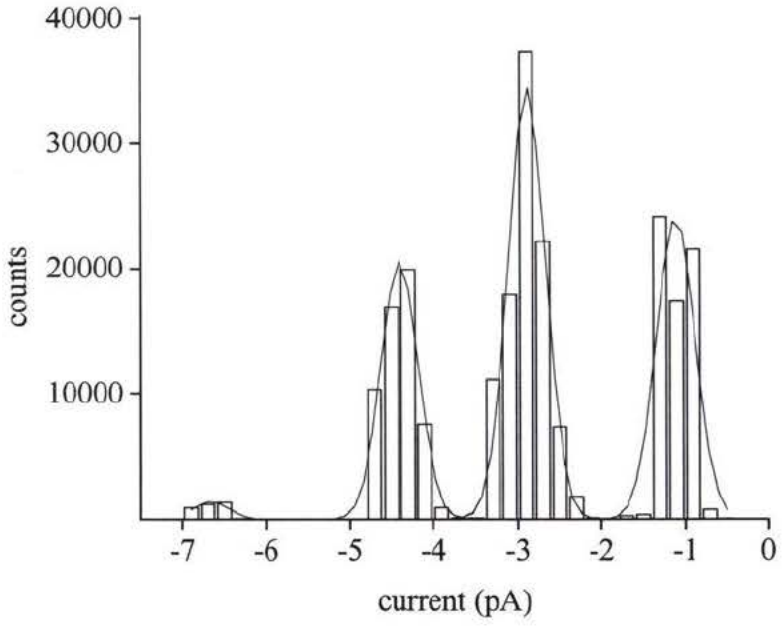

Figure 11: Histogram of step-changes in conductance by **17**, data of Figure 10.

Are the events in Figure 10 the same within experimental error? To address this question, the data was transformed into an all-points histogram in Figure 11. The Gaussian distribution is widely used to analyze histograms of current amplitude from single-channel activity.[43] This "normal" distribution is used to describe the continuous distribution of a population of measurements, which vary by randomly occurring error about the most probable value, or mean. This random error is mostly due to background noise. The 12 seconds of data from this trace was low-pass filtered and then put into 0.2 pA bins to yield the histogram in Figure 11.

Three levels are made obvious from the histogram. A level centered at –1.1 pA represents the baseline. Two dominant levels are centered about the distributions at –2.9 pA and –4.4 pA. A fourth level, from the step-change in conductance just after 93 seconds in Figure 10, is centered at –6.7 pA. The centroids of these distributions represent mean current amplitude of the single-channel conductances, and are plotted against an integral number of events in Figure 12.

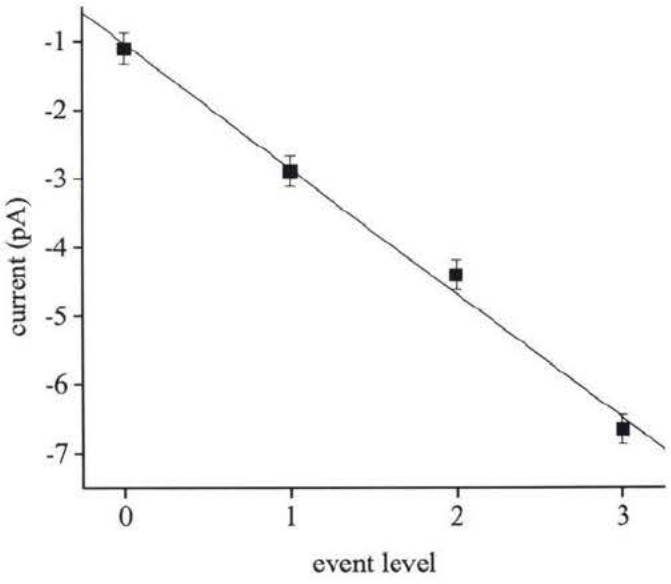

Figure 12: Events plot of K^+ single-channel conductances in Figure 10.

Whether the events are the same or different (within error) can be addressed once the mean current amplitudes (centroids) have been plotted against event level number (integers). A linear regression can then be performed on the points, and if the fit is reasonable, then the events are one and the same. The events plot for the trace in Figure 12, plotted from the histogram in Figure 11, illustrates that the events are the same within one standard deviation error. Figure 10 is then concluded to represent three copies of the same channel, which are all open at the same time just after 93 seconds in the trace.

Isophthalate **17** also induced well-defined step-changes in conductance under positive polarity. Distinct event levels were observed in the voltage clamp traces, such as the one depicted in Figure 13. This example is more complex than the one at negative potential (Figure 10), as there are apparently two predominant step heights present.

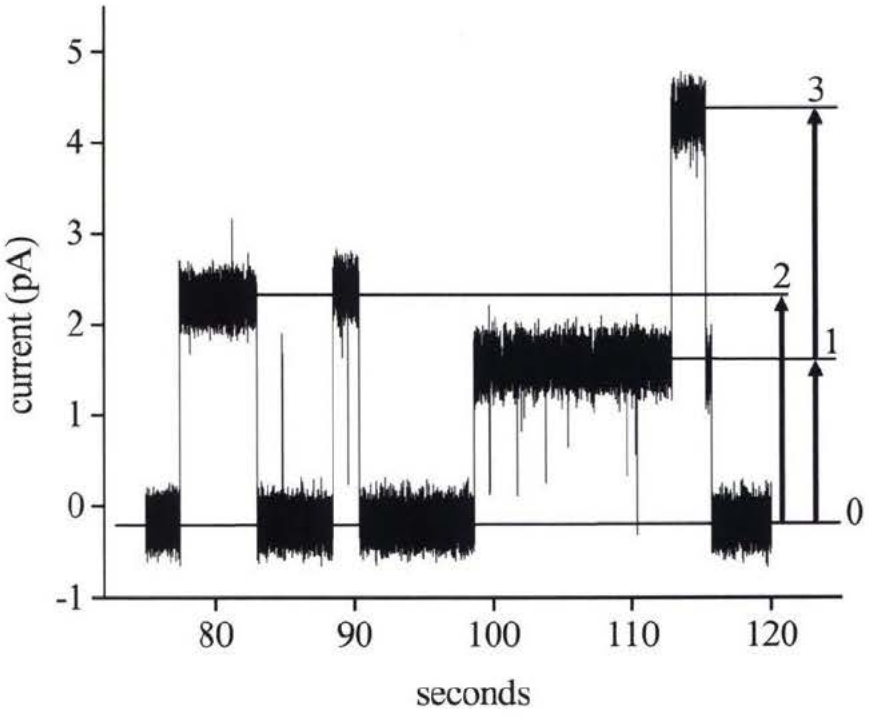

Figure 13: Two types of step-changes apparent from **17** at a transmembrane potential of +140 mV (1M KCl).

These are noted "1" and "2" to the right of Figure 13. On the face of it, these two states have different conductances. Vertical arrows to the right indicate discrete step changes in conductance to 3 levels of continuous current. The level noted as "3" has opened on top of the level noted "1." The levels at one, two and three in Figure 13 represent the open states of single channel conductances. The duration of typical single channel conductances by **17** varied from flickering events of the time scale of a second to prolonged openings of 10 to 15 seconds, which is illustrated in Figure 13.

Are levels one and two significantly different (within error)? To address this and determine if there was more than one type of event, the data in Figure 13 was filtered and plotted as a histogram (Figure 14 at left). The arrows represent the discrete transitions from one mean current amplitude to another as observed from the data in Figure 13. As at negative transmembrane potentials, the means, - 0.18 pA (baseline), +1.58 pA, +2.31 pA and +4.31 pA, were plotted against event level (Figure 14) and a line was fitted through them.

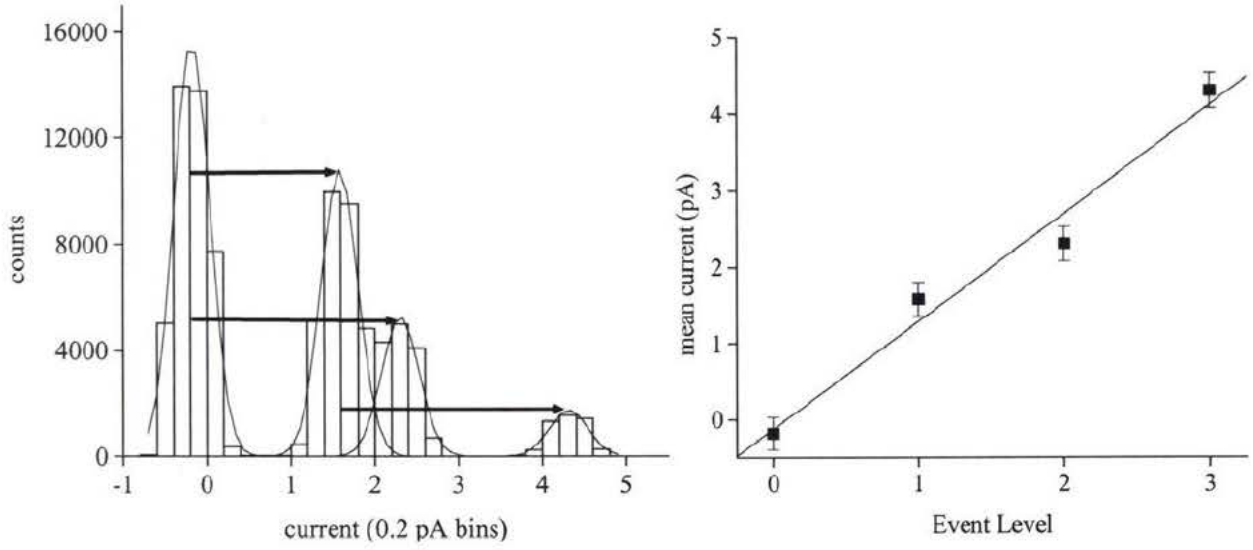

Figure 14: Histogram (left) and mean current ± SD (right) as a function of event level ($R^2 > 0.98$) for K^+ single channel conductances by **17** at a transmembrane potential of +140mV (1M KCl).

Level two clearly falls outside the best fit line. The difference *between* the centroids of 0.72 is 1.6 times the sum of the standard deviation (0.45) for the two distributions in question, and therefore levels one and two can be said to be significantly different ($p > 0.9$). Thus, the events in Figure 13 are not all the same, but occur as two different types.

The two types of events plots discussed are typical of the plots generated. In general, two types of data are produced: average step-changes in conductance (similar to Figure 10), and discrete observations which occur in a particular data set (similar to Figure 13). Average behavior is typically observed in the transition between the baseline (zero) level distribution and the first level distribution because they tend to have the largest number of points. Subsequent levels can be of the same size as the zero to one transition (linear events plot) or may vary significantly, as is the case of Figure 14 at right. Both average (predominant) and discrete (secondary) step-changes in conductance are taken into account to characterize the behavior of the isophthalate **17**.

Figure 15 summarizes all the data from K^+ single channel conductances analyzed for **17** in 1M KCl. Solid circles represent average behavior, and open circles symbolize the discrete single-channel observations. The linear fit plotted in Figure 15 includes only the solid (predominant) behavior.

Approximately the same amount of current was observed on average at both polarities. Voltage gating is defined by exhibiting greatly diminished (rectified) current at one polarity, and this is not the case for **17**. The slope of this plot represents the specific conductance of 15.4 pS ± 0.2 pS by the channel formed by **17** for transport of the potassium cation. The channels formed by **17** appear to be more stable under negative potentials as the specific conductance is limited to a tight range of values, whereas the conductances plotted for positive transmembrane potentials vary more, especially at

higher positive potentials. This is evident from the discrete values plotted for positive potentials.

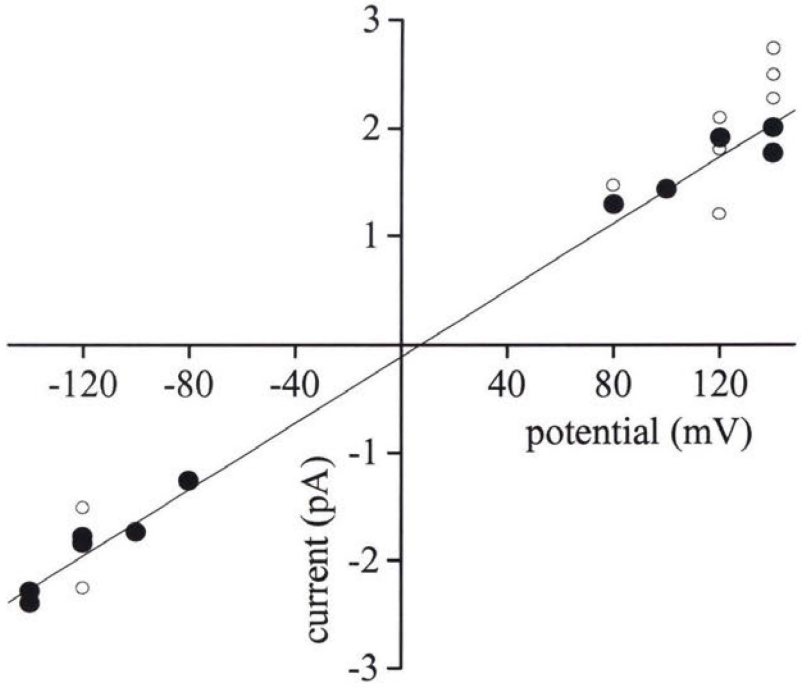

Figure 15: Current-voltage dependence of single-channel potassium conductances by **17.**

The greater variation at positive potentials will be encountered again with other electrolytes. This is consistent with simple electrostatics. At positive potentials, a dianionic compound will be drawn out of the bilayer, back towards the aqueous pool (*cis*) where it was introduced.

Occasionally, sloped events (like the first event illustrated in Figure 16) were observed in potassium experiments. This type of event is still clearly a step-change in conductance because, after filtering, the noise bands of the zero level and the conducting level do not overlap. Conductance is uniformly decreasing over the lifetime of the

opening in such sloped events, possibly a result of the shrinking in diameter of the conducting pathway. Events like this indicate a flexible active structure; however, the occurrence of this type of opening is fairly rare, so no quantitative analysis has been performed.

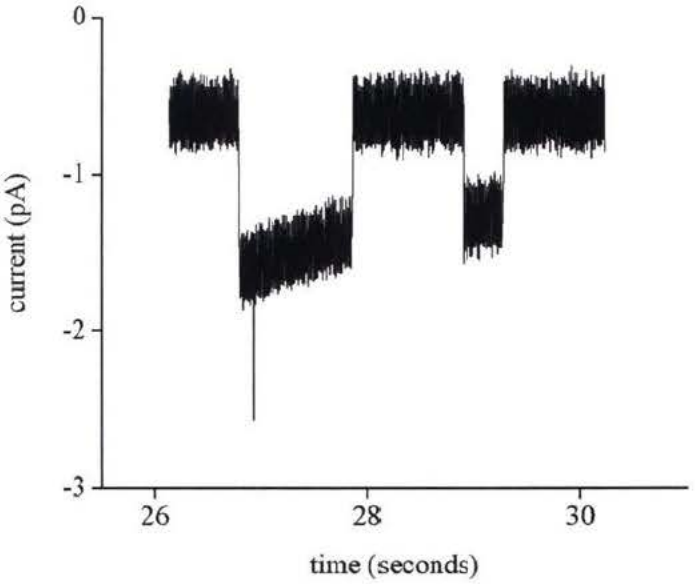

Figure 16: An example of an infrequently occurring sloped K^+ conductance by **17** (-120 mV, 1M KCl)

2.4.2 Experiments in 1M CsCl

Step-conductances by **17** for Cs^+ were generally larger in magnitude and more prevalent than for those observed for K^+. Several conductance levels were typical of Cs^+ single channel activity. The 30 seconds of data shown in Figure 40 represents five distinct conductance levels stacked with some intermediate levels apparent. Events like the one under the arrow in Figure 17 make it visually difficult to discern whether the events are of the same magnitude. Of particular interest is the elevated baseline which was typical for experiments in cesium chloride. The baseline at 5 pA was continuous throughout the duration of the experiment, and can be attributed to the increased ionic permeability of the bilayer in cesium chloride. As the charge on the cesium cation is

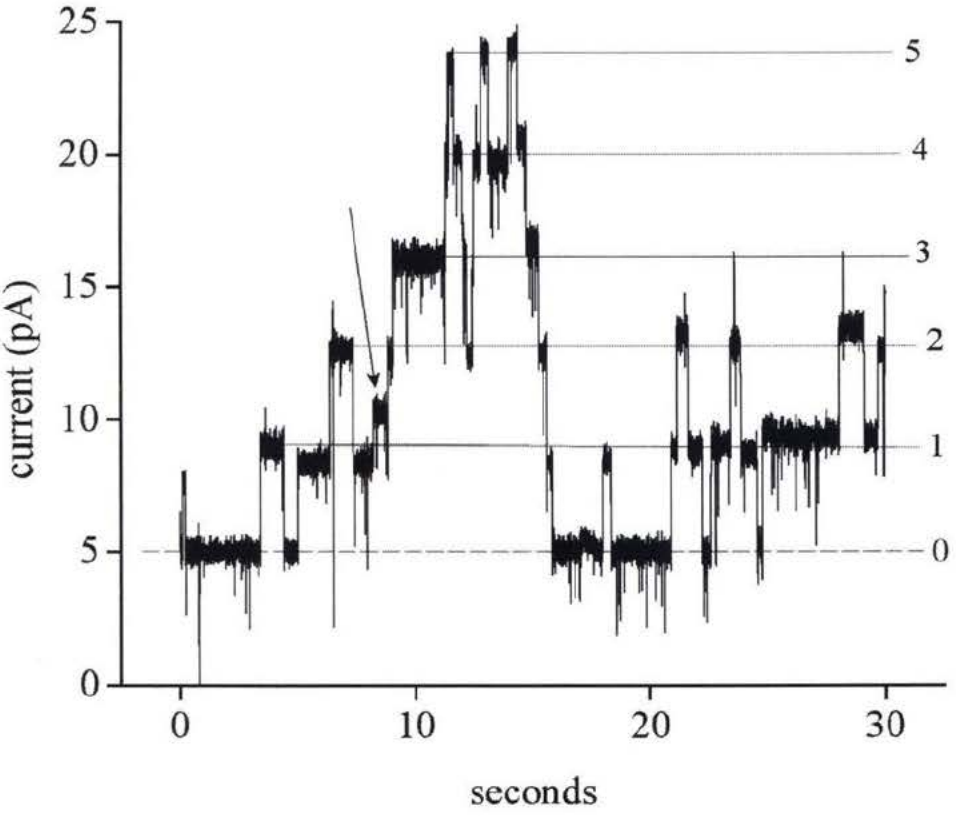

Figure 17: Single-channel Cs^+ conductances induced by isophthalate **17** at a transmembrane potential of +120mV (1M CsCl).

more diffuse than potassium, this cation is more permeant into the membrane.

At level 5 in Figure 17, there are 5 channels open, each of which passes what appears to be the same amount of current. The probability of an integral number of openings (event level) relative to another level is proportional to the populations of the distributions for the two levels. The data in the trace were plotted as an all points histogram in Figure 18. Gaussians were fitted to these distributions, from which a regular progression of means is apparent.

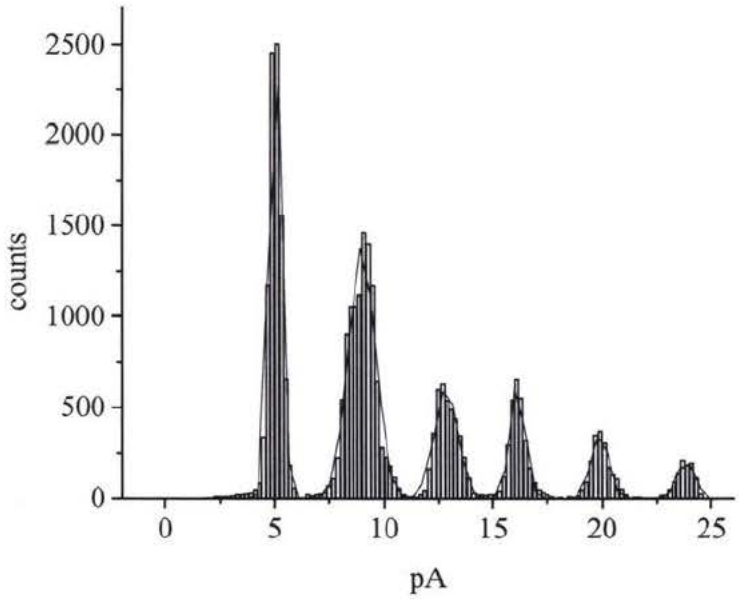

Figure 18: Histogram of Cs^+ channel conductances derived from Figure 17.

The smaller step-change of irregular magnitude indicated in Figure 17 is not apparent as in its own distribution in Figure 18. Only the principal activity of the five levels, indicated by lines in Figure 17, is made apparent in the histogram above.

In Figure 19, the events plot for the above histogram (at +120 mV) and one at negative polarity (-120 mV) are compared. Both summarize the events observed for 30 seconds of data.

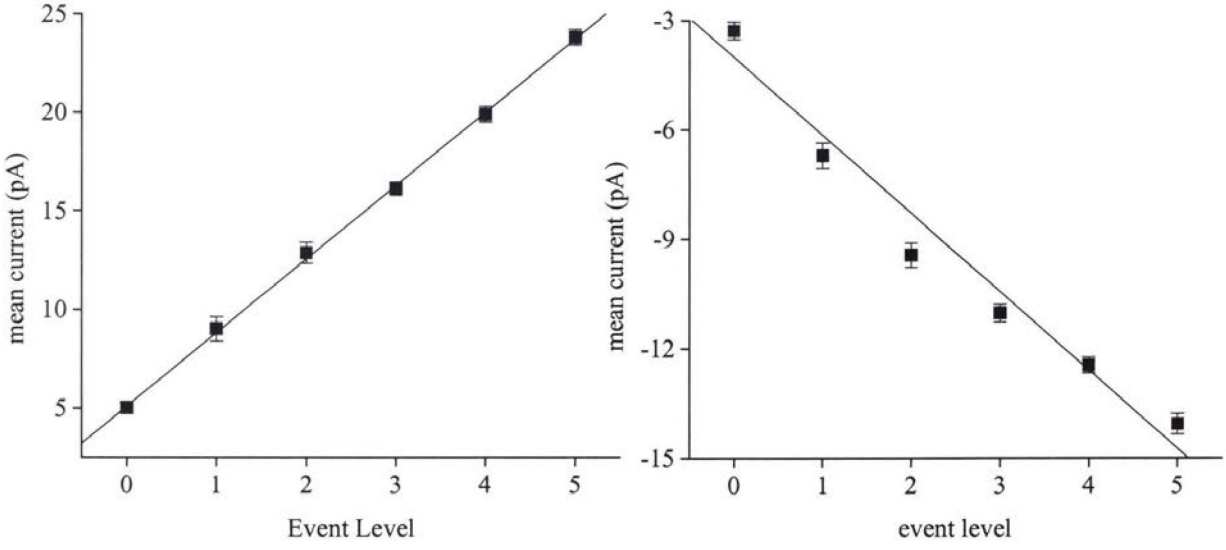

Figure 19: Events plots of 30 seconds of data from histogram in Figure 18 (left) and from an experiment at a negative transmembrane potential of -120mV (right).

From the excellent linear fit of the plot at left in Figure 19, it can be concluded that there is one predominant type of behavior. An example of an events plot that is not linear is at right in Figure 19. Four of the six points lie outside one standard deviation of the best fit line. More deviation from linearity was observed under negative potentials for the cesium cation than for experiments with potassium and sodium cations.

The I-V relation in Figure 20 describes the overall ohmic conductivity of **17** over a range of transbilayer potentials by plotting average (solid circles) and discrete observations (empty circles). The linear regression, however, was performed only on the solid points, yielding a slope of 31.0 pS describing the specific conductance for the

cesium cation. At positive potentials, a wider range of discrete conductances is observed, most of which are of smaller magnitude in relation to the predominant behavior. This supports the idea of enhanced flexibility in the conducting structure at positive potentials,

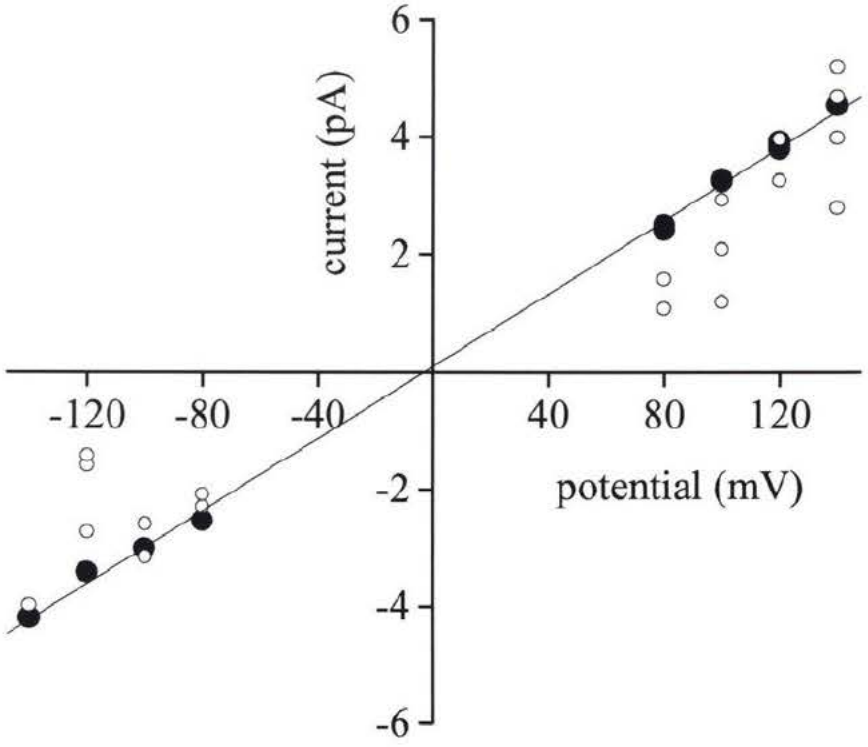

Figure 20: I-V plot of predominant (solid) and secondary (empty) observations for Cs^+.

and is consistent with the single-channel potassium observations for isophthalate **17**. In Figure 20, the linear fit illustrates discrete observations deviating from the best fit to the predominant step-changes in conductance. In general, more discrete observations were found under positive transmembrane potentials, which indicates an inherent flexibility that is not apparent at negative potentials. At negative potentials, the predominantly dianionic isophthalates are effectively driven into the bilayer, as a net

driving force is exerted on them, pushing them towards the anode (*trans*). At positive potentials, the net driving electromotive force is away from the bilayer, so the active structure the isophthalate is assuming can be said to have some "elasticity" in inserting at positive potentials relative to negative potentials. At negative potentials, the dianionic molecules are effectively driven into the bilayer from the *cis* side.

2.4.3 Experiments in 1M NaCl

Sodium cation single-channel conductance events by **17** were smaller in magnitude, and less prevalent than in potassium and cesium experiments. Usually only one or two channels were observed as "on" at any given moment.

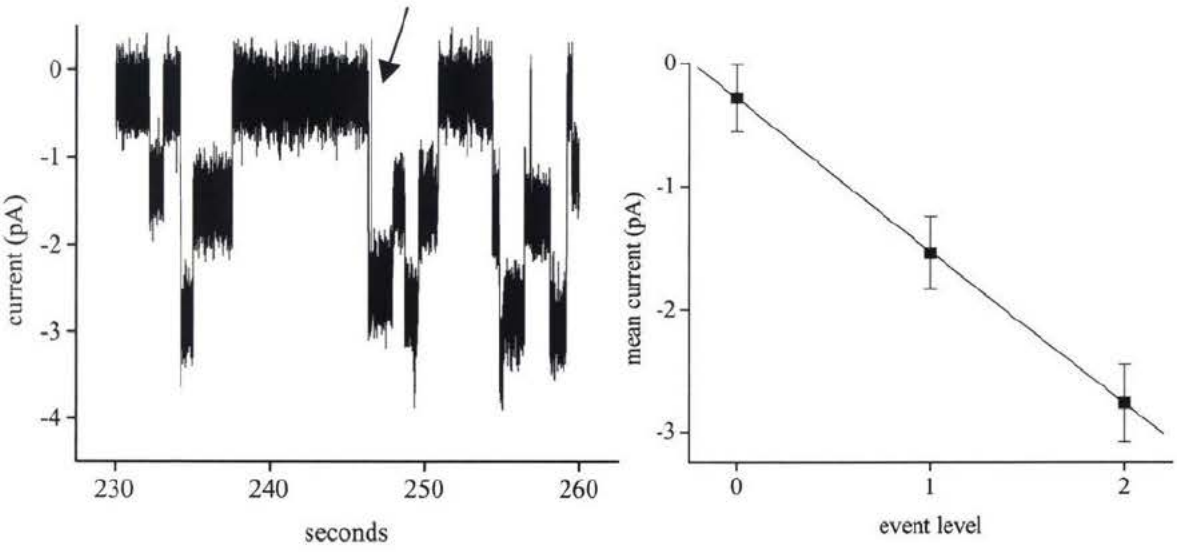

Figure 21: Sodium cation single-channel conductances induced by **17** at a transmembrane potential of −120 mV (left). Linear fit of mean event currents as a function of level number (right) (1M NaCl).

Typical single-channel conductance was observed upon injection of 14 to 42 nanomoles of isophthalate **17**, and activity was usually observed within 5 to 30 minutes. Single-channel occurrences were observed for periods of up to an hour. In Figure 21, two levels of channels in the "on" state are apparent. That is, either zero, one, or two channels are conducting at any given time. The linear fit of the mean current amplitude of each conductance level as a function of event level (integers) suggests the levels are equivalent. Is the second level statistically different from the first? In this case, the

difference in means between the two levels is twice the sum of their standard deviations (1.23 > 0.61), which indicates they are significantly distinct populations.

As depicted in Figure 21, the duration between switching "on" and "off" in single-channel conductances from **17** can vary widely, from subsecond flickering events to prolonged conductances of several seconds. The switching "on" and "off' of a given channel is a completely random process, which means the duration of a given conducting pathway will vary. Flickering events were occasionally observed in K^+ and Na^+ voltage clamp experiments, whereas Cs^+ conductances tended to be of longer duration (1 to 3 seconds) and with less "flickering." The arrow in Figure 21 indicates a subsecond flickering event, just before a very brief return to baseline and the subsequent opening of two channels at once. The very brief return to baseline could either represent (A), a channel that does not completely close for a moment, and then re-opens before a new one opens, or (B), a channel that closes forever and two new ones open in some other area of the membrane. This situation reflects the stochastic nature of single-channel analysis.

More flickering events are evident in the 30 seconds of data in Figure 22. The event

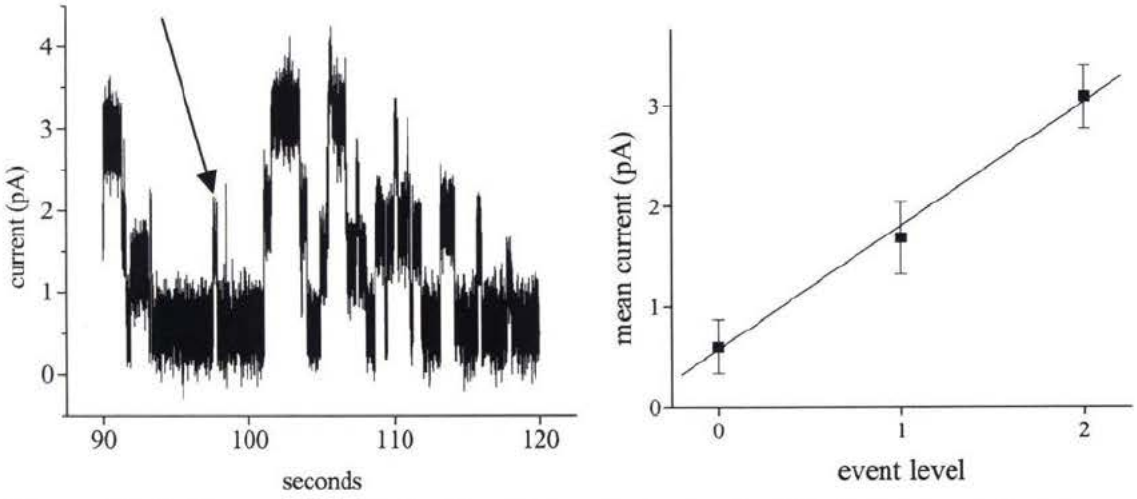

Figure 22: Sodium cation single-channel conductances by **17** at a transmembrane potential of -120 mV (left). Linear fit of mean currents as a function of integral level numbers (right) (1M NaCl)

under the arrow indicates what is meant by a "flickering" event. The data in the trace at left in Figure 22 were converted to a histogram. The events plot at right of Figure 22 demonstrates that the event levels plotted are all within one standard deviation of the best fit line, and thus statistically of the same magnitude.

The I-V plot in Figure 23 indicates that the sodium-cation single-channel conductances were generally ohmic in behavior, as was the case for experiments in KCl and CsCl.

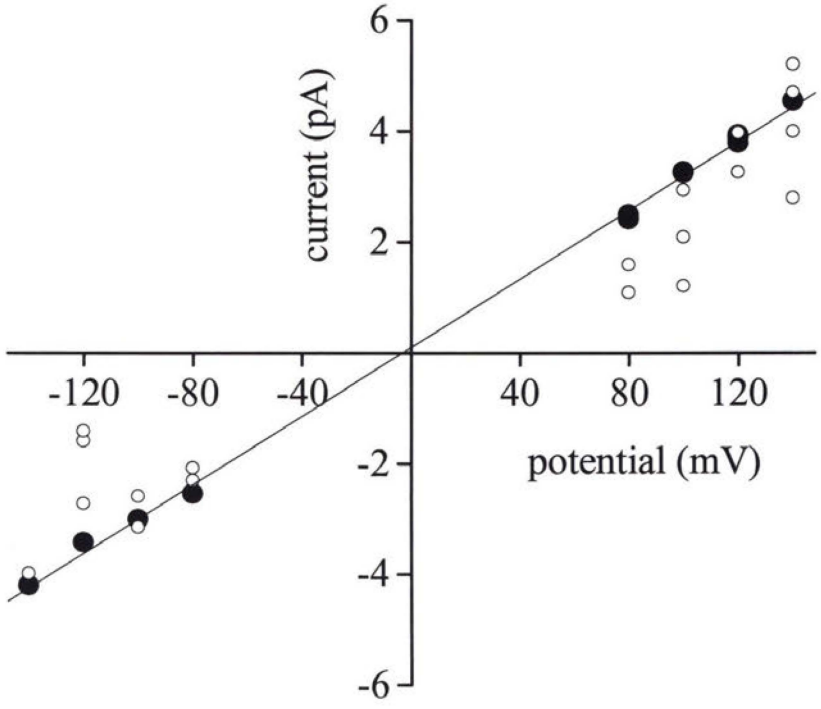

Figure 23: Current-voltage dependence of Na^+ single-channel conductances by isophthalate **17.**

The linear regression was performed on the solid circles, which represent the predominant (average) behavior. The slope describes the specific conductance of 9.2 pS

for the sodium cation. Discrete observations were made as well and are important in characterizing the activity. In Figure 23, conductances appear to conform more to Ohm's law at negative potentials, but at positive transmembrane potentials the active structure had greater flexibility since more discrete observations were scattered about the average conductance at positive polarity. The Na^+ conductances at positive polarity tended to deviate from linearity more than at negative potentials, especially at higher positive transmembrane potential i.e. (+140 mV).

2.5 Summary of results from the survey

This survey examined 15 alkoxy isophthalates by the planar bilayer voltage-clamp technique, and found only one compound, **17**, active under the conditions of the survey (see Table 2). Isophthalate **17** is concluded to have demonstrated cation selectivity in the order $Cs^+ > K^+ > Na^+$. These values were derived from the means of the predominant conductances over a range of potentials (I-V plots) for the three electrolytes. The left side of Table 2 shows specific conductances only considering the mean observations (fitted only to filled circles), whereas the right side shows the specific conductance when a linear regression is performed on all observations (solid and empty circles).

Table 2: Specific Conductance of isophthalate* 17 *for three alkali chlorides

Cation	Mean Specific Conductance (pS) ± SD	Linear Fit (R^2)	Mean + Discrete Specific Conductance (pS) ± SD	Linear Fit (R^2)
Na^+	9.2 pS ± 0.1	> 0.993	9.9 pS ± 0.2	> 0.98
K^+	15.4 pS ± 0.2	> 0.997	16.0 pS ± 0.3	> 0.98
Cs^+	31.0 pS ± 0.1	> 0.999	27.2 pS ± 0.8	> 0.97

In all cases, the standard deviation for the linear fit increases when both mean and discrete observations are taken into account (right side of Table 2). Furthermore, the mean and discrete fit suffered more deviations from linearity as the R^2 values indicate. The linear regressions for mean conductances only had R^2 values greater than 0.999, whereas when both discrete and mean observations are fitted R^2 was greater than 0.98 (for cesium, greater than 0.97).

The cesium cation has the highest specific conductance of the three alkali metal chlorides, which can be attributed to the surface charge on cesium being the most diffuse of the three alkali cations examined. As a cation enters the channel, it is effectively forced to reduce its hydration sphere. For a narrow conduction pathway, the cation which can shed water most easily will enter the channel most efficiently. The relatively small specific conductances, combined with the order of cation selectivity, suggest that the active structure is relatively small. The more prevalent "flickering" events in potassium and sodium experiments generally suggests that the active structure is more stable in conducting cesium cations over potassium and sodium. These short-lived "flickering" events have been described before for the bola-amphiphile **6** as "fast open-close transitions" of one single-channel conductance where "the active structure does not close completely".[12]

In the following chapter, two closely related homologs to isophthalate **17** are synthesized and are examined under the conditions of the survey. Surprisingly, both of the homologs synthesized were inactive under the conditions of the survey. This brought us to wonder about the characterization and purity of **17**. Since isophthalate **17** originated from another institution, one becomes curious about the characterization and purity of the compound which reliably induced transport in planar lipid bilayers.

Upon careful analysis of mass spectra, and proton and carbon NMR, the compound was confirmed to be a pure sample. However, the positive FAB LSIMS revealed the molecular ion peak to be 28 mass units heavier than what was expected, with a molecular weight of 504 g/mol rather than 476 g/mol. No trace of a methyl ester singlet was visible in the ^{1}H NMR spectra, and all the expected resonances in ^{1}H and ^{13}C NMR were apparent. In the ^{1}H NMR, the ratio of the areas of methylene (broad multiplet) to terminal methyl (broad triplet) was found to be 7.7, whereas it should be (36:6), or 6, in compound **17**. In light of the proton NMR and mass spectra, it is likely that compound **17** has two more methylene groups in the alkoxy moiety than what was originally thought. The expected ^{1}H integration of methylene to terminal methyl for **17a** is 40:6, or 6.67, still not in agreement with the experimental observation. The mass spectrum is in agreement with the **17a** structure and gave the m+1 peak of 505.3. The exact mass m+1 peak of 505.3900 (mean of three trials) is in complete agreement with **17a**. This reassignment of structure **17** to structure **17a** in no way alters the finding of cation channel-forming activity of **17a**.

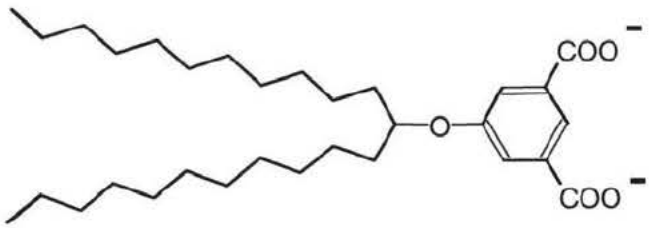

17a

3 Ether Isophthalate Synthesis

3.1 Synthesis of two homologs of 17

Two homologs of the isophthalate **17** were proposed to further elucidate the mechanism of action of this active cation channel. This was a worthwhile endeavour because isophthalate **17** was active by the guidelines of the survey, inducing well-defined behavior in three different alkali metal chloride electrolytes. Many simple structural variations of **17** could be proposed: ether substitution at position 4 of the aryl ring (instead of 5), ester moieties in place of carboxylates, a polyamine chain linked via an amide bond, a naphthyl ring in place of an aryl one, a fluorinated alkyl chain instead of a saturated hydrocarbon alkyl moiety, to name a few.

The structural variation which we thought would have the greatest impact on interpreting how isophthalate **17** was forming the active structure was alkyl chain length. We did not want to vary the structure too greatly, so as to increase the probability of finding another active isophthalate by the bilayer clamp technique. The bilayer is a barrier which must be spanned to some degree. The overall length of the molecule is a critical factor in forming a conducting structure, even if the molecule is not acting unimolecularly. The alkyl chain length was varied in an attempt to understand the critical factor of overall molecular length in producing an active cation-conducting structure. Upon shortening, at some point the length of an active motif will become too short to pose a cation-conducting pathway through the hydrophobic interior of the bilayer. Probing this "critical length" is consistent with the overall goal of investigating what "minimal" structural motif will induce cation channel formation.

The two homologs of **17** that were proposed are one which is four carbons shorter in the alkyl chain, and one which is four carbons longer than isophthalate **17**. These derivatives of the active structure were synthesized to elucidate the relationship between observed activity and functioning structure. The two homologs of isophthalate **17** synthesized were: 5(9-heptadecyloxy) isophthalate (**31**) and 5(13-pentacosanoxy) isophthalate (**32**). At this point in the project, the correct structure for the active compound was still believed to be **17**, and the targets **31** and **32** were derived according to the incorrect structure (**17**) and not the revised structure (**17a**). Had the correct structure (i.e. **17a**) been known at that time, these homologs would have been adjusted to increase the alkoxy chain lengths.

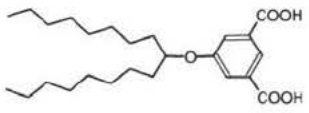

31

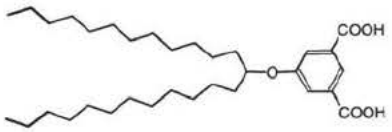

32

The two homologs were synthesized starting with the commercially available 5-hydroxy isophthalic acid **39** and respective ketones **33** and **34**, as illustrated in Scheme 4. The ketones were reduced to the respective alcohols **35** and **36** using lithium aluminum hydride. Absence of the carbonyl stretch around 1750 cm^{-1} and the presence of an OH stretch at 3300 cm^{-1} in the IR confirmed the reduction to the alcohols.** The work-up of the alcohols was performed using Steinhardt's procedure.[49] These alcohols were subsequently brominated (Scheme 4), and the bromides **37** and **38** were isolated on a silica column using pentane as eluent.

** Both **35** and **36** are known compounds, but **36** is known only as a component of sulfur-rich nonpolar macromolecular fractions isolated from crude oil and sediment extracts and characterized as the TMSi-ether by GC-MS.[47] Compound **35** is a reported compound with ^{1}H and ^{13}C NMR resonances consistent with **35**, but misnamed as "10-nonadecanol".[48]

The 5-hydroxy isophthalic acid **39** was converted to the dimethyl ester **40**. The methyl ester carbon was visible in the ^{13}C NMR at δ 52.9 ppm, and the six protons as the dominant singlet in the ^{1}H NMR at δ 4.9 ppm. Known procedures for the alkylation of phenols with secondary bromides were employed[34,50] to prepare the protected ethers **41** and **42**. Sodium hydride was used to deprotonate the phenol moiety of **40** in the coupling reaction of the bromides **37** and **38**, carried out in dimethyl formamide (DMF) with a catalytic amount of potassium iodide. The proton on the ether-linked carbon was evident as a broad quintet in the ^{1}H NMR at δ 4.3 ppm. The presence of the aforementioned resonances for methyl ester indicated that this moiety was intact.

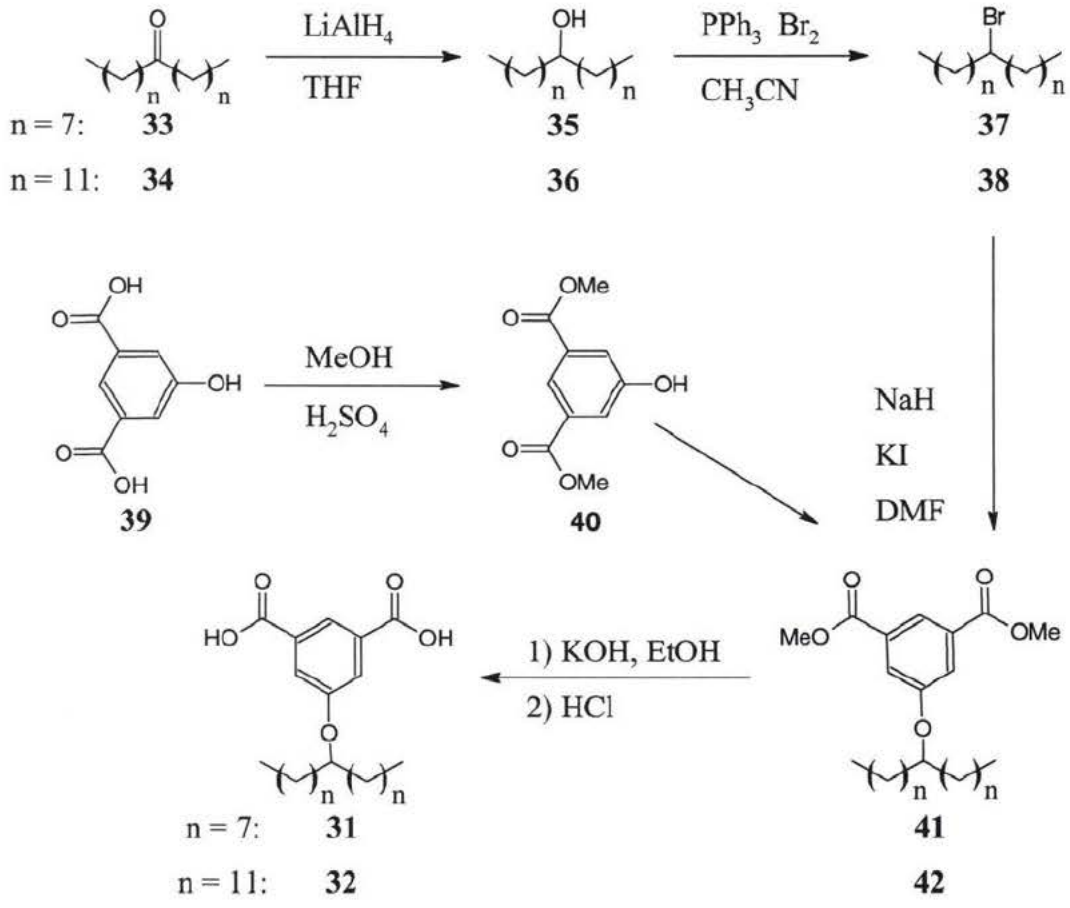

***Scheme 4: Synthesis of compounds* 31 *and* 32**

Ether formation for **41** and **42** was confirmed by the distinct upfield shift of the ether-linked alkyl carbon at δ 78.5 (**42**) and 78.6 ppm (**41**) in the ^{13}C NMR. The dimethyl esters of the product **41** and **42** were dried, taken up in dichloromethane, and the aqueous layer(s) were put under continuous extraction with dichloromethane (overnight).

The crude dimethyl ester of the product was purified on a silica column using hexanes and ethyl acetate as eluent. Alkenes and unreacted bromides were initially flushed out using hexanes, and the dimethyl ester eluted with increasing proportions of ethyl acetate. The dimethyl ester was finally isolated by Chromatotron silica plate chromatography using hexanes and chloroform as eluent (1:1).

The subsequent hydrolysis of the ester groups of **41** and **42** to the diacids **31** and **32** was performed in 2:1 ethanol:water using 2.5 equivalents of potassium hydroxide. The two diacids were precipitated in an ice bath by adding concentrated HCl. The success of the reaction was confirmed by loss of the methyl ester line in the ^{13}C NMR and the singlet in the proton NMR. The ether-linkage was still evident in the ^{13}C NMR from the line at δ 78.6 ppm (**31**) and δ 79.6 ppm (**32**), and the broad quintet at δ 4.3 ppm for both compounds.

The products **31** and **32** were further characterized by proton and carbon NMR, positive Fast-Atom Bombardment Liquid Secondary Ion Mass Spectrometry (+FAB LSIMS), exact mass analysis (by +FAB LSIMS), elemental analysis (by Canadian Microanalytical Service, Ltd.), and melting point determinations. For the homolog **31**, the +LSIMS revealed a predominant m+1 peak of 421.2 and an exact mass m+1 (mean of 3 runs) of 421.2955 (matrix: *meta* nitro benzyl alcohol, mNBA) in good agreement with the theoretical m+1 value of 421.2954 g/mol. The solid melted completely between 141°C to 144 °C.

The homolog **32** was characterized by the same techniques. The mass spectra (+LSIMS) was dominated by an m+1 peak of 533.3 (matrix mNBA). The m+1 for the exact mass was reported as 533.4223(mean of 3 runs, matrix mNBA), as compared to a theoretical "isotopically weighted" m+1 value of 533.4206 g/mol. The solid completely melted in the range of 77°C to 78.5°C.

3.2 Survey of channel-forming activity of 31 and 32

The homologs of **17,** compounds **31** and **32**, were examined by the bilayer voltage-clamp technique in the same manner as the previous 15 isophthalates. Under the conditions of the survey, no activity was observed for either of these homologs. This was rather unexpected, given the close structural similarity of these homologs to **17**. It was at this point that **17** was characterized as **17a**.

Unfortunately, the compounds synthesized ended up being two carbons longer (**32**) and 6 carbons shorter (**31**) than the active isophthalate **17a**. Six carbons shorter is a big leap to still expect a membrane spanning structure, but an isophthalate two carbons longer would seem to still have a good chance of being active. The fact that neither of the new compounds was active under the survey implies that the length of the alkyl moiety in **17a** is critical, in that the right alkyl length is a key factor in promoting the active structure in the bilayer.

Chapter 4: Further evaluation of transport activity of alkoxy isophthalates by the pH stat technique

4.1 Vesicles: spheres of bilayers

There are two main methodologies for assessing cation transport across a phospholipid membrane: techniques such as the bilayer clamp experiment that use planar lipid bilayers (with a cuvette, a thin partition, or pipette tip) and techniques that employ liposomes, or vesicles. Vesicles consist of a spherical bilayer surrounding an entrapped aqueous compartment. Planar lipid bilayers are more difficult to form than vesicle bilayers, but the advantage for the former is that resolution of the data obtained is on the scale of a single channel. Vesicles are facile to prepare, and the pH stat experiment utilized has been more robust than the bilayer clamp experiment in past experimental work.[44] The use of vesicles provides a bulk, macroscopic view of cation channel formation, that has been employed successfully in structure-activity surveys. Thus, a vesicle survey is a reasonable proposal to uncover if there are other active compounds from the original suite of ISA derivatives (Schemes one through three), plus the homologs **31** and **32**, which were all deemed inactive by the bilayer clamp survey.

Vesicles are analogs of cell membranes,[51] having the same overall lipid-packing morphology in a lyotropic unilamellar phase.[7] Analogous to cell membranes, vesicles contain an aqueous compartment encapsulated by one or several bilayer(s). Membrane-forming lipids have low solubility in water (CMC about 10^{-8} molar),[7] and spontaneously reassemble in water upon thermal disruption (ultrasonication)[52] to form vesicles. Sonication eventually makes the globules dissociate to a minimum size. Vesicles can be small (10 nm) or rather large (500 nm), and uni- or multi-lamellar. Uni-lamellar vesicles refer to aqueous compartments surrounded by a single lipid bilayer, and multi-lamellar

describes vesicles that are aqueous pools surrounded concentric bilayers. For channel-forming compounds, a rather large proportion of Large Unilamellar Vesicles (LUV's) is required. The vesicles used in the experiments (below) were found to be bimodally distributed from large (233 nm) in diameter to medium (81 nm). More than 80% were found to be in the larger diameter category, which is important in ensuring a large enough internal aqueous volume to generate a well-defined signal in the pH stat experiment.

Cation transport experiments rely on the impermeability of the bilayer to hold ionic and proton gradients across the inner and outer aqueous pools. Approximately 650 kJ/mol would be required to move a sodium cation to the midplane of a membrane 30 Å thick.[44] Thus, the bilayer is quite impermeable to cations, and cation gradients are readily imposed across the membrane. Agents that effect the collapse of such gradients are of interest to probe the cation-transporting ability of ionophores.

The vesicles prepared in this thesis were formed by reverse evaporation of a mixture of PC:PA:cholesterol (8:1:1), followed by sizing through a polycarbonate membrane and size-exclusion chromatography. Cholesterol is an important regulating influence in biological membranes, as it decreases the net fluidity of phospholipid membranes above the main transition temperature but augments it in the gel phase below the main transition temperature.[51] Above the main transition temperature, addition of cholesterol to phospholipid bilayers promotes a reduction in amplitude of acyl chain motions of the hydrophobic core.[5] The main effect of cholesterol on headgroup packing appears to be disruption of interactions between choline and phosphate moieties.[5] At the temperature of the experiment, egg PC is in the fluid phase and cholesterol is a rigidifying presence.

Experimental methods typically used to investigate the collapse of a gradient imposed on the vesicle bilayer include acid/base titration, ^{23}Na NMR, UV/Vis or fluorescence

emission. Sodium NMR is used to monitor the transport of ^{23}Na nuclei (I = ½). In the presence of an external paramagnetic shift reagent, such as Dy^{3+}, the external resonance of sodium cations is shifted up field. A sodium transporter will alter the line widths of the external and internal resonances, and a rate can be calculated from this change.[53] Line-broadening becomes saturated, however, limiting the useful concentration range for the experiment. Fluorescence experiments often employ a pH sensitive dye which is encapsulated in the vesicles.[44] A common fluorophore employed is 2,7-bis-carboxyethyl-5(6)-carboxyfluorescein, which is quite sensitive to changes in pH. It can be enclosed inside the internal aqueous compartment, and the externally residing probe molecules removed by gel filtration.[54] The emission spectra is monitored as the proton gradient collapses at the onset of cation transport. At the end of the experiment, the liposomes can be lysed, releasing all of the dye, and the emission response monitored over a range of pH values through titration.[54] The technique using carboxyfluorescein, however, suffers from slow leakage.[54] This detriment has been put to use by using carboxyfluorescein as a leakage probe to determine how well-sealed the vesicles are.

The pH stat technique is effectively a base titration to maintain a set pH when a pH gradient collapses and releases protons to the external solution. In a typical pH stat experiment, a two-unit pH gradient is imposed across the membrane of the vesicles, which establishes a transmembrane potential of about 120 mV. A potassium-cation gradient is established by introducing potassium sulfate to the external solution (see Figure 24). Before candidates channels were introduced, FCCP (carbonyl cyanide p-(trifluoromethoxy) phenylhydrazone)was added to the external solution so as to ensure a

proton conducting pathway. FCCP is a known protonophore[5] and is capable of depolarizing plasma membranes[55] and mitochondrial membranes.[56]

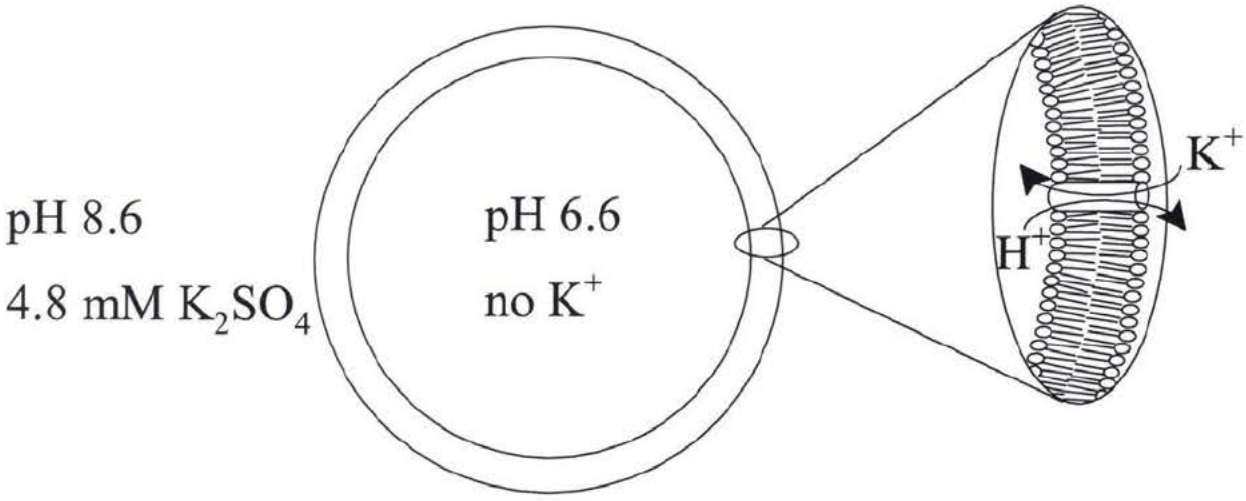

Figure 24: Schematic diagram of a vesicle under the conditions of the pH-stat experiment.

Cation transport is assessed by knowing that the transport of cations is directly proportional to the transport of protons, through antiport exchange. Antiport exchange dictates a one for one exchange rate as the cation and proton gradients collapse (Figure 24). In a cation-proton antiport, the ratio (internal to external) of concentrations for the one substrate [H^+] is equal to the ratio of concentrations (internal to external) for the second substrate [K^+].[4] Kinetic data for cation translocation are derived from the rate of addition of titrant to maintain a set pH. An initial sudden "jump" of few microlitres over the first couple of seconds is expected as the candidate and solvent are brought to the pH of the system (8.6). The rate is calculated from the data after this quick (but small) step up in titrant volume.

4.2 Cation Transport by Isophthalates in Vesicles

Two compounds were found to be active in the survey of activity in vesicles by the pH stat technique. Isophthalates **29** (monoalkoxy, perfluorinated) and **30** (diazacrown) clearly demonstrated cation transport activity in pH stat vesicle experiments. A typical pH stat experiment, using the perfluorinated candidate **29,** is shown in Figure 25.

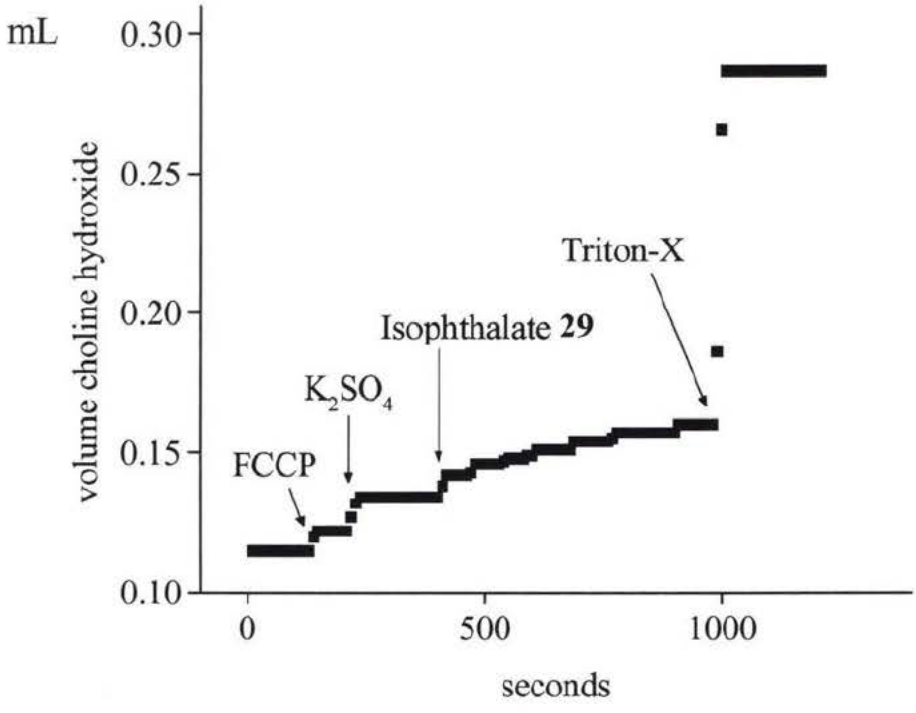

Figure 25: Cation transport activity of isophthalate **29** in PC:PC:cholesterol vesicles by the pH stat technique.

All of the candidates were introduced at the same stock solution concentration (8 mM) into the external solution, and were given equal amounts of time (25 minutes) to effect cation transport. For pH stat experiments, 100 μL of vesicles were put into five mL of electrolyte solution, and the solution was stirred and titrated with choline hydroxide to

bring the solution to pH 8.6. The system was verified to be at equilibrium (i.e. not adding base to maintain pH 8.6), which is the flat region in the beginning of the plot in Figure 25. Upon introduction of FCCP (19 nmol), a small amount of choline hydroxide (6 to 9 μL) was immediately required to maintain the set pH of 8.6, hence the small jump in volume under the arrow labeled in Figure 25. After an immediate jump, however, sealed vesicles did not require more titrant to maintain the set pH. Potassium sulfate (25μmol) was injected under the arrow labeled "K_2SO_4" in Figure 25. This amount of potassium sulfate normally produced an immediate 10 to 15 μL consumption of titrant, but the vesicles quickly equilibrate (20 to 30 seconds) to the set pH.

Candidate isophthalates (0.8 μmol) were introduced in either methanol or DMSO to the external solution. Isophthalate **29** was introduced to the external solution at the labeled arrow in Figure 25. Activity is generally observed immediately, as it is in Figure 25. Isophthalate **29** induced a prolonged consumption of titrant in the vesicles, as the progression of small steps indicate. Right before the end of a 25 minute file, dilute Triton-X (see arrow Fig. 25) was introduced to lyse the vesicles and allow any remaining protons to equilibrate with the external solution. This is important in ensuring that a proton gradient was present through out the experiment. Control experiments were conducted with blank solvent solutions in place of the candidate compound solutions to assess the leakiness of the vesicles. Gramicidin was used as a known compound to make sure that each batch of vesicles formed was conducive to cation translocation.

Titration curves following the introduction of **29** were exponential in character. An exponential was fitted to the titration curve, and a rate in milliliters per second was derived. This rate was converted to the reported rate of moles of protons per second by using the molarity of the standardized base and the stoichiometry of the titration. This

non-linear fit procedure produced an apparent first order rate constant from which an initial rate of 5.9 x 10^{-9} H^+ mol· s^{-1} was calculated.

Diazacrown isophthalate **30** demonstrated cation transport through prolonged release of protons from the vesicles, as shown in Figure 26. The titration of the proton flux from this compound was also found to be exponential in character, and an initial rate constant of 9.3 x 10^{-9} H^+ mol· s^{-1}, was derived. This is about 58% faster than perfluorinated **29** at the same concentration.

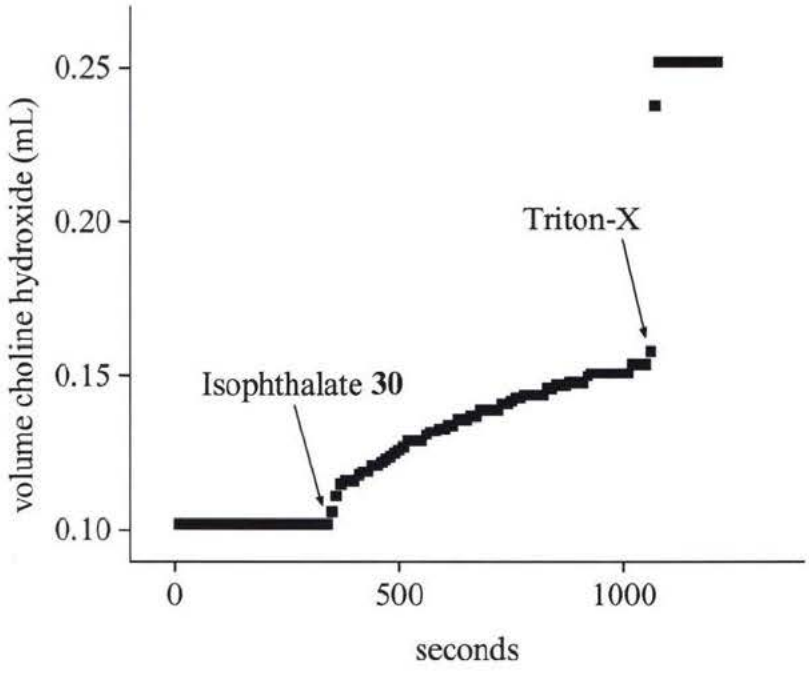

Figure 26: Cation transport activity of diaza-18-crown-6 alkoxy isophthalate **30** in vesicles by the pH stat method.

The data for a cesium-cation pH stat experiment with **30**, however, was found to have a lower rate than that for the potassium experiment (4.5 x 10^{-9} H^+ mol· s^{-1}). These data are summarized in Table 3. It is remarkable that this minimized isophthalate (**30**) version of Gokel's tris-diaza design is still able to induce cation transport, with only one isophthalate replacing the two terminal diazacrown headgroups.

Table 3: Comparison of pH-stat transport rates of Isophthalates 29 and 30 with Gramicidin

Compound	Concentration (M)	Cation	Absolute Rate mol $H^+ \cdot s^{-1}$
perfluorinated **29**	1.5×10^{-4}	K^+	5.9×10^{-9}
diazacrown **30**	1.5×10^{-4}	K^+	9.3×10^{-9}
diazacrown **30**	1.5×10^{-4}	Cs^+	4.5×10^{-9}
Gramicidin[a]	13.3×10^{-9}	K^+	3.3×10^{-9}

a) as determined by Kaye (25 °C), [K+] = 43 mM, no FCCP[44]

Table 3 compares the rate constants determined with the well-know cation-channel forming compound, Gramicidin. The results clearly indicate that the active isophthalates **29** and **30** are relatively inefficient cation channels compared to the naturally occurring pentadecapeptide. Gramicidin effects roughly the same (within an order of magnitude) cation flux as the two isophthalates, but at a concentration five orders of magnitude more dilute.

At this point in the project, the data from planar bilayer survey were compared with the data from the vesicle survey. The two surveys conducted yielded conflicting results. Isophthalates **29** (perfluorinated) and **30** (diazacrown) were consistently active in the pH stat experiments, yet these two derivatives had previously been shown to be inactive in planar bilayers. Isophthalate **17a** was the only compound active in the bilayer clamp survey, yet it was inactive in the vesicle survey. The homolog of **17a**, compound **32**, is only two carbons longer than **17a**, yet was inactive in both vesicle and planar bilayer surveys. In order to clarify these conflicting observations, a return to the bilayer clamp

with a more conventional approach was made. The goal was to determine whether these compounds could give single-channel behaviors under conditions less stringent than the fixed survey protocol described in chapter 2. The return to the voltage-clamp will be covered in the beginning of the next chapter, with a focus on Isophthalates **29**, **30**, and **32**.

Chapter 5: Conclusion

5.1 Revised bilayer clamp survey

Compounds **29**, **30**, **31** and **32** were examined with three revisions to the survey: (1) solutions of the compounds were simultaneously injected on both sides (i.e. into *cis* and *trans* compartments) of the bilayer, (2) the solutions in which compounds were introduced were made 5.7 times more concentrated (8 mM), and (3) more experiments were attempted to effect cation transport. Even with these modifications to the survey, isophthalate **31** failed to give any sign of single-channel formation in five different planar bilayer experiments under the revised conditions.

Inconsistent activity for the diazacrown isophthalate **30** was observed under the revised survey. On average "irregular" conductances were observed for isophthalate **30**, although three observations of events resembling more well-defined "square top"

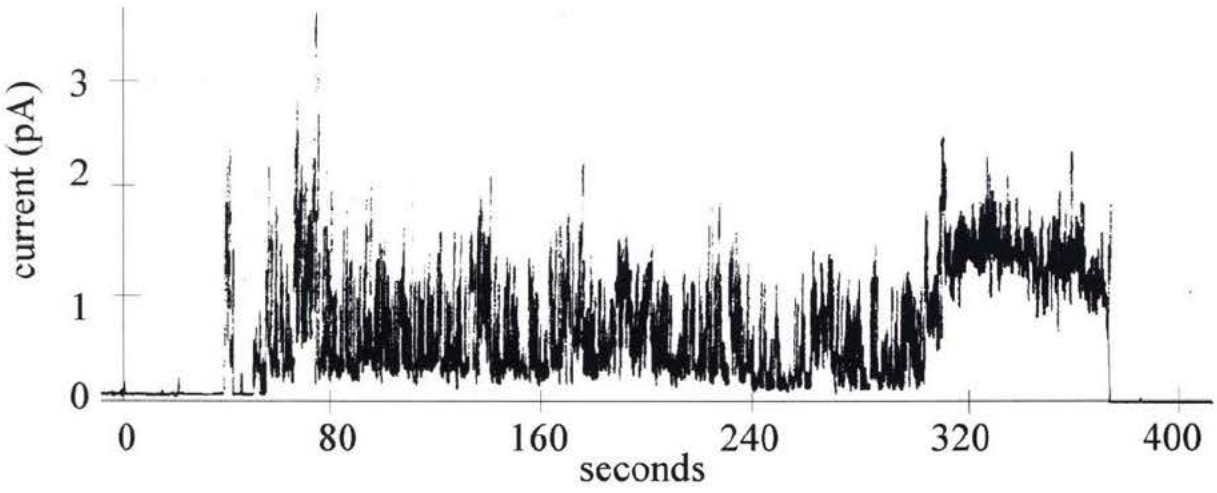

Figure 27: Irregular activity induced by diazacrown **30** at a transmembrane potential of +120 mV in 1M KCl (not filtered).

step-changes in conductance have been made for this compound. Typical irregular conductance behavior for the diazacrown derivative **30** is depicted in the current-time trace in Figure 27. Unfortunately, this trace was not digitized, filtered and recorded, because at the time it was not considered worthwhile data. The raw trace from a chart recorder was scanned to exemplify what is meant by irregular, hard to characterize activity. Although irregular, there is clearly continuous current of approximately 1.5 pA flowing for nearly 60 seconds (~ 310 to 370 s) towards the end of the trace in Figure 27. This type of irregular activity would be sufficient to give the transport results obtained from the vesicle survey, since the vesicle experiment can not distinguish irregular activity from well-defined single-channel behavior.

The tridecafluoro-5-alkoxy isophthalate **29** induced 26 clear step-changes in conductance under the revised conditions, although this is a handful compared to the thousands observed for the active compound **17a** under the initial survey. A few observations (4) were made at positive transmembrane potentials, although the majority (22) were made at negative potential.

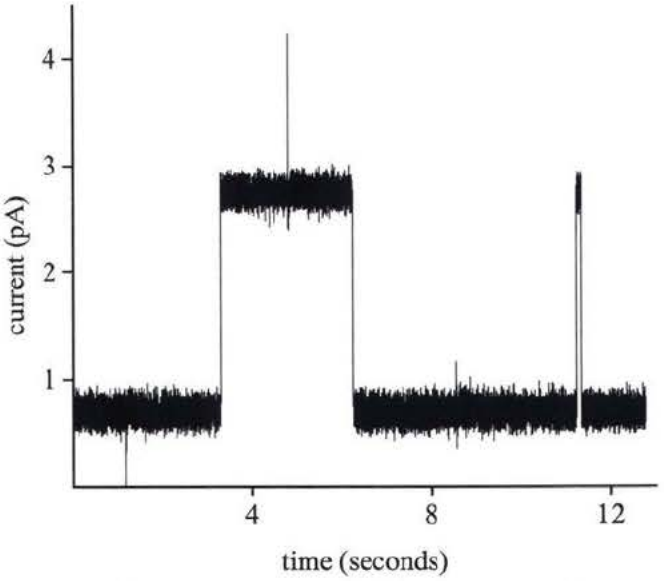

Figure 28: Isophthalate **29** induced regular step-changes in conductance of widely varying duration under the revised survey (+120 mV, 1M KCl).

At both negative and positive transmembrane potentials, a range of step-changes in conductance was observed: -0.7 to –2.9 pA at a negative transmembrane potential of –120 mV and +1.6 to +2.5 pA at +120 mV. Two typical observations of step-changes in conductance for **29** are depicted in Figure 28. Figure 28 illustrates the longest conductance observed for the fluorinated compound 29 in the first step change in conductance (3 seconds), but also show a typical, short yet clear step-change in conductance (less than a quarter of a second) after 11 seconds in the trace. Both are +2.1 pA in magnitude. The second conductance is more representative of average channel activity from **29**. It is significant that over four times as many observations were made for **29** at negative potentials over positive potentials. The histogram in Figure 29 summarizes the 22 observations of step changes in conductance made for **29** at a transmembrane potential of –120 mV. The distribution is broad, and no clear value is evident. Although the events are of short duration, the current carried is consistent with the relatively low level of activity observed in vesicles by the pH stat technique.

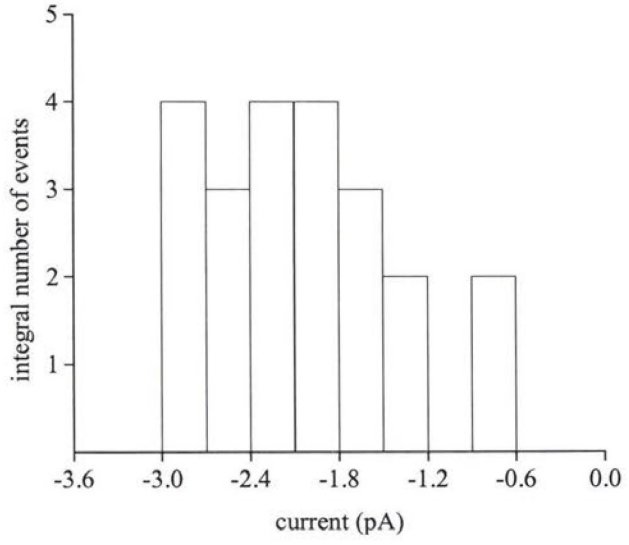

Figure 29: Histogram of all observations at negative potential indicating a range of step-changes in conductance for the tridecafluoro compound **29** (-120 mV, 1M KCl).

Compound **32** induced regular step-changes in conductances, although observations were few and far between and of rather short duration (relative to **17a**). An example of a regular step change in conductance is shown in Figure 30.

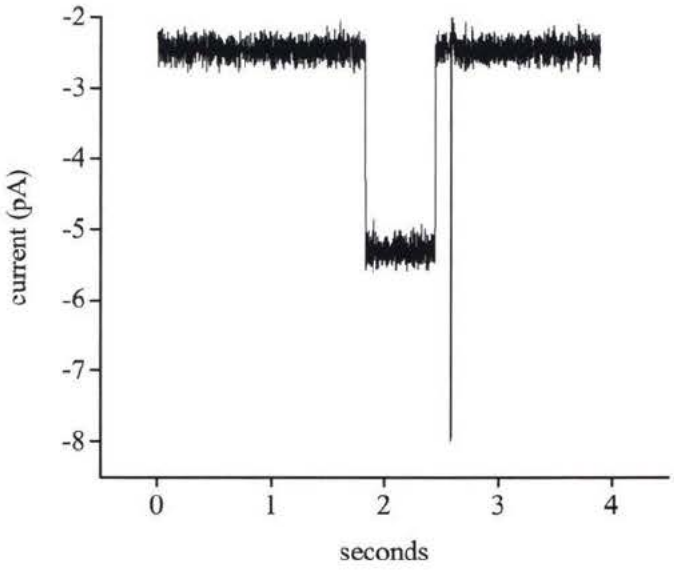

Figure 30: Isophthalate **32** induced step-changes in conductance following simultaneous injection on both sides of the bilayer (transmembrane potential of -120 mV, 1M KCl).

The activity of **32** was expected, as it is structurally very similar (two methylenes longer) than the active parent homolog **17a**. The step-change in conductance in Figure 30 is –2.8 pA in magnitude at a transmembrane potential of -120 mV, resulting in a conductance of 23 pS. In total, five clear step-changes in conductance were observed over a series of five experiments. All the observations were made at negative potentials, as shown in Table 4. The majority of observations for the terminal tridecafluoro compound **29** were also made at negative potential, in agreement with the fact that the dianions are driven towards the bilayer at negative polarity.

Table 4: Observed step-changes in conductance by compound 32 (-120 mV, K^+).

Event Number	Magnitude (pS)	Approx. Duration (ms)
1	17	82
2 (Fig. 30)	23	623
3	21	199
4	23	112
5	24	266

In comparison to the parent homolog **17a** (with step-changes in conductance 15.4 to 16 pS), a range of conductances varying from slightly larger in magnitude (17.5 pS), to significantly larger step-changes (23 pS in Fig. 27), were observed in 1M potassium chloride for homolog **32**. This demonstrates some flexibility in the active structure, as was the case for **17a**. However, no step changes were observed at positive potentials, which supports the aforementioned premise that isophthalates are driven into the bilayer at negative transmembrane potentials. The event in Figure 30 is the one of longest duration (623 ms) of the handful of observations made, indicating that the active structure of this homolog, although somewhat flexible like **17a**, is not as stable as the parent molecule. However, the events induced by **32** are clearly step changes in conductance, so the active structure retains a structural regularity. The greater magnitude of step-changes in conductance promoted by **32** relative to **17a** suggests that the two extra methylenes of **32** are providing a larger diameter conducting pathway for cation to flow. This provides some evidence that the active structure for both the homolog and the parent compound is an aggregate. The infrequency of events in planar bilayers is consistent with the very

inconsistent results provided by the pH stat technique (sometimes small cation flux was observed in vesicles).

5.2 Mechanistic Speculations

Although the step-changes in conductance observed for **17a** imply a regular, well-defined conducting pathway for cations, the challenge remains in proposing motifs for the collaboration of molecules of **17a**. The molecules of **17a** must follow a fine balance to form a structure that is consistent with the amphiphilic nature of the isophthalate, yet positions electron-rich moieties in key positions to stabilize, or temporarily bind, cations in transit.

An ester isophthalate **15** was shown to form hexameric aggregates in toluene (10 mM)[37] in Figure 6. Hexameric ISA aggregates have been estimated to have an internal diameter of 14 Å.[37] In comparison to Gramicidin, which has an aqueous pore 4 Å in diameter[2] and demonstrates conductances of approximately 30 pS for the cesium cation[4] to 15 pS for the sodium cation,[5] this is a massive cavity. Compound **17a** demonstrates step-changes in conductance nearly equal to Gramicidin for the cesium cation (31.0 pS, Table 2) and over a third less for the sodium cation (9.2 pS), thus, whatever the structure formed by **17a** is, it is certainly not the hexamer in Figure 6 proposed by Yang.

It is very doubtful that a single molecule or dimer of **17a** would create a large enough hydrophilic cavity or "defect zone" for cation translocation to occur. It is difficult to envisage a hydrated cavity spanning at least 35 Å in length formed by only one or two molecules.

Section 1.7 described several supramolecular architectures that have been observed for ISA derivatives in pure form and in a variety of solvates. The motifs presented

in section 1.7 provide a reasonable starting point for a cation channel model. For example, compound **17a** could be forming some type of extended ladder structure, as shown in Figure 31 (Model 1).

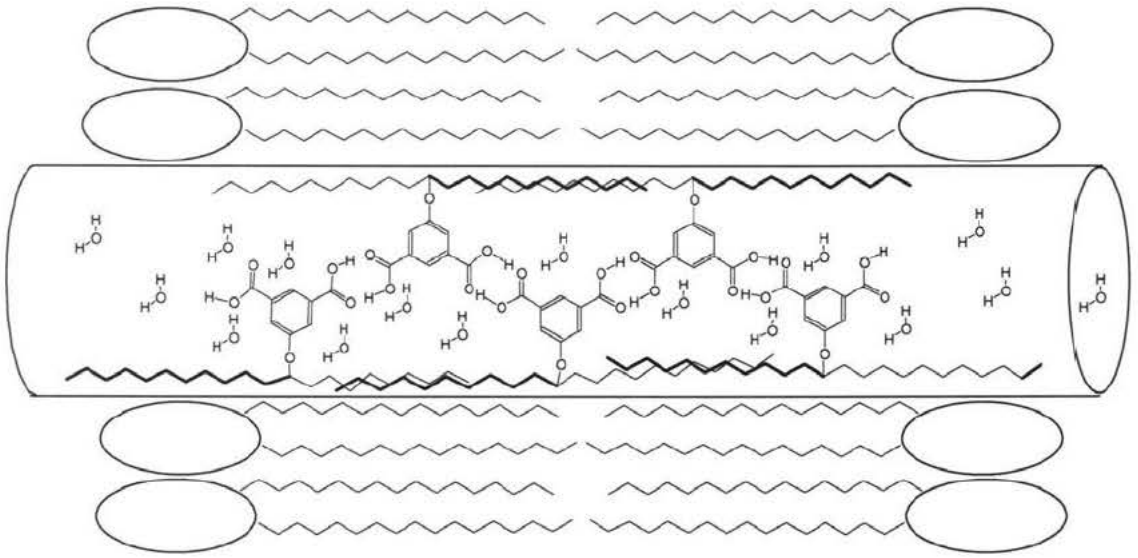

Figure 31 Model 1: Hydrated cylinder formed by oligomeric aggregate of **17a** as a model for a cation channel spanning a planar bilayer.

The isophthalate headgroups in Figure 31 are in a conformation similar to that for pure 5-alkoxy isophthalic acid as illustrated in Figure 2. This ladder structure would most likely have a three dimensional component if this were the active supramolecular architecture taken on by **17a** in the bilayer. This type of ladder architecture could only be assumed if the molecules were mostly protonated, which is highly unlikely since these isophthalates are predominantly deprotonated at the pH of the experiment. Since the isophthalates are typically introduced to the aqueous electrolyte in methanol, solvent or water incorporation in the active structure is likely.

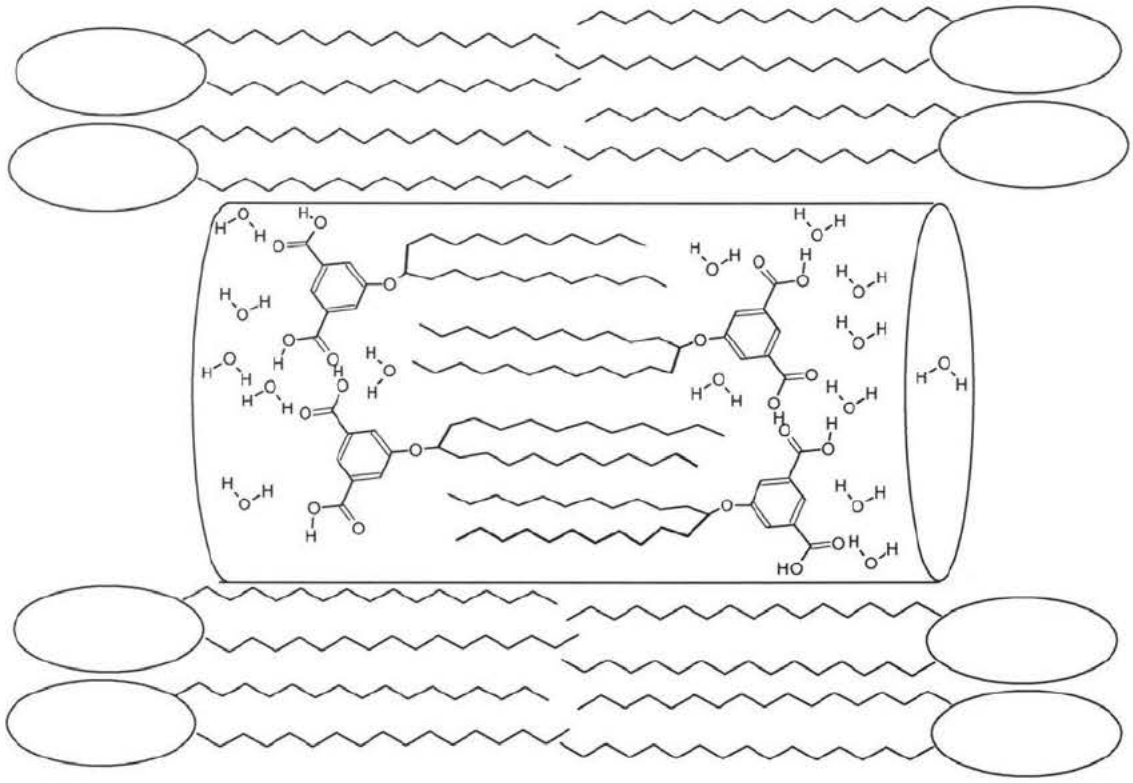

Figure 32 Model 2: Oligomeric aggregate as a bilayer-spanning structure formed by interdigitated **17a** exhibiting hydrogen-bonding with water.

An alternative model derived from structural studies in section 1.7 is depicted in Figure 32 (Model 2). Such an interdigitated arrangement would have a short planar section in the middle of the bilayer. Figure 32 suffers from the fact that it is a sheet structure like Figure 30, and probably would not be significantly hydrated at the midplane of the bilayer. The "defect zone" promoted by **17a** is most likely a hydrated, three dimensional cavity, which is not evident from Figures 31 and 32.

The most probable hypothesis proposed for isophthalate **17a** is that this amphiphile is forming a small aggregate of a few molecules, giving rise to an aqueous pore extending into the hydrophobic interior of the bilayer. Given the relatively small magnitude of the

conductance exhibited by this amphiphile relative to other synthetic architectures, this aqueous bundle could be as small as three molecules (trimeric).

Figure 33 (Model 3a) illustrates the columnar shape that such a pore could have, and shows how the negative charges of the carboxylates project outward and would be in close proximity to the positively charged choline of the phosphatidylcholine zwitterion. In model 3a as drawn, the dianionic charges would tend to push the aggregate apart.

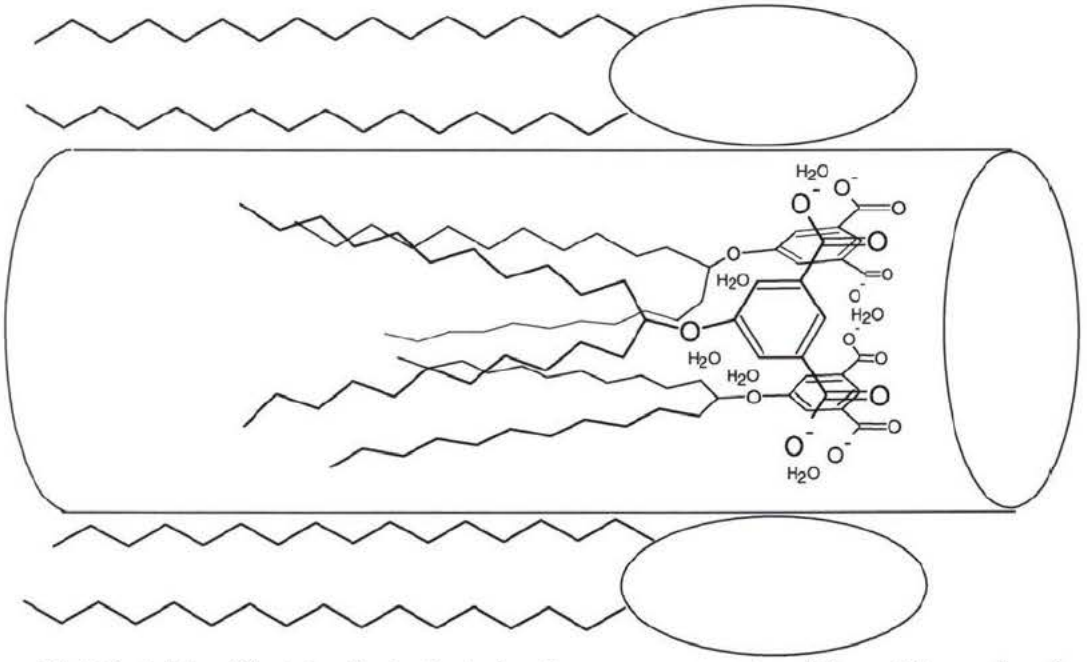

Figure 33 Model 3a: Sketch of a hydrated columnar aggregate of three **17a** molecules in one face of the bilayer.

Interactions with a sea of outward directed, positively charged choline could be the critical stabilizing force in the motif proposed in one face of the bilayer in Figure 33. Hydrogen-bonding with water could keep the dianions from repelling one another enough to hold the aggregate together. Furthermore, any degree of protonation would stabilize such an aggregate.

Isophthalate **17a** has been estimated to be 33 Å long (Cache program) with the alkoxy chain fully extended, as in Figure 31. With the alkoxy moiety in the "U" conformation as

in Figure 32, it is not likely that a membrane spanning structure will be achieved when the inner hydrocarbon "slab" of the bilayer has been estimated at 34Å.[53]

If the configuration in Figure 33 were indeed the active conformation, a "defect zone" would have to be promoted in the opposite monolayer large enough to permit the passing of cations. Phase separations are known to be induced by the addition of another substance, occurring in small clusters due to incomplete miscibility, with an otherwise intact overall bilayer morphology.[57] If a "defect zone" is promoted through incomplete miscibility in one face of the bilayer, cations can be hydrated near the midplane, and it would be likely that they are driven through the opposite monolayer, even without a concerted "pathway" through the second monolayer. However, this scenario is speculative at best.

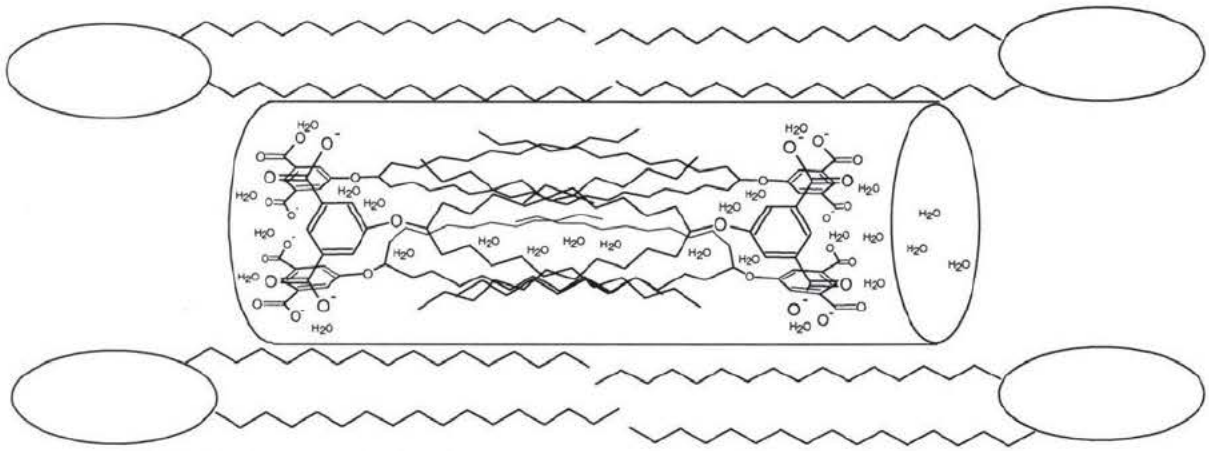

Figure 34 Model 3b: Sketch of bis columnar structure for **17a.**

Since a single-sided column structure is just at the threshold of being long enough to form a membrane-spanning structure, a bis columnar structure is also possible, shown in Figure 34. This type of structure would definitely have a higher entropic cost in self-associating into the double-ended column than the single-ended structure in Figure 33. However, it is possible, given the structure determined for monoalkoxy isophthalates in

Figure 7.[38] The crystal morphology of this isophthalate is the most relevant of prior ISA work, and provides some insight into how **17a** and **32** could form an active membrane-spanning structure. Figure 34 is larger than the minimum proposed motif of three to four molecules in Figure 33, yet would still provide a restricted cation-conducting pathway. There is no way of knowing the exact conformation of **17a** from the bilayer clamp data acquired. All that is known with certainty is that **17a** can consistently form a well-defined, regular conduction pathway.

Hypothetically, the alkyl chain of the active isophthalate **17a** was of just the right length to form a compact aggregate in the bilayer. Interestingly, the ether substitution of **17a** was on an even numbered carbon (12), whereas the other two derivatives synthesized had the ether substituted to an odd numbered carbon (9, 13). Although the alkoxy moieties for compounds **17a**, **31** and **32** all have odd numbers of carbons, the number of carbons on each side of the ether-substituted carbon is odd for **17a** and even for **31** and **32**. The odd number of carbons to each side of the ether-linked carbon in isophthalate **17a** may influence the stability of such an aggregate in solution. Even-numbered alkanes are known to have higher enthalpies and entropies in reaching the solid/liquid phase transition over their odd-numbered counterparts.[57] The odd number of carbons to each side of the ether-substituted carbon in **17a** should be closer to a "melted" state than the odd number to each side in **32**, and this may very well explain the stability demonstrated by **17a** over **32**. Short-lived flickering events were observed for the longer isophthalate **17a** homolog synthesized, **32**. Although short lived (i.e. less than half a second), the activity for **32** consisted of well-defined step-changes in conductance. The brevity of the activity suggests that the active structure for the homolog **32** is not as stable as the active structure for the parent compound, **17a**.

5.3 Principle findings of the project

Both surveys concur that the cation flux observed for the active isophthalates is relatively small, implying that the active cation conducting passageway(s) are relatively small. Although the step-changes in conductance exhibited by isophthalates **17a** and **32** were relatively small, this is no way diminishes the finding of clear, resolved step-changes in conductance. Isophthalate **17a** induced unambiguous, well-defined ohmic step-changes in conductance in planar bilayer voltage-clamp experiments, with three different alkali chlorides, yet produced inconsistent activity in the pH stat vesicle survey. The two compounds that were active in vesicles, **29** and **30**, were active at five orders of magnitude higher concentration than the concentration of the well-known pore-former Gramicidin (Table 3), producing approximately the same (within an order of magnitude) cation flux. It is still remarkable, however, that these single isophthalate derivatives are clearly active channel-forming compounds, at only one-sixth the molecular weight of Gramicidin (with respect to **17a**). Higher concentrations can be expected as required for an active structure that functions through aggregation beyond dimerization.

The results of the surveys are summarized in Table 5. Four compounds, isophthalates **17a**, **29**, **30** and **32,** were found to be consistently active by the guidelines of the two surveys conducted in this thesis. There was some inconsistency between the two surveys. Isophthalate **17a** produced very inconsistent results in vesicles, but was active under the original bilayer clamp survey. Isophthalate **30** induced irregular conductances in planar bilayer, but the activity observed would be enough to explain the titration curve produced in vesicles. Although vesicles are spheres of bilayers, the lipid packing

morphology in vesicles is curved and not planar, and this is a critical factor for the insertion of a molecule into the bilayer.

It is noteworthy that these four compounds represent three structurally unique motifs: monoalkoxy, *n*-monoalkoxy perflouronated, and diazacrown, respectively. Compounds **29** and **32** were found to be active under the revised survey. The fact that **32** was inactive in vesicles is in agreement with the observation of very infrequently occurring subsecond channel openings which promote relatively low cation flux in the bilayer clamp experiments. The channels observed through step-changes in conductance for **32** would not be expected to induce a significant cation flux in vesicles. Although cation flux from isophthalates was not great enough to be applicable, the single-channel conductances for **17a** are the best evidence that isophthalates can form ordered structures in phospholipid bilayers (although the exact ordering remains elusive).

Table 5: Summary of surveys

survey	monoalkoxy						dialkoxy			naphthyl, perfluoro					diaza crown	homologs of **17a**	
	16	**17a**	**18**	**19**	**20**	**21**	**22**	**23**	**24**	**25**	**26**	**27**	**28**	**29**	**30**	**31**	**32**
bilayer clamp		●												●	○		●
pH stat		○												●	●		

Consistently active under either the original or revised survey (●) and inconsistent activity observed (○)

Isophthalates **29** and **30** induced small but clear cation-flux in medium-large vesicles as probed by the pH stat technique. Isophthalate **30** exhibited a significantly faster K^+ transport rate than **29** in vesicle experiments, implying a larger cation conducting pathway. The diazacrown derivative **30** induced inconsistent activity in planar lipid bilayer experiments, but the terminal tridecafluoro compound **29** induced clear step changes in conductance at both polarities whereas **30** was typically irregular. Compared to Gokel's tris diazacrown derivative, **30**, should be more amphiphilic (dianionic head group), however, it only has the central diaza-18-crown-6 cation-conduction site, and not three as in Gokel's compound **7**. These cation conducting diazacrowns on each end are concluded to be important as cation-conducting headgroups, since analogs of **7** have induced regular, well-defined activity in planar lipid bilayers. The fluorinated alkoxy terminus of **29** adds an element of rigidity to the alkyl end of the molecule that other alkoxy isophthalate derivatives do not possess, and hence may facilitate insertion into the vesicles over the saturated hydrocarbon analogs examined.

In summary, the motifs presented in section 1.7 are most likely not related to the active structures in this thesis (i.e. Models 1 and 2). The most probable channel conformation is Model 3a, as it is consistent with isophthalates being amphiphilic and inducing relatively small step-changes in conductance. Although speculative, this model should have the lowest hypothetical entropic cost in arrangement, as compared to models 1, 2 and 3b. In any case, compounds **17a**, **29** and **32** are the lowest molecular weight channel-forming compounds. This research revises what was previously thought as requisite to form a membrane-spanning structure.

6 Experimental

6.1 Bilayer voltage-clamp experiments

6.1.1 Chemicals

Egg phosphatidylcholine (PC), diphytanoyl phosphatidylcholine (diPhyPC), cholesterol (chol.), and egg phosphatidic acid (egg PA) were purchased from Avanti Polar Lipids. They were shipped on dry ice and stored in a freezer. FCCP (carbonyl cyanide *p*-(trifluoromethoxy) phenylhydrazone), methanol, D-mannitol, and Bis-Tris (2,2-bis(hydroxymethyl)-2,2',2"-nitrilotriethanol), and sulfuric acid (ultrapure) were purchased from Aldrich. HPLC grade chloroform and anhydrous diethyl ether were bought from BDH. Gramicidin and Triton-X were purchased from Aldrich. Methanol (HPLC grade), chloroform (HPLC grade), decane (99%), and silver chloride were purchased from Sigma-Aldrich. Chloride salts of sodium, potassium, and cesium cations were purchased from Aldrich. Electrolyte solutions were made up with D^3 (deionized, distilled twice) water.

6.1.2 Instrumentation

To apply potentials and monitor current, a BC-525A bilayer clamp (Warner Instrument) was employed. The output signal was monitored with a 100 MHz Oscilloscope (Tektronix), analog filtered with a model 902 8-pole Bessel filter (Frequency Devices), fed to a Digidata 1200A 333kHz digitizer (Axon Instruments), and recorded on a PC. All data acquisition was performed using the Fetchex program of the pClamp 6 software suite (Axon Instruments).

The experimental cell was placed inside a solid aluminum Faraday cage (Machine Shop, UVic), which floats atop a pneumatically dampened table (TMC). Bilayer cuvettes

with 250 μm apertures made of either Delrin™ (polyacetal) or polystyrene (Warner Instrument) were slid into cuvette holders fabricated from Delrin™ blocks (Machine Shop, UVic).

Salt bridges were used to stabilize junction potentials, and were employed between the electrolyte in each well and the Ag/AgCl electrode. Glass "U" tubes (3 mm o.d.) were filled with a solution of boiling 1% w/w agar in electrolyte (either 3M NaCl, KCl, or CsCl) using 3 cc disposable syringes. The ends of the bridges must be flat (cut cleanly, perpendicular to the tube) for a good seal to the syringe which inhibits air bubbles. The bridges met the electrodes in small vials (Kimax, 9 x 30mm, ¼ dram) filled with 3M electrolyte. Once bridges were exposed to candidate compounds, they were boiled to remove all agar, soaked in a concentrated base bath and rinsed profusely with tap water, 100% ethanol and finally rinsed with D^3 water (double distilled, deionized water).

Electrical contact between the salt bridge wells and the headstage was made by silver/silver chloride electrodes. These electrodes were fabricated by repeatedly dipping one end of a silver wire (typically 0.5mm dia.) in molten silver chloride (as it starts to cool) and crimping a male copper pin to the other end, which provided contact to the headstage. Concentrated HCl was used to clean the silver chloride end of the electrodes, followed by D^3 water.

6.1.3 Bilayer Clamp Method

Stock solutions of either PC, PA, cholesterol (8:1:1) or diPhyPC were made up in half dram vials in HPLC grade chloroform under argon in a glove bag and were kept in the freezer in a dessicator. Aliquots of the stock solutions were transferred to 10 mL round bottom flasks and left under vacuum overnight; the lipids formed colourless films on the

bottoms of the flasks. Decane was added to form 17 to 25 mg/mL mixtures, purged with Nitrogen, swirled to pick up lipid, and sonicated for 1 minute in a small bath sonicator. Lipid made up in decane rarely gave suitable bilayers on the second day. Camel hair brush tips (size 10/0) were cut down around the base until about a dozen hairs were left at the tip. Teflon tape was used to wrap the base of the brush such that the hairs at the tip were slightly splayed. The aperture in the bilayer cuvette was prepared for bilayer formation by applying primer coats of the lipid in decane solution with the brush to both sides of the aperture. Decane was then evaporated under a gentle flow of nitrogen before applying another coat (three to four coats were typically applied). The bilayer cuvette was then inserted into one well of the holder. Electrolyte levels were made equal so as not to create a pressure gradient across the bilayer: 2.6 mL of 1M electrolyte were added into the cuvette and 5.0 mL into the free well of the holder.

Once electrodes and salt bridges were in place, the junction potential was corrected before the bilayer was formed. The bilayer clamp provides potential to compensate for voltage drops which occur at each interface, or junction, with significant resistance. The salt bridges helped to stabilize the junction potential, which was typically 0 or ±1 mV. Junction potentials greater than ±4 mV were attributed to electrode degradation. Minor adjustments in junction potential were typical from one experiment to the next.

Bilayers were formed by two methods: brushing and dipping. In the brushing method, a very small amount of lipid solution was placed on the tip of the brush, and lipid was spread with downward strokes using the side of the bristles. An immediate plummet in conductance observed on the oscilloscope indicated a film had formed. At this point, the "capacitance test" function of the bilayer clamp was enabled, feeding a 100 Hz triangle wave to the headstage. This triangle wave was integrated over the input capacitance, and

this integration was manifest as a square wave on the oscilloscope. The height of this wave is inversely proportional to the capacitance between the two wells of electrolyte. Brushing was continued, drying the brushtip on a Chemwipe between strokes, until the observed capacitance was 190 to 220 pF. The manufacturer's suggested capacitance is 0.4 $\mu F/cm^2$. For a 250 μm diameter hole, this would be an area of 4.91×10^{-4} cm^2, so the suggested capacitance is about 196 pF. The observed capacitance, however, is also a function of the area of the annulus, or the ring of solvent around the bilayer aperture. Bilayers formed by brushing are known to contain significant amounts of hydrocarbon (decane) from examination of bilayers through electron microscopy[58] and analysis of their composition,[59] therefore, an annulus (or bulk decane ring) can be expected to form around the lipid film. The typical 200 to 220 pF capacitance indicates a small solvent annulus and a thin bilayer over the aperture.

After lipid in decane had been introduced by brushing, a lipid/decane film formed on the surface of the electrolyte, and bilayers could then be formed by the dipping method. The dipping method is usually the method used for forming bilayers in an experimental setup where an aperture in a thin sheet partition (PTFE)[60, 45] is clamped between pools of electrolyte, and the bilayer is formed by dipping through the air-water interface by withdrawl and replacement of the cuvette. In this apparatus, the entire cuvette was pulled up vertically to expose one face of the aperture to the air-water interface held in the cell holder to oppose monolayers. The dipping method tended to more readily yield bilayers of high capacitance. Many bilayers were formed by initially dipping to form a bilayer that was brushed with downward strokes to sufficiently high capacitance. Both the painting and dipping methods have been used conjointly by other researchers.[45]

Once a bilayer of sufficient capacitance was formed, potential was applied across the bilayer (± 100 mV) to test for leakiness. A period of conductivity was recorded for 40 minutes (alternating polarity every 10 minutes) to establish that the bilayer was of low conductance (0.1 pA to 0.4 pA continuous current, or 1 to 4 pS conductance). Bilayers which exhibited 3 spikes greater than 0.5 pA above the baseline were not used to survey the candidate isophthalates.

Once a bilayer of sufficient quality was formed, aliquots of the candidate isophthalates (typically 1.5 mM in methanol, trifluoroethanol, or DMSO) were injected with a microlitre syringe as closely as possible to the bilayer in the free well of the cuvette holder (*cis* side). The measured voltage was applied with respect to the trans (cuvette) side of the bilayer,[12] making the trans side the relative ground. Every 10 to 15 minutes, successive aliquots of isophthalate were injected and the polarity was switched. For a typical experiment, 10 µL of candidate isophthalate were injected and +120 mV were applied for 15 minutes, at which point another 10 µL aliquot was injected and –120 mV were applied for another 15 minutes, when another 10 µL were injected and the polarity switched for the third time.

Once activity was observed, data files of current as a function of time were acquired using the Fetchex program of the pClamp 6 suite. Cation transport activity was identified as discrete step-changes in conductance, as the switch is made to an "open" state. Five minute files were recorded at a sampling rate of 20 kHz for each potential and polarity, i.e. +80 mV, -80 mV, + 100 mV, -100 mV, + 120 mV, -120 mV. Files were recorded at ± 140 mV if the baseline was not excessively noisy at ± 120 mV. Once it was established through analysis that the observed activity was on the time scale of seconds (and not faster), the sampling rate was decreased to 5 kHz to conserve disk space. The files were

imported into the spreadsheet Origin as DAT files and low pass filtering was performed at 100Hz using a Fast Fourier Transform.

6.2 Vesicle experiments using the pH stat technique

6.2.1 Instrumentation

A Metrohm automatic burette (655 Dosimat) was used in conjunction with an automatic titrator (614 Impulsomat) and pH meter (632). Data was fed to an HP-85 from the automatic burette, and interfaced with a 486 PC which recorded the data. The ultrasonic sonicator (Heat Systems W385) was located in the University of Victoria's Biochemistry department. The vesicle sizer was a LiposoFast (Avestin, Ottawa, ON), using a 19 mm (dia.) polycarbonate membrane (pore dia. 400 nm). The particle sizer used to characterize the vesicles was a Nicomp Submicron Particle Sizer Model 370 (Nicomp, Santa Barbara, CA, USA)

6.2.2 Vesicle preparation and sizing

Vesicles were prepared using the same lipid mixture that was used for the majority of planar bilayer experiments, PC:PA:cholesterol in an 8:1:1 ratio. Vesicles were obtained through sonication, reverse phase evaporation, sizing through a membrane and gel filtration, following a documented procedure.[44] The stock solutions required for "internal" and "external" buffers were prepared and handled as described by Kaye[44]. A stock solution of 25 mg/mL PC:PA:cholesterol (8:1:1) in chloroform (8.3 mg/mL) was kept in the freezer. Using a pipette, 6 mL of this stock solution was transferred to a special round bottom flask with a sunken bottom and was left under vacuum overnight at room temperature. To the completely dry film, 6 mL diethyl ether was added and when

dissolved 2 mL of internal buffer (pH 6.6) was added. The round bottom was stoppered with a nitrogen filled balloon [44] to limit the lipid's exposure to atmospheric air and water.

A 13 mm flat tip was fitted on the probe sonicator (Heat Systems) and tuned, and the lipid mixture was sonicated (30 two second pulses at output level 5, duty cycle 50). After sonicating, the previously clear, colourless lipid mixture took on an opaque, dull grey appearance. The round bottom was re-stoppered with the balloon. The diethyl ether was removed on a rotary evaporator with the water bath set to 25°C to yield predominantly large unilamellar vesicles with a large portion of the buffer entrapped.[44] After 5 to 10 minutes when most of the ether has evaporated, the vesicles go through a soapy, gelatinous phase and bumping is prevalent. Once bubbling and bumping subside, the vesicles take on a thicker appearance and settle in the bottom of the flask. At this point, 3 mL of external buffer (pH 7.6) was added, and rotary evaporation was continued at 25 °C under slightly reduced pressure for an hour.[44]

The vesicles were sized using two 500 µL syringes, one on each side of the LiposoFast membrane apparatus (Avestin, ON). The vesicles were slowly passed through the polycarbonate membrane (400 nm) back and forth and odd number of times (typically 21). Size-exclusion chromatography was then performed on the vesicles. Two disposable size-exclusion columns (Sephadex G-25) were first flushed with external buffer solution before loading half the vesicles into each column. The first 14 opaque drops were allowed to pass through, and drops 15 through 55 from each column were collected.

The vesicles which were used for the bulk of the survey were characterized by dynamic light scattering using a Nicomp Submicron Particle Sizer, Model 370 (Nicomp, CA). Blank external buffer solution was filtered using a Gelman 0.45 μm filter (gave a reading of 14 kHz) and was used to perform successive serial dilutions on a sample of vesicles (51 hours old) until a reading of 60 to 63 kHz was obtained. The results of the volume-weight Nicomp distribution analysis were two predominant vesicle diameters in a bimodal distribution: 231.5 nm (83.1%) and 81.3 nm (18.7%).

6.2.3 pH stat method

The vesicle cell was maintained at 22.5°C and continuously purged with nitrogen to inhibit carbon dioxide uptake. The cell was washed with methanol and rinsed with D^3 water in between experiments. All of the candidates were deprotonated with 25 μL of 90.7 mM choline hydroxide, so that when added to the external solution, the pH would not lower past the "stat" pH of 8.6. An aliquot (100 μL) of vesicles was diluted with 5 mL of the external choline sulfate solution. Titrant was added to bring the pH of the system to 8.6, thus establishing a 2 pH unit gradient across the vesicle bilayer. As soon as the pH stabilized, the pH stat program was started and the titrant volume was recorded as a function of time. A proton gradient decoupler, FCCP (carbonyl cyanide 4-(trifluoromethoxy)phenylhydrazone), was added (19.3 nanomol), to facilitate the release of protons. An alkali cation gradient was posed by introducing potassium sulfate (25 μmol) to the vesicle mixture. Candidate isophthalic acids (0.8 μmol) in either methanol or DMSO were mixed with a small amount of base (23 to 29 μL of 90.7 mM choline hydroxide) to deprotonate the diacids and make them slightly basic. This was necessary so that the pH would not fall below the set pH of 8.6 as a result of candidate acidity. A

prolonged decrease in pH could then be attributed to protons being released from inside the vesicles. When the gradients collapse, protons released to the external solution cause the external pH to drop, and the pH stat controlled auto-titrator begins adding titrant to maintain the set pH. After several minutes, the volume as a function of time plot flattens out, and the detergent Triton-X was added to lyse the vesicles and release the remaining protons to the external solution. The raw rate was expressed in milliliters of choline hydroxide per second, as derived from an exponential fit using the spreadsheet Origin. The rate obtained was converted to an absolute rate of moles of protons per second.

6.3 Synthesis of 5-(9-heptadecoxy) isophthalic acid (31)

9-Heptadecanol (**35**)

9-Heptadecanone (10.0 g, 39.3 mmol) **33** was combined with lithium aluminum hydride (1.3 equiv., 1.94 g, 51.1 mmol) in dry THF. The reaction mixture was stirred at reflux for three hours under nitrogen. The crude reaction mixture was placed in an ice bath, and excess $LiAlH_4$ was deactivated with distilled water (1.9 mL), followed by 1.9 NaOH (15% w/w, 1.9 mL), and distilled water (5.7 mL). Solids were removed by filtration and the organic phase was isolated. The aqueous phase was extracted three times with 10mL aliquots of diethyl ether. The combined organic extracts were washed twice with distilled water. The organic phase was dried over magnesium sulfate and the solvent was removed on a rotary evaporator to yield 9.08g (35.4 mmol, 90%) of **35**.

^{1}H NMR: ($CDCl_3$): 3.55 (1H, quin.), 1.5 to 1.2 (28H, m.), 0.9 (6H, br.t.)

^{13}C NMR: ($CDCl_3$) 72.0, 37.5, 31.9, 29.7, 29.6, 29.28, 25.7, 22.7, 14.1

FTIR (KBr pellet): strong absorbance at 3305 cm^{-1} (O-H stretch), absence of carbonyl around 1750 cm^{-1}

9-Bromoheptadecane (**37**)

9-Heptadecanol (9.08 grams, 35.4 mmol) **35** was added to 80 mL dry, distilled acetonitrile, and was heated until dissolved. Triphenylphosphine (10.21 grams, 38.9 mmol) were then added, and the mixture was brought to 60°C. Bromine in acetonitrile (2.0 mL Br_2 in 20 mL) was added dropwise at a rate to maintain the temperature above 60°C. The reaction was stirred for an hour at 62 to 64°C. Distilled water (250 mL) was added to the reaction mixture and it was cooled in an ice bath. Solids were removed by vacuum filtration. Distilled water was added to the filtrate until the total volume was 1 litre, and the filtrate was extracted four times with 40 mL aliquots of diethyl ether. The combined extracts were dried over magnesium sulfate and the solvent was removed. The crude product was chromatographed on a silica column using pentane as the eluent to yield 9.47 g (29.7 mmol, 84%) of **37**.

^{1}H NMR: ($CDCl_3$): 4.0 (1H, br. quin.), 1.8 to 1.2 (28H, br.m.), 0.85 (6H, br.t.)

^{13}C NMR: ($CDCl_3$): 58.9, 39.2, 31.9, 29.7, 29.5, 29.3, 27.6, 22.7, 14.1.

Dimethyl 5-hydroxy isophthalate (**40**)

5-Hydroxy ISA (32.69 g, 179 mmol) **39** was stirred in methanol (400 mL) until dissolved. Concentrated sulfuric acid (1.0 mL) was added dropwise, and the reaction mixture was brought to reflux while stirring in an oil bath (2 hours, 100°C). The solvent was removed on a rotary evaporator, and residue was dissolved in ethyl acetate (450 mL). Water (100 mL) was added and the organic phase was extracted with 5% w/w sodium bicarbonate solution (200 mL). The organic phase was isolated, and dried by vacuum filtering through magnesium sulfate to yield 21.67g dimethyl isophthalate **40** (103.1 mmol, 57.6%).

^{1}H NMR (CD_3OD): 8.1 (1H, s), 7.55 (2H, s), 4.9 (1H, s), 3.9 (6H, s).

^{13}C NMR: (CD_3OD): 167.6, 159.2, 133.0, 122.4, 121.5, 52.9.

Dimethyl 5-(9-heptadecoxy) isophthalate (**41**)

Compound **40** (3.68g, 17.5 mmol) was dissolved in dry, distilled DMF (15 mL) under nitrogen. Sodium hydride (60% w/w in oil washed with pentane, 0.63 g, 26.3 mmol) was added and the solution was stirred under nitrogen for two hours at room temperature before addition of **37** (5.57 g, 17.5 mmol) and a catalytic amount of KI. The mixture was stirred at 55°C to 60°C for 18 hours. Excess NaH was deactivated with water. The solvents were removed on a rotary evaporator and the solid was dried under vacuum.

The solid was dissolved in dichloromethane, and extracted with NaOH (0.5M, 600 mL). The organic phase was isolated and the dichloromethane was removed on a rotary evaporator. The aqueous phases were extracted with dichloromethane in a continuous liquid/liquid extractor for 12 hours, at which time an opaque organic phase and a clear aqueous phase were present. The organic layers were combined to yield 4.14 g of product (9.22 mmol, 52.7%).

The product was isolated on a silica column using hexanes and ethyl acetate as the eluent. Final purification was achieved by chromatotron plate chromatography using 1:1 hexanes:chloroform as the eluent. One mm and two mm plates were combined to yield 0.347 g of **41** (0.773 mmol, 4.4%).

^{1}H NMR ($CDCl_3$): 8.2 (1H, s), 7.7 (2H,s), 4.3 (1H, br. quin.), 3.9 (6H, s), 1.7 to 1.2 (28H, br.m.), 0.85 (6H, br.t.).

^{13}C NMR: ($CDCl_3$): 166.3, 158.8, 131.7, 122.5, 121.0, 78.6, 52.3, 33.6, 31.8, 29.7, 29.5, 29.2, 25.2, 22.6, 14.1.

MS (+LSIMS, mNBA, m+1): 449.3

5-(9-Heptadecoxy) isophthalic acid (**31**)

The dimethylester **41**(0.173 g, 0.388 mmol) was dissolved in ethanol (100%, 20 mL) and brought to 100°C. With stirring, KOH (0.109g, 1.94 mmol) was added in 2:1 ethanol:water. The reaction mixture was maintained at 100°C for 25 minutes, was cooled and lowered into an ice bath. Concentrated HCl was added dropwise until the pH was 1. The ethanol was removed on a rotary evaporator, and the product precipitated in an ice bath; the precipitate (0.045 g, 0.106 mmol) was collected by vacuum filtration. The hydrolysis was repeated with 0.386 mmol **41** to yield 0.0888 g (0.211 mmol, 54.7%). The combined yield of the diacid **31** for both hydrolyses was 0.134g (0.317 mmol, 41%).

^{1}H NMR ($CDCl_3$): 8.4 (1H, s), 7.7 (2H, s), 4.35 (1H, br. quin.), 1.75 to 1.3 (28H, br.m.), 0.85 (6H, br.t.)

^{13}C NMR ($CDCl_3$): 171.5, 158.7, 130.9, 124.4, 122.0, 78.6, 33.7, 31.9, 29.8, 29.6, 29.3, 25.3, 22.7, 14.1.

MS (+LSIMS, mNBA, m+1): 421.2.

Exact Mass (+LSIMS, mNBA, m+1, mean of 3 runs) 421.2955

m.p. 141 to 144 ° C

Calculated for $C_{25}H_{40}O_5$: 71.39% carbon and 9.59 % hydrogen).

Found: 70.54% carbon and 8.73% hydrogen (Canadian Microanalytical Service, Ltd.)

6.4 Synthesis of 5-(13-pentacosanoxy) isophthalic acid (32)

13-Pentacosanol (**36**)

13-Pentacosanone **34** (10g, 27 mmol, Lancaster Synthesis) was dissolved in dry, distilled THF. Lithium aluminum hydride (1.95 g, 51.4 mmol) was added and the reaction mixture was stirred at reflux for 3.5 hours under nitrogen. The crude reaction mixture was placed in an ice bath, and excess $LiAlH_4$ was deactivated with distilled water

(2 mL), followed by sodium hydroxide (15% w/w, 2 mL), and distilled water (6 mL). Solids were removed by vacuum filtration and the organic phase was isolated. The aqueous phase was extracted with diethyl ether (30 mL). Extracts were combined and washed with distilled water (20 mL). The organic phase was dried over magnesium sulfate and the solvent was removed on a rotary evaporator to yield 2.85 g (7.73 mmol, 28.6%) of **36**.

^{1}H NMR ($CDCl_3$): 3.5 (1H, br. quin.), 1.45 to 1.2 (44H, br.m.), 0.85 (6H, br.t.).

^{13}C NMR ($CDCl_3$): 72.0, 37.5, 31.9, 29.7, 29.6, 29.4, 25.7, 22.7, 14.1.

FTIR (KBr pellet): strong O-H stretch at 3391 cm^{-1}, absence of carbonyl stretch around 1750 cm^{-1}

13-Bromopentacosanane (**38**)

13-Pentasosanol **36** (2.85 g, 7.73 mmol) was added to dry, distilled acetonitrile (80 mL). Triphenylphosphine (2.23 g, 8.5 mmol) was added and the mixture was brought to 56°C. A 1.1 equivalent bromine solution (0.44 mL Br_2 in 4.4 mL acetonitrile) was added dropwise to maintain the reaction mixture at 58°C. The temperature was increased to 65°C and was stirred for an hour at 65°C. The solution was allowed to cool, and the bulk of the solvent was removed on a rotary evaporator. Solids were removed by vacuum filtration. Distilled water (200 mL) was added to the reaction mixture and the filtrate was extracted with diethyl ether (200 mL). The extracts were combined, dried over magnesium sulfate and the solvent was removed on a rotary evaporator. 13-bromopentacosanane **38** was isolated on a silica column using pentane as the eluent, to yield 1.45 g (3.36 mmol, 43.5%).

^{1}H NMR ($CDCl_3$): 4.0 (1H, br. quin.), 1.85 to 1.2 (44H, br.m.), 0.85 (6H, br.t.).

^{13}C NMR ($CDCl_3$): 130.3, 59.0, 39.2, 31.9, 29.7, 29.6, 29.5, 29.4, 29.2, 29.1, 27.6, 27.2, 14.1.

Dimethyl 5-(13-pentacosanoxy) isophthalate (**42**)

Isophthalate **40** (0.982 g, 4.67 mmol) was dissolved in dry, distilled DMF (12 mL). Sodium hydride (60% oil dispersion washed with pentane, 1.86 equiv., 0.144 g, 6.02 mmol) was added to the solution, which was stirred under nitrogen for two hours. 13-bromopentacosanane (1.4 g, 3.24 mmol) **38** and a catalytic amount of KI (0.153 g) were added at room temperature, and the mixture was stirred for 12 hours at 55 to 60°C under nitrogen. The solution was allowed to cool, the DMF removed on a rotary evaporator, and the crude product dissolved in dichloromethane (100 mL) and extracted with sodium hydroxide (0.5 M, 200 mL). The aqueous phases were extracted with dichloromethane in a continuous liquid/liquid extractor overnight, and organic phases were combined and the solvent removed on a rotary evaporator. The alkoxy isophthalate **42** was isolated on a silica column using hexanes and ethyl acetate as eluent to yield 0.152 g (0.271 mmol, 8.4%).

^{1}H NMR ($CDCl_3$): 8.2 (1H, s), 7.65 (2H, s), 4.25 (1H, br.quin.), 3.85 (6H, s), 1.95 to 1.15 (44H, br.m.), 0.8 (6H, br.t.).

^{13}C NMR ($CDCl_3$): 166.2, 158.8, 130.3, 122.5, 121.0, 78.5, 52.3, 33.7, 32.6, 31.9, 29.8, 29.7, 29.6, 29.4, 29.2, 29.1, 25.2, 22.7, 14.1.

MS (+LSIMS, mNBA, m+1): 561.4

5-(13-Pentacosanoxy) isophthalic acid (**32**)

The alkoxy isophthalate **42** (0.152 g, 0.271 mmol) was dissolved in ethanol (100%, 25 mL) and was brought to 100°C. While stirring, potassium hydroxide (0.096 g, 1.71 mmol) was dissolved in water (12.5 mL) and added. The reaction mixture was

maintained at 100°C for 8 hours. The mixture was allowed to cool, lowered into an ice bath and concentrated HCl was added dropwise until the pH was 1. The ethanol was removed on a rotary evaporator, and the product **32** precipitated in an ice bath to yield 0.029 g (0.054 mmol, 20.1%).

^{1}H NMR (CD_3OD): 8.1 (1H, s), 7.6 (2H, s), 4.8 (1H, s), 4.3 (1H, br. quin.), 1.65 to 1.1 (44H, br.m.), 0.8 (6H, br.t.).

^{13}C NMR (CD_3OD): 168.8, 160.3, 133.8, 124.0, 121.9, 79.6, 34.8, 33.1, 30.8, 30.7, 30.6, 30.5, 26.2, 23.8, 14.5.

MS (+LSIMS, matrix mNBA, m+1): 533.3

Exact Mass (+LSIMS, matrix mNBA, m+1, mean of 3 runs) 533.4223

m.p. 77 to 78.5°C

Calculated for $C_{33}H_{56}O_5$: 74.38% carbon and 10.59 % hydrogen.

Found: 73.62 % carbon and 10.38 % (Canadian Microanalytical Service, Ltd.)

References

(1) Abel, E.; Meadows, E. S.; Suzuki, I.; Jin, T.; Gokel, G. W. *Chem. Comm.* **1997**, 1145 - 1446.

(2) Hille, B. *Ionic Channels of Excitable Membranes*; Sinauer Associates, Inc.: Sunderland, 1984.

(3) Dougherty, D. A.; Lester, H. A. *Angew. Chem. Int. Ed.* **1998**, *37*, 2329-2331.

(4) Stein, W. D. *Channels, Carriers, and Pumps*; Academic Press, Inc.: San Diego, 1990.

(5) Yeagle, P. *The Structure of Biological Membranes*; CRC Press, Inc.:Boca Raton, 1992.

(6) Bezrukov, S. M.; Rand, R. P.; Vodyanoy, I.; Parsegian, V. A. *Faraday Discuss.* **1999**, *111*.

(7) Ringsdorf, H.; Schlarb, B.; Venzmer, J. *Angew. Chem.* **1988**, *27*, 113 - 158.

(8) Nagawa, Y.; Regen, S. L. *J. Am. Chem. Soc.* **1991**, *113*, 7237-7240.

(9) Doyle, D.; Cabral, J. M.; Pfuetzner, R. A.; Kuo, A.; Gulbis, J. M.; Cohen, S. L.; Chait, B. T.; MacKinnon, R. *Science* **1998**, *280*, 69-77.

(10) Heginbotham, L.; Lu, Z.; Abramson, T.; MacKinnon, R. *Biophys. J.* **1994**, *66*, 1061-1067.

(11) Kumpf, R. A.; Dougherty, D. A. *Science* **1993**, *261*, 1708-1710.

(12) Loock, D. , Ph.D. Thesis: University of Victoria, 1997.

(13) MacKinnon, R. *Nature* **1991**, *350*, 232.

(14) Meillon, J. C.; Voyer, N. *Angew. Chem. Int. Ed.* **1997**, *36*, 967-968.

(15) Ghadiri, M. R.; Granja, J. R.; Buehler, L. K. *Nature* **1994**, *369*, 301-304.

(16) Murrillo, O.; Suzuki, I.; Abel, E.; Murray, C. L.; Meadows, E. S.; Jin, T.;

Gokel, G. W. *J. Am. Chem. Soc.* **1997**, *119*, 5540-5549.

(17) Abel, E.; Maguire, G. E. M.; Meadows, E. S.; Murillo, O.; Jin, T.; Gokel, G. W. *J. Am. Chem. Soc.* **1997**, *119*, 9061-9062.

(18) Fyles, T. M.; Loock, D.; van Straaten-Nijenhuis, W. F.; Zhou, X. *J. Org. Chem.* **1996**, *61*, 8866 - 8874.

(19) Fyles, T. M.; Heberle, D.; van Straaten-Nijenhuis, W. F.; Zhou, X. *Supramolecular Chemistry* **1995**, *6*, 71 - 77.

(20) Fyles, T. M.; Loock, D.; Zhou, X. *Can. J. Chem.* **1998**, *76*, 1015-1026.

(21) Fyles, T. M.; Loock, D.; Zhou, X. *J. Am. Chem. Soc.* **1998**, *120*, 2997-3003.

(22) Hu, C. W. Unpublished Results: Activity for hexaester acyclic in vesicles.

(23) Deng, G.; Merritt, M.; Yamashita, K.; Janout, V.; Sadowink, A.; Regen, S. L. *J. Am. Chem. Soc.* **1996**, *118*, 3307 - 3308.

(24) Deng, G.; Dewa, T.; Regen, S. L. *J. Am. Chem. Soc.* **1996**, *118*, 8975-8976.

(25) Otto, S.; Osifchin, M.; Regen, S. L. *J. Am. Chem. Soc.* **1999**, *121*, 7276-7277.

(26) Kobuke, Y.; Morita, K. *Inorganica Chimica Acta* **1998**, *283*, 167-174.

(27) Troiano, G. C.; Tung, L.; Sharma, V.; Stebe, K. J. *Biophys. J.* **1998**, *75*, 880 - 888.

(28) Stadler, E.; Dedek, P.; Yamashita, K.; Regen, S. L. *J. Am. Chem. Soc.* **1994**, *116*, 6677-6682.

(29) Kobuke, Y.; Ueda, K.; Sokabe, M. *J. Am. Chem. Soc.* **1992**, *114*, 7618-7622.

(30) Kobuke, Y.; Ueda, K.; Sokabe, M. *Chem. Lett.* **1995**, *6*, 435-436.

(31) Eichhorst-Gerner, K.; Stabel, A.; Moessner, G.; Declerq, D.; Valiyaveettil, S.; Enkelmann, V.; Müllen, K.; Rabe, J. P. *Angew. Chem. Int. Ed.* **1996**, *35*, 1492-

1495.

(32) Pfaadt, M.; Moessner, G.; Pressner, D.; Valiyaveettil, S.; Boeffel, C.; Müllen, K.; Spiess, H. W. *J. Mater. Chem.* **1995**, *5*, 2265-2274.

(33) Enkelmann, V.; Valiyaveettil, S.; Moessner, G.; Müllen, K. *Supramol. Sci.* **1995**, *2*, 3.

(34) Vanoppen, P.; Grim, P. C. M.; Rucker, M.; Feyter, S. D.; Moessner, G.; Valiyaveettil, S.; Müllen, K.; Schryver, F. C. D. *J. Phys. Chem.* **1996**, *100*, 19636-19641.

(35) Valiyaveettil, S.; Enkelmann, V.; Müllen, K. *J. Chem. Soc., Chem. Commun.* **1994**, 2097-2098.

(36) Valiyaveettil, S.; Müllen, K. *New J. Chem.* **1998**, *22*, 89-95.

(37) Yang, J.; Marendaz, J.-L.; Geib, S. J.; Hamilton, A. D. *Tet. Lett.* **1994**, *35*, 3665-3668.

(38) Meiners, C.; DeFeyter, S.; Lieser, G.; Stam, J. v.; Soltermann, A.; Berghmans, H.; Schryver, F. C. D.; Müllen, K. *Langmuir* **1999**, *15*, 3374-3380.

(39) van Genderen, M. H.; Pfaadt, M.; Moller, C.; Valiyaveettil, S.; Spiess, H. W. *J. Am. Chem Soc.* **1996**, *118*, 3661-3665.

(40) Menger, F. M.; Lee, S. J. *J. Am. Chem. Soc.* **1994**, *116*, 5987-5988.

(41) Kato, T.; Uryu, T.; Kaneuchi, F.; Jin, C.; Frechet, J. M. *Liq. Cryst.* **1993**, *14*, 1311-1317.

(42) Advanced Chemistry Development, Inc.; ACD/I-Lab Web Service: 2000. http://www2.acdlabs.com/ilab

(43) Ashley, R. H.; ed. *Ion Channels: A Practical Approach*; IRL Press at Oxford

University Press: Oxford, 1995.

(44) Kaye, K. , M.Sc. Thesis: University of Victoria, 1991.

(45) Miller, C., ed. *Ion Channel Reconstitution*; Plenum Press: New York, 1986.

(46) Mish, F. C., ed. in chief *Webster's Ninth New Collegiate Dictionary* Springfield, MA, 1989.

(47) Jenisch-Anton, A.; Adam, P.; Schaeffer, P.; Albrecht, P. *Geochimica et Cosmochimica Acta* **1999**, *63*, 1059-1074.

(48) Kabalka, G. W.; Mohammadi, M.; Kunda, S. A.; Finn, R. D. *Org. Prep. and Proc. Int.* **1985**, *17*, 17 - 22.

(49) Fieser and Fieser, *Reagents for Organic Synthesis, Volume 1*; John Wiley and Sons, Inc.: NY, 1967.

(50) Valiyaveettil, S.; Gans, C.; Klapper, M.; Gereke, R.; Müllen, K. *Polymer Bulletin* **1995**, *34*, 13-19.

(51) Philippot, J. R.; Schuber, F. *Liposomes as Tools in Basic Research and Industry*; CRC Press: Boca Raton, 1995.

(52) Fuhrhop, J. H.; Krull, M. *Frontiers in Supramolecular Organic Chemistry and Photochemistry*; VCH Weinheim: NY, 1991.

(53) Abel, E.; Maguire, G. E. M.; Murillo, O.; Suzuki, I.; Wall, S. L. D.; Gokel, G. W. *J. Am. Chem. Soc.* **1999**, *121*, 9043-9052.

(54) New, R. R. C.; ed. *Liposomes: A Practical Approach*; IRL Press at Oxford University Press: Oxford, 1990.

(55) Tretter, L. et. al., *Mol. Pharmacol.* **1998**, *53*, 734-741.

(56) Buckler, K. J.; Vaughan-Jones, R. D. *J. Physiol. (Lond.)* **1998**, *513*, 819-833.

(57) Tanford, C. *The Hydrophobic Effect: Formation of Micelles and Biological Membranes*; John Wiley & Sons, Inc.: New York, 1980.

(58) Henn, F. A.; Deeker, G. L.; Greenawalt, J. W.; Thompson, T. E. *J. Mol. Biol.* **1967**, *24*, 51-58.

(59) Henn, F. A.; Thompson, T. E. *J. Mol. Biol.* **1968**, *31*, 227-235.

(60) Benz, R.; Fröhlich, O.; Läuger, P.; Montal, M. *Biochimica et Biophysica Acta* **1975**, *394*, 323-334.

(61) Hartshorne, R. *Ion Channel Reconstitution*; Plenum Press: NY, 1986.

VITA

Surname: Knoy | Given Names: Ryan Lee

Place of Birth: Mesa, Arizona, USA

Educational Institutions Attended:

University of Victoria	1998 to 2000
Northern Arizona University	1993 to 1998

Degrees Awarded:

B. S. in Chemistry	1998
B. A. in Spanish	1998

Honours and Awards:

NAU Chemistry Departmental Award	1998
ACS Analytical Chemistry Award	1997

Conference Presentations:

T. M. Fyles, R. Knoy, *Membrane Transport Activity of Isophthalate Amphiphiles*, 83rd Canadian Society for Chemistry Conference and Exhibition, May 27th through 31st 2000, Calgary Alberta

PARTIAL COPYRIGHT LICENSE

I, Ryan Knoy, grant the right to lend my thesis to users of the University of Victoria Library, and to make single copies only for such users or in response to a request from the library of any other university, or similar educational institution, on its behalf or for one of its users. Further, I agree that permission for extensive copying of this thesis for scholarly purposes may be granted by me or a member of the University designated by me. It is understood that copying or publication of this thesis for financial gain shall not be allowed without my expressed written consent.

Title of Thesis: *Membrane Transport Activity of Isophthalate Amphiphiles*

Author [redacted]

Ryan L. Knoy
November, 2000